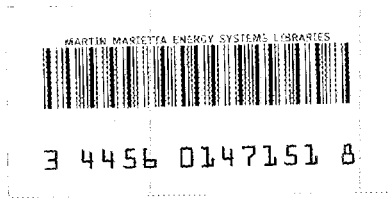


ornl

OAK RIDGE
NATIONAL
LABORATORY

MARTIN MARIETTA



ORNL/TM-9695

Annual Progress Report of the Materials Project of the Energy Conversion and Utilization Technologies (ECUT) Program for Fiscal Year 1983

L. E. Morris
A. Jordan
J. A. Carpenter, Jr.

OAK RIDGE NATIONAL LABORATORY
CENTRAL RESEARCH LIBRARY
CIRCULATION SECTION
ROOM 600N 123
LIBRARY LOAN COPY
DO NOT TRANSFER TO ANOTHER PERSON
If you wish someone else to use this
report, send in note with report and
the library will arrange a loan.

OPERATED BY
MARTIN MARIETTA ENERGY SYSTEMS, INC.
FOR THE UNITED STATES
DEPARTMENT OF ENERGY



Printed in the United States of America. Available from
National Technical Information Service
U.S. Department of Commerce
5285 Port Royal Road, Springfield, Virginia 22161
NTIS price codes—Printed Copy: A06 Microfiche A01

This report was prepared as an account of work sponsored by an agency of the United States Government. Neither the United States Government nor any agency thereof, nor any of their employees, makes any warranty, express or implied, or assumes any legal liability or responsibility for the accuracy, completeness, or usefulness of any information, apparatus, product, or process disclosed, or represents that its use would not infringe privately owned rights. Reference herein to any specific commercial product, process, or service by trade name, trademark, manufacturer, or otherwise, does not necessarily constitute or imply its endorsement, recommendation, or favoring by the United States Government or any agency thereof. The views and opinions of authors expressed herein do not necessarily state or reflect those of the United States Government or any agency thereof.

ORNL/TM-9695
Distribution
Category UC-95a

METALS AND CERAMICS DIVISION

ANNUAL PROGRESS REPORT OF THE MATERIALS PROJECT OF THE ENERGY
CONVERSION AND UTILIZATION TECHNOLOGIES (ECUT)
PROGRAM FOR FISCAL YEAR 1983

L. E. Morris, A. Jordan, and J. A. Carpenter, Jr.

Date Published - February 1987

Prepared for the
Assistant Secretary for Conservation and Renewable Energy
Office of Energy Utilization Research
Energy Conversion and Utilization Technologies (ECUT) Program

NOTICE: This document contains information of a preliminary nature. It is subject to revision or correction and therefore does not represent a final report

Prepared by the
OAK RIDGE NATIONAL LABORATORY
Oak Ridge, Tennessee 37831
operated by
MARTIN MARIETTA ENERGY SYSTEMS, INC.
for the
U.S. DEPARTMENT OF ENERGY
under Contract DE-AC05-84OR21400



3 4456 0147151 8

CONTENTS

ABSTRACT	1
OVERVIEW	1
HIGH TEMPERATURE MATERIALS	2
DUCTILE ORDERED INTERMETALLIC ALLOYS	2
Aluminides	2
Long Range Ordered (LRO) Alloys	13
WEAR TESTING OF DUCTILE LRO AND NICKEL ALUMINIDES	27
DIFFUSION STUDIES OF DUCTILE LRO AND NICKEL ALUMINIDES	28
MECHANICAL ALLOYING OF DUCTILE NICKEL ALUMINIDE ALLOYS	28
METALLIC BRAZING FILLER METALS FOR CERAMIC-CERAMIC AND CERAMIC-METAL JOINING	28
WORKSHOP ON CERAMIC JOINING	35
MODELING OF CERAMIC ATTACHMENTS	36
ASSESSMENT OF ELECTROMAGNETIC JOINING OF CERAMICS	36
ASSESSMENTS OF SUPERALLOYS AND METAL FORMING	41
LIGHTWEIGHT MATERIALS	42
RECOVERY AND REUSE OF PLASTIC SCRAP VIA BONDING AND SEPARATION - COORDINATION	42
PREPARATION AND TESTING OF LABORATORY SPECIMENS OF COMPATIBILIZER-BONDED AUTO SHREDDER RESIDUE	44
DEVELOPMENT OF HYDROGEN-BONDING COMPATIBILIZERS FOR AUTO SHREDDER RESIDUE	51
IN SITU POLYMERIZATION FOR BONDING AUTO SHREDDER RESIDUE	53
SEPARATION AND ANALYSIS OF AUTO SHREDDER RESIDUE	57
PLASTICS REUSE VIA DECOMPOSITION	58
ASSESSMENT OF ECONOMIC POTENTIAL OF PLASTICS REUSE	60
AGING OF RIGID URETHANE FOAM INSULATION	61
PLASTIC-COATED LOW-TEMPERATURE HEAT EXCHANGERS	69
MATERIALS BY DESIGN	70
NEW ASSESSMENTS AND INITIATIVES	71
CUBIC BORON NITRIDE AND DIAMOND-LIKE CARBON COATINGS BY CVD	71
CERAMIC COMPOSITES	73
MAGNETRON-SPUTTERED AMORPHOUS METAL WEAR-RESISTANT COATINGS	75
INSTRUMENTS FOR HARSH ENVIRONMENT	76

SUPERCRITICAL FLUID EQUATIONS OF STATE	83
COATINGS FOR HIGH TEMPERATURE ENERGY CONVERSION SYSTEMS	84
LASER SURFACE MODIFICATION OF CERAMICS	85
ION IMPLANTATION OF ZIRCONIA	85
FY 1983 PUBLICATIONS	85
ACKNOWLEDGMENTS	86
REFERENCES	86

ANNUAL PROGRESS REPORT OF THE MATERIALS PROJECT OF THE ENERGY
CONVERSION AND UTILIZATION TECHNOLOGIES (ECUT) PROGRAM
FOR FISCAL YEAR 1983*

L. E. Morris, A. Jordan, and J. A. Carpenter, Jr.

ABSTRACT

This is the annual technical progress report for fiscal year 1983 of the Materials Project of the U.S. Department of Energy (DOE) Energy Conversion and Utilization Technologies (ECUT) Program. In fiscal year 1983, the ECUT Materials Project conducted research in four technical areas, or "work elements," entitled High Temperature Materials, Lightweight Materials, Materials by Design, and New Assessments and Initiatives. The progress of the various tasks of the work elements is discussed in this report.

OVERVIEW

The U.S. Department of Energy (DOE) established the Energy Conversion and Utilization Technologies (ECUT) Program to develop and promote utilization of an expanded technology base and advanced concepts in energy conversion and utilization. The purpose of the Program is to meet the Conservation and Renewable Energy Program goals of improved productivity (utilization efficiency) and alternate resource utilization in the mid to long term.

The Materials Project is one of several projects within the ECUT Program. It is managed for DOE by the Oak Ridge National Laboratory (ORNL) in a lead laboratory role. The mission of the ECUT Materials Project is to identify and conduct base technology research and development to overcome any materials limitations impeding the achievement of the above goals of the Conservation and Renewable Energy Program.

*Research sponsored by the Office of Energy Utilization Research, Energy Conversion and Utilization Technologies (ECUT) Program, U.S. Department of Energy, under contract DE-AC05-84OR21400 with Martin Marietta Energy Systems, Inc.

This is the second annual progress report of the ECUT Materials Project. Project progress since FY 1982 has been chronicled in a previous report.¹

The main purpose of this report is to chronicle the project's work for future reference. It is not intended as a timely reporting of developments emanating from the work. In general, such timely reporting of development from the ECUT Materials Project is done in open literature reports and publications. See the PUBLICATIONS section for a list of reports and publications published in FY 1983 and the REFERENCES section for publications in which the results of work contained in this document have been reported.

In FY 1983, the DOE ECUT Program elevated the subject of tribology (the science of friction, wear, and lubrication) to full-fledged project status. In FY 1981 and FY 1982, tribology was a work element under the Materials Project; progress in that area in FY 1982 was reported in the annual report of the Materials Project for that year. In FY 1983 and beyond, progress in the tribology area will be reported under a separate annual report.

HIGH TEMPERATURE MATERIALS

DUCTILE ORDERED INTERMETALLIC ALLOYS - C. T. Liu, A. DasGupta, J. A. Horton, R. O. Williams, E. H. Lee (Oak Ridge National Laboratory), and N. S. Stoloff (Rensselaer Polytechnic Institute)²⁻¹²

The objective of this task is to develop and characterize new high-temperature structural materials based on ductile ordered alloys and assess them for energy conservation applications. The work on ductile aluminides based on Ni₃Al was initiated in fiscal year 1983, while work from fiscal year 1982 on ductile long-range-ordered alloys based on (Fe,Ni)₃V and (Fe,Ni)₃(V,Al) continued. The general development work on each type of material is reported separately below.

Aluminides* -- C. T. Liu, J. A. Horton, and E. H. Lee (Oak Ridge National Laboratory)

The aluminides were selected for development because they were known to be strong and resistant to corrosion in hostile environments at elevated

*Work sponsored jointly by the ECUT Program and the AR&TD Fossil Energy Materials Program.

temperatures. Success in development and commercialization of structural aluminides could substantially reduce the nation's dependence on critical strategic elements, such as chromium and cobalt, which are used extensively in current heat-resistant alloys.

Poor ductility and fabricability had been considered to be the major problems with using aluminides as structural materials. However, recent study of microalloying at ORNL had demonstrated that additions of a few hundred parts per million of boron dramatically improved the fabricability and ductility of polycrystalline Ni_3Al . Thus, boron-doped Ni_3Al served as an attractive basis for the development of ductile and strong structural aluminides. The development work of this task has involved: (1) hardening Ni_3Al by solid solution and particle strengthening; (2) improving oxidation and corrosion resistances at high temperatures (e.g., $>900^\circ\text{C}$); (3) improving creep resistance; and (4) preparation and characterization of large heats for structural uses in advanced engines and energy conversion systems. Much of the work for the first two of these tasks has been successfully accomplished, and current work is concentrating on improving high-temperature ductility and hot fabricability of hafnium-modified aluminides. Also, Cabot Corporation is interested in trying to scale up these materials in hundred-pound quantities.

Two aluminides, IC-32 and IC-33, were prepared based on Ni_3Al , where 10.6 wt % of iron and small amounts ($<1.2\%$) of manganese, titanium, and carbon were added for solid-solution hardening and carbide strengthening. Both alloys were fabricated into 0.8-mm-thick sheets by repeated cold rolling with intermediate anneals at 1000 to 1050°C . Second-phase particles were observed metallographically, and they were identified as titanium carbide (TiC) with a lattice parameter of 0.43 nm by transmission electron microscopy (TEM). The particles ranged in size from 0.1 to 1.0 μm in diameter and covered about 2% of the areas examined. A preliminary analysis of the orientation relationship of these particles to the matrix showed that the $(001)_{\text{ppt}}$ is parallel to the $(001)_{\text{matrix}}$ and the $[200]_{\text{ppt}}$ is parallel to the $[220]_{\text{matrix}}$.

Mechanical properties of well-annealed IC-32 and IC-33 were determined by tensile tests as functions of temperature. Figure 1 compares the yield strength of IC-32 with boron-doped Ni_3Al (500 ppm B) and with

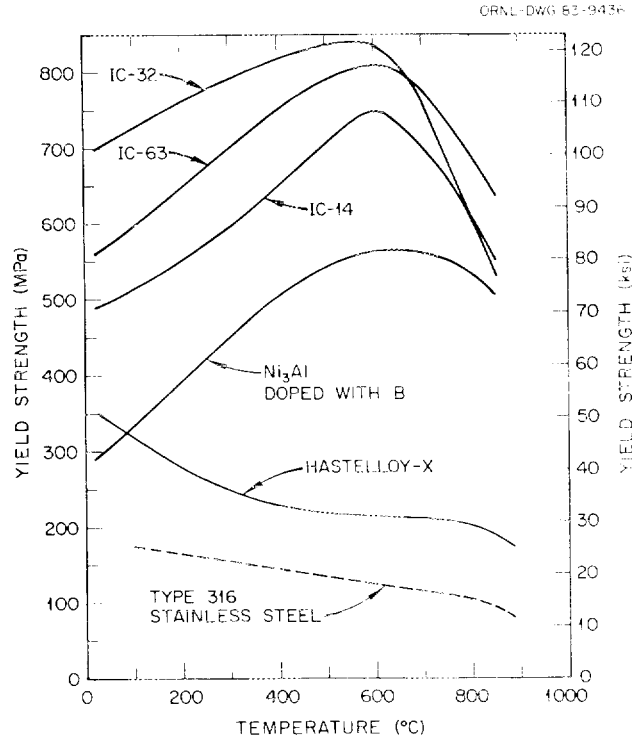


Fig. 1. Comparison of yield strength as a function of temperature of the aluminide alloy IC-32 with boron-doped Ni₃Al and commercial wrought alloys Hastelloy X and type 316 stainless steel.

the commercial wrought alloys Hastelloy X and type 316 stainless steel. Unlike the commercial alloys, the strengths of boron-doped Ni₃Al and IC-32 increase with increasing temperature, reaching a maximum around 600°C. This experiment demonstrated that Ni₃Al could be effectively strengthened by macroalloying. IC-32 displays a yield strength at 600°C of 830 MPa (120,000 psi), which is over 4 times that of Hastelloy X and 9 times that of type 316 stainless steel.

The boron-doped Ni₃Al showed light spalling during cyclic oxidation above 900°C. In order to improve the adhesion between aluminide oxide and base metal, a small amount of hafnium (approximately 0.5 at. %) was added to nickel aluminides containing 23.5 to 24.5 at. % aluminum. The hafnium-modified aluminide with 24.5 at. % aluminum was cracked during cold rolling, but the aluminides with 24% aluminum (IC-49) and 23.5% aluminum (IC-50) were successfully fabricated into sheets.

The oxidation behaviors of IC-49 and IC-50 were determined by exposure of samples to air at 1000°C. The samples were removed from a furnace after each 25- to 75-h exposure. Figure 2 is a plot of weight gain due to oxidation in IC-50 as a function of exposure time at 1000°C. The hafnium-modified aluminide showed a parabolic oxidation and exhibited no apparent spalling. The total weight gain was 0.6 mg/cm after a 571-h exposure. The oxidation rate of the aluminide was much lower than that of stainless steels and commercial superalloys. The good oxidation resistance of IC-50 resulted from formation of aluminide oxide films which protect the base metal from excessive oxidation.

A number of experiments had been initially unsuccessful in attempting to raise the temperature for maximum strength. However, work on solid-solution hardening has indicated that hafnium is most effective in

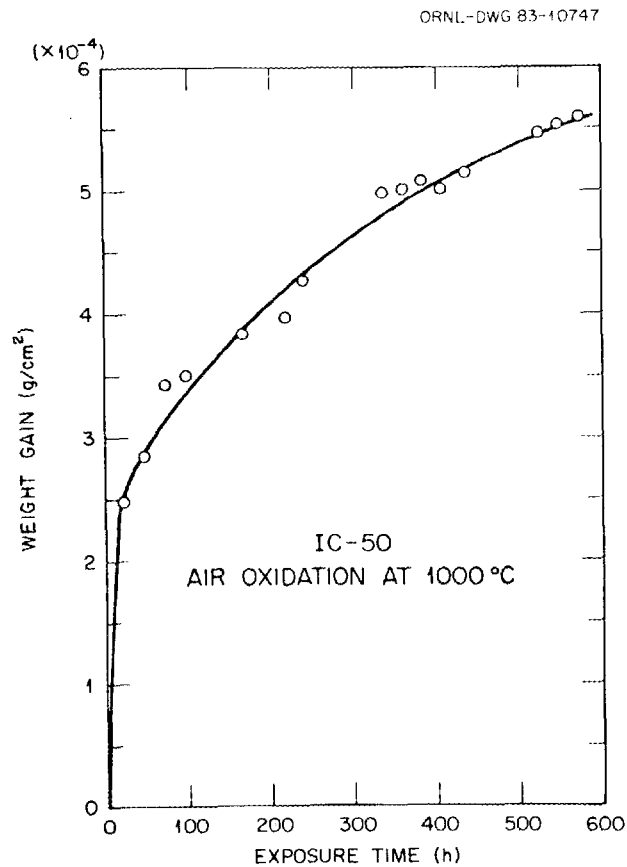


Fig. 2. Weight gain in IC-50 sample as a function of exposure time at 1000°C in air.

improving the strength of boron-doped Ni₃Al above 600°C. In order to optimize the hafnium content in Ni₃Al, a series of nickel aluminides was prepared with 0.25, 0.5, 1.0, 1.5, 2.0, and 3.0 at. % hafnium. All the hafnium-modified aluminides were doped with 500 ppm boron for ductility improvement. The alloy ingots were homogenized at 1000°C and fabricated by repeated cold rolling with intermediate anneals at 1000 to 1050°C. All the aluminides were successfully cold rolled into 0.8-mm-thick sheet, except the 3.0 at. % hafnium alloy, which cracked during early stages of cold fabrication.

Tensile properties of the hafnium-modified aluminides were determined as a function of test temperature in vacuum. It was found that hafnium is very effective in hardening Ni₃Al at elevated temperatures. Table 1 shows the tensile results at 850°C.

Table 1. Effect of hafnium additions on tensile specimens of boron-doped Ni₃Al tested at 850°C

Hafnium concentration (at. %)	Yield strength		Tensile strength		Elongation (%)
	(MPa)	(ksi)	(MPa)	(ksi)	
0	498	72.3	660.1	95.8	7.1
0.25	548	79.5	692.5	100.5	3.1
0.50	640.1	92.9	866.1	125.7	14.1
1.0	744.1	108.0	926.0	134.4	5.5
1.5	922.6	133.9	1085.9	157.6	9.6
2.0	788.9	114.5	788.9	114.5	<0.1

At 850°C both tensile and yield strengths increase with hafnium content and peak at 1.5 at. % hafnium. This hafnium-modified aluminide has a yield strength of 922.6 MPa (133.9 ksi) and ultimate tensile strength of 1085.9 MPa (157.6 ksi). These properties are higher than those of commercial superalloys including cast superalloys. The aluminides show a decrease in strength (and a sharp drop in tensile elongation) with an increase in hafnium content from 1.5 to 2.0 at. % at 850°C. Figure 3 graphically illustrates the effects of hafnium additions on strength at 850°C and also at room temperature. It is quite surprising

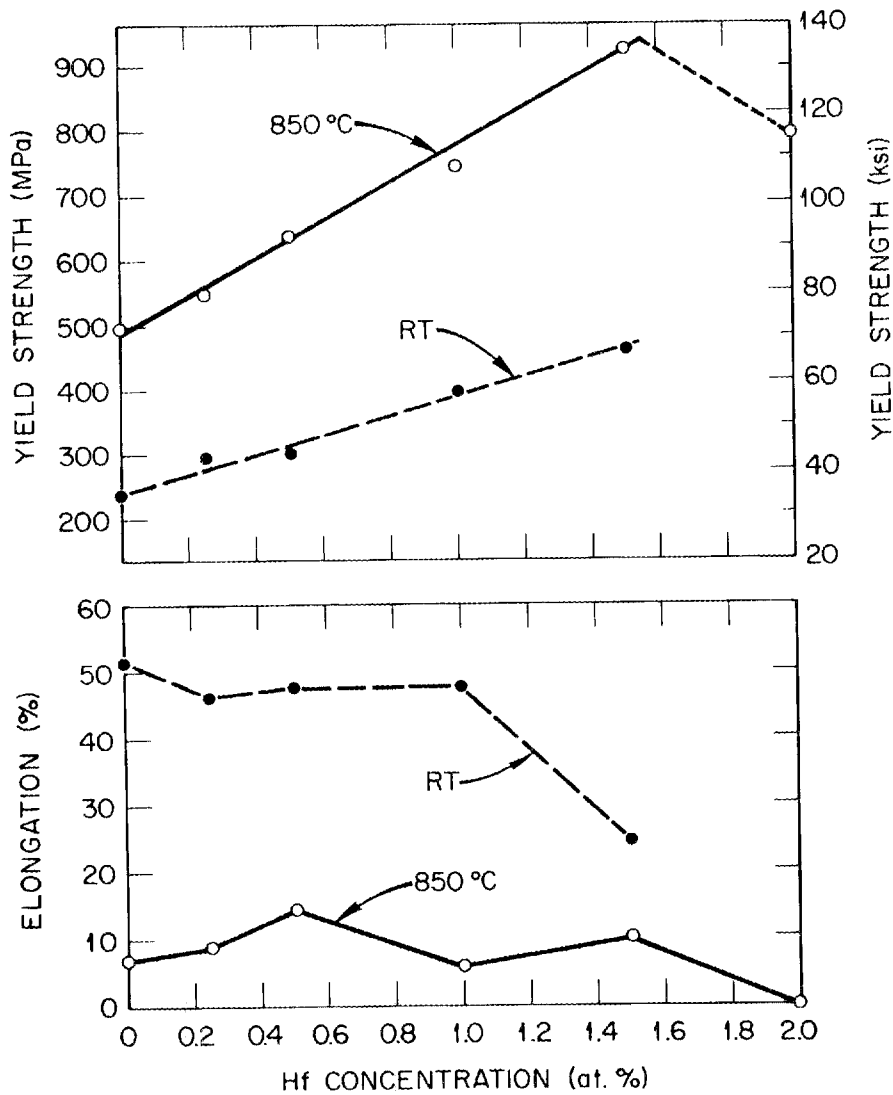


Fig. 3. Effects of hafnium concentration on the tensile properties of Ni_3Al at room temperature and at 850°C .

that the slope for the 850°C yield strength curve is higher than that of the room temperature curve, indicating that hafnium is more effective in improving the strength at 850°C .

The yield strength of boron-doped Ni_3Al and hafnium-modified Ni_3Al (1.5 at. % Hf) is plotted as a function of test temperature in Fig. 4. Hastelloy X and type 316 stainless steel are also included for comparison.

The ductility of Ni_3Al is not sensitive to the hafnium content up to about 1% hafnium at room temperature and to about 1.5% hafnium at 850°C .

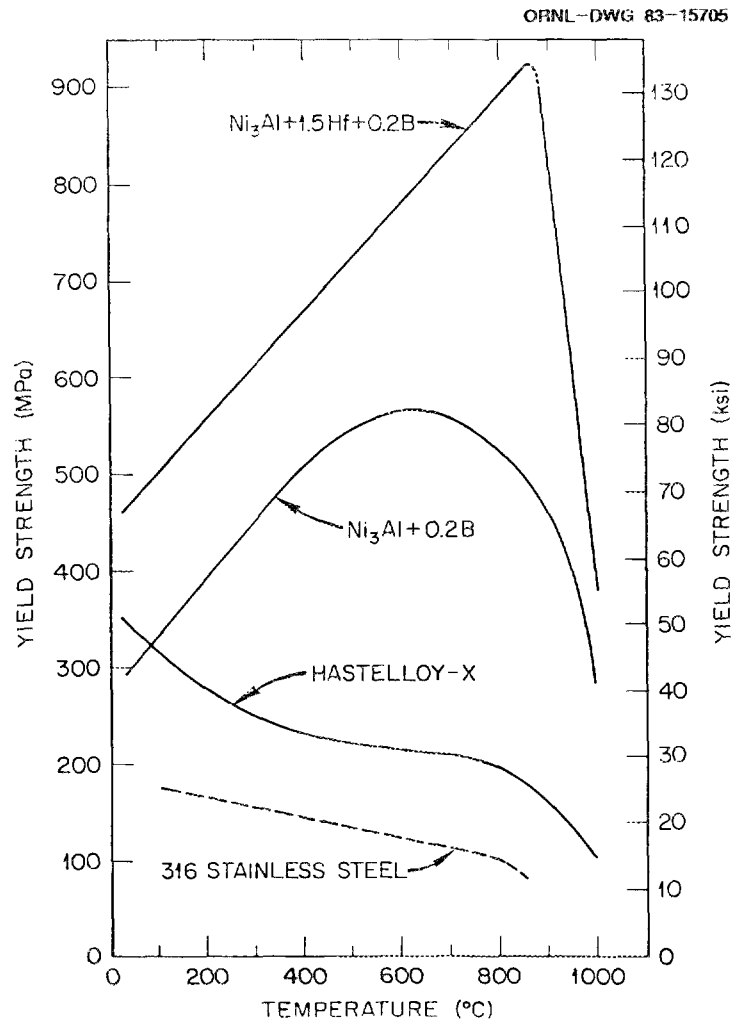


Fig. 4. Comparison of yield strength as function of temperature of hafnium-modified aluminide with boron-doped Ni₃Al and commercial solid-solution alloys Hastelloy X and type 316 stainless steel.

Above these levels, the ductilities of the hafnium-modified aluminides decrease significantly, as shown in Fig. 3. We are working on improving the high temperature ductility of the hafnium-modified Ni₃Al by control of alloy stoichiometry and boron concentration. It is suspected that boron additions improve the room temperature ductility, but they may lower the ductility at temperatures above 800°C.

An aluminide with 0.5% hafnium was alloyed with 10 at. % iron, which was designated as IC-63. This aluminide was readily fabricated into 0.8-mm-thick sheets by repeated cold rolling. Tensile properties of IC-63

were determined as a function of test temperature. Figure 5 compares the yield strength of IC-63 with the yield strengths of boron-doped Ni₃Al (500 ppm B), iron-modified IC-14, and carbide-strengthened IC-32. The yield strengths of the commercial alloys Hastelloy-X and type 316 stainless steel are also included in the plot for comparison. The carbide-strengthened aluminide, IC-32, has the best strength at temperatures to 700°C; above that temperature, the hafnium-modified IC-63 was the strongest among the aluminides at that time.

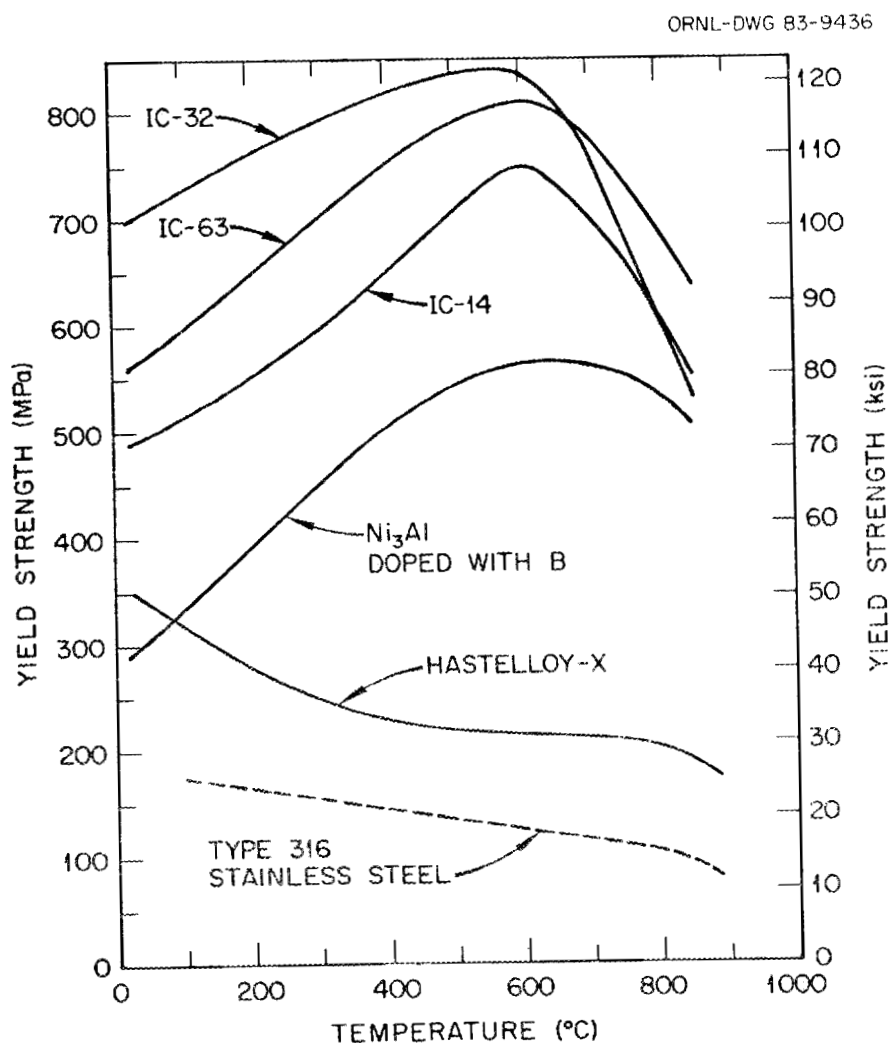


Fig. 5. Comparison of yield strength as a function of temperature of the aluminide alloys (IC-14, IC-63, and IC-32) with boron-doped Ni₃Al and commercial wrought alloys Hastelloy X and type 316 stainless steel.

Creep properties of the hafnium-modified aluminides were determined at 760°C in vacuum under a dead-load arrangement. The results are summarized in Table 2, which includes comparable data for Waspaloy, Hastelloy X, and type 316 stainless steel for comparison. The creep rate decreases and the rupture life of the modified Ni₃Al increases with increasing hafnium content. The data in Table 2 suggest that a minimum level of hafnium is required in order to substantially improve the steady state creep rate. The minimum hafnium level appears to be 0.5 at. % for the creep tests at 138 MPa (20,000 psi) and 1.0 at. % at 276 MPa (40,000 psi). The creep rate of the aluminide alloyed with ≥0.5% Hf is lower than that of Hastelloy X by more than two orders of magnitude. The creep resistance of the aluminide alloyed with ≥1 at. % Hf is comparable or better than that of Waspaloy.

Table 2. Comparison of creep properties of hafnium-modified nickel aluminides^a with those of commercial alloys

Alloy composition (at. %)	Steady state creep rate (10 ⁻⁶ /h)	Rupture life (h)
760°C, 183 MPa (20 ksi)		
Ni ₃ Al	91.0	352
Ni ₃ Al + 0.25 Hf	31.0	>600 ^b
1.0 Hf	3.3	>600 ^b
1.5 Hf	3.7	>500 ^b
2.0 Hf	0.5	>500 ^b
Type 316 stainless steel	8500.0	65
Hastelloy X	1300.0	252
760°C, 276 MPa (40 ksi)		
Ni ₃ Al + 0.25 Hf	130	285
0.5 Hf	130	340
Ni ₃ Al + 1.0 Hf	42	>600 ^b
1.5 Hf	23	>600 ^b
Waspaloy		~1000 ^b

^aAll aluminides were doped with 0.2 at. % boron.

^bTests discontinued without rupture.

Structural features in hafnium-modified aluminides were studied by TEM. Specimens were recrystallized prior to thinning by electropolishing. As can be seen in Fig. 6, no obvious precipitation occurs in the aluminide with 0.5% Hf. This suggests that the hafnium added to Ni_3Al remains in solution, rather than forming second-phase particles.

The microstructures of Ni_3Al alloys modified with up to 2 at. % Hf were examined by TEM. The TEM disks were prepared from the shoulders of tensile specimens that were annealed for 1 h at 1050°C plus 30 min at 600°C , followed by tensile testing at 600°C . Dislocation networks with what appeared to be extended dislocation nodes were observed in the aluminide modified with 2.0 at. % hafnium, as shown in Fig. 7. These dislocation structures were not observed in any of the other alloys with a lower hafnium content, although these specimens were not all deformed the same amount. Possibly the hafnium addition lowers the antiphase boundary (APB) or stacking fault energy sufficiently for the dislocations to separate enough to be imaged.

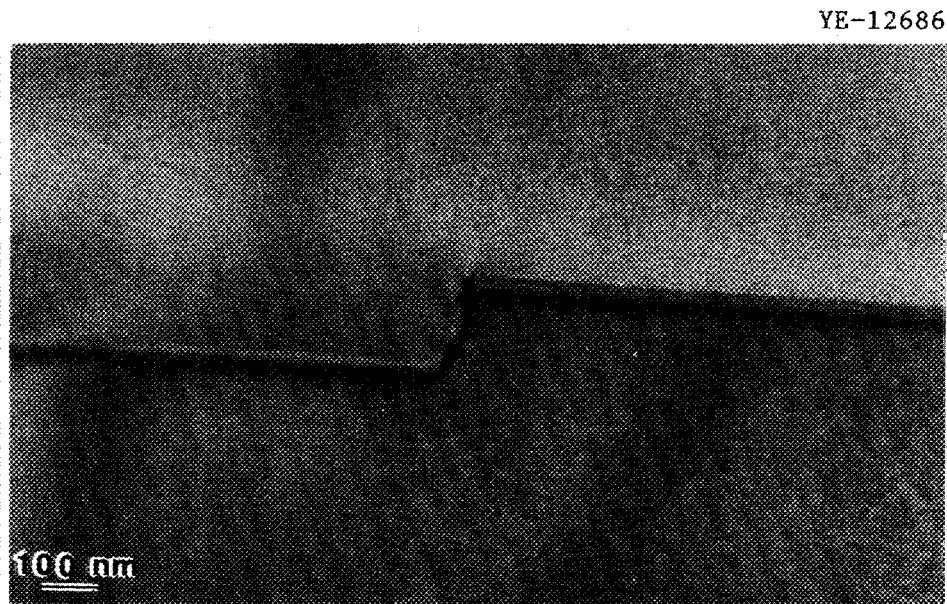
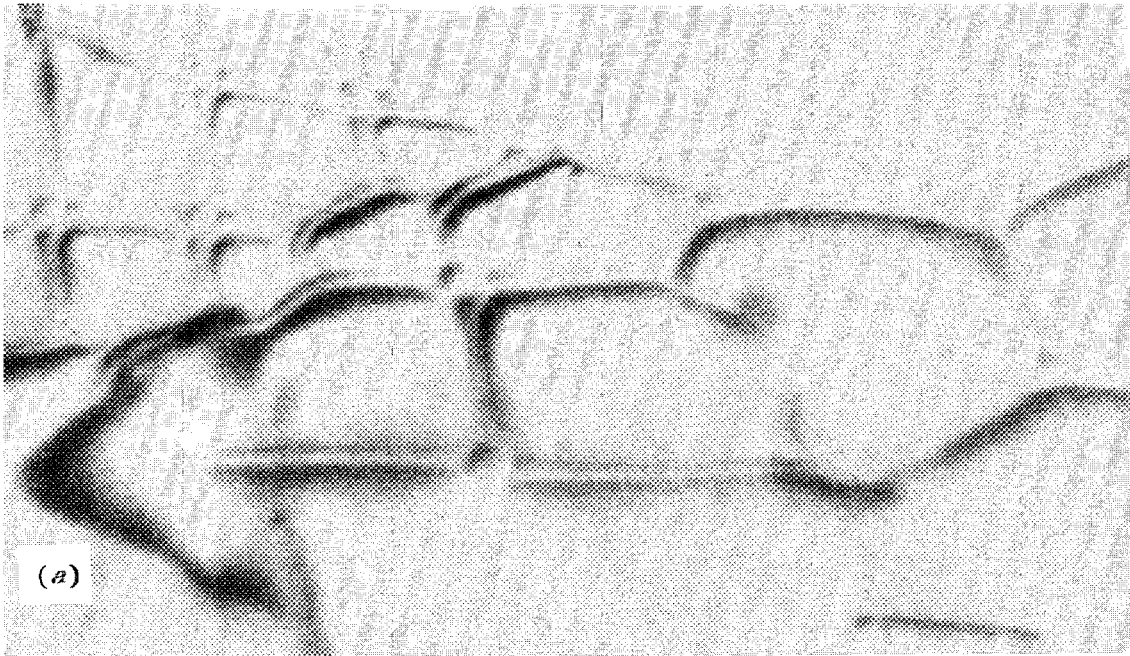


Fig. 6. Transmission electron micrograph showing no precipitates in hafnium-modified aluminide (0.5 at. % Hf). Feature visible traversing center of micrograph is a grain boundary.

YE-12695



YE-12696



Fig. 7. (a) Bright-field and (b) dark-field transmission electron micrographs of aluminide with 2 at. % hafnium, showing possible superlattice dislocations and extended nodes. The dark-field micrograph was made with weak beam $g, 3g$ conditions with a $[220]$ diffraction vector and an electron beam direction near $[110]$.

The separation between the dislocations is approximately 8 nm. The separated dislocations could be either dipoles, superlattice dislocations, or partials. Dislocation dipoles are rather common in these materials during low-temperature deformation, but it is unlikely that an intersection would occur between dipoles without the dislocations annihilating. No stacking fault fringe contrast was observed in normal bright-field imaging, indicating that these dislocations are probably not partials. Several of the nodes appear to be similar to the normal extended nodes formed from partial dislocations in fcc metals, but no corresponding contracted nodes were found. A complete dislocation analysis of these dislocation networks is in progress.

There has been considerable industrial interest in these aluminides. To date more than 300 letters of inquiry have been received, 25 requesting material for tests. Of these, we have been able to supply only one. The Cabot Corporation is interested in trying to scale up the fabrication of these materials in hundred-pound quantities.

The development of these aluminides was cited for an IR-100 award for 1983 by *Industrial Research and Development* magazine.

The National Materials Advisory Board is beginning a study for the U.S. Department of Defense to assess the potential of these aluminide materials for military applications.

Long Range Ordered (LRO) Alloys* - C. T. Liu, A. DasGupta, J. A. Horton, R. O. Williams (Oak Ridge National Laboratory), and N. S. Stoloff (Rensselaer Polytechnic Institute)

The development of LRO alloys for advanced heat engine applications has been focusing on the alloy system $(\text{Ni}_{70}\text{Fe}_{30})_3(\text{V}_{98-X}\text{Al}_X\text{Ti}_2)$, where vanadium atoms are partially replaced by aluminum atoms. The function of adding aluminum is to increase the critical ordering temperature (T_C) and oxidation resistance of the LRO alloys.

The progress of phase transformations with temperature has been studied in detail in the alloy system $(\text{Ni}_{70}\text{Fe}_{30})_3(\text{V}_{98-X}\text{Al}_X\text{Ti}_2)$, with

*Work sponsored jointly by the ECUT Program and the AR&TD Fossil Energy Materials Program.

$x = 0$ to 80, by using X-ray diffraction, differential scanning calorimetry (DSC), optical microscopy, and transmission electron microscopy (TEM). Preliminary studies were made on LRO-45 ($x = 0$), which indicated that the sequence of transformations was

tetragonal \rightarrow tetragonal + cubic \rightarrow disordered cubic.

In alloys with aluminum additions the situation was found to be more complicated, with a general trend toward the stability of cubic ordered structure ($L1_2$) at low temperature. With still higher aluminum content, e.g., in LRO-55 ($x = 40$), the presence of second-phase particles was found to complicate the transformation and microstructure. Studies by TEM indicated that the second-phase particles had the ordered NiAl structure with a lattice parameter of 0.283 nm. These particles ranged from 0.1 to 1.0 μm in diameter and covered an area fraction of about 5%. Analysis gave the following orientation relationship:

$(001)_{\text{ppt}}$ parallel to $(011)_{\text{matrix}}$, and
 $[010]_{\text{ppt}}$ parallel to $[011]_{\text{matrix}}$.

The alloy with $x = 20$ (LRO-54) was studied next. Figure 8 depicts the disordering phase transformations for LRO-54. The microstructures of LRO-54 shown in Figs. 8(a) and 8(b) were produced by quenching specimens after annealing for 120 min at 770°C and 80 min at 860°C, respectively. All the micrographs are superlattice dark fields on the [110] ordered reflections, which show ordered regions as bright areas. The specimen quenched from 770°C had the "Chinese script" structure containing ordered tetragonal regions. The matrix appeared to be disordered. The strain fields present suggest that the matrix was cubic and the precipitates were tetragonal. The specimen quenched from 860°C [Fig. 8(b)] also contained ordered tetragonal regions with a much lower area fraction covered, although the precipitates were larger in a cross section. These results suggested that the actual disordering process starts with a disordered cubic phase.

Figure 9 shows TEM micrographs of the disordering process in LRO-55 ($x = 40$) quenched from 860°C [Fig. 9(a)] and 965°C [Fig. 9(b)]. The specimen quenched from 860°C is mostly ordered, with only small disordered bands separating the ordered areas. The specimen quenched from 965°C has only a small amount of remaining area which is ordered, but these ordered

YE-13292

YE-13293

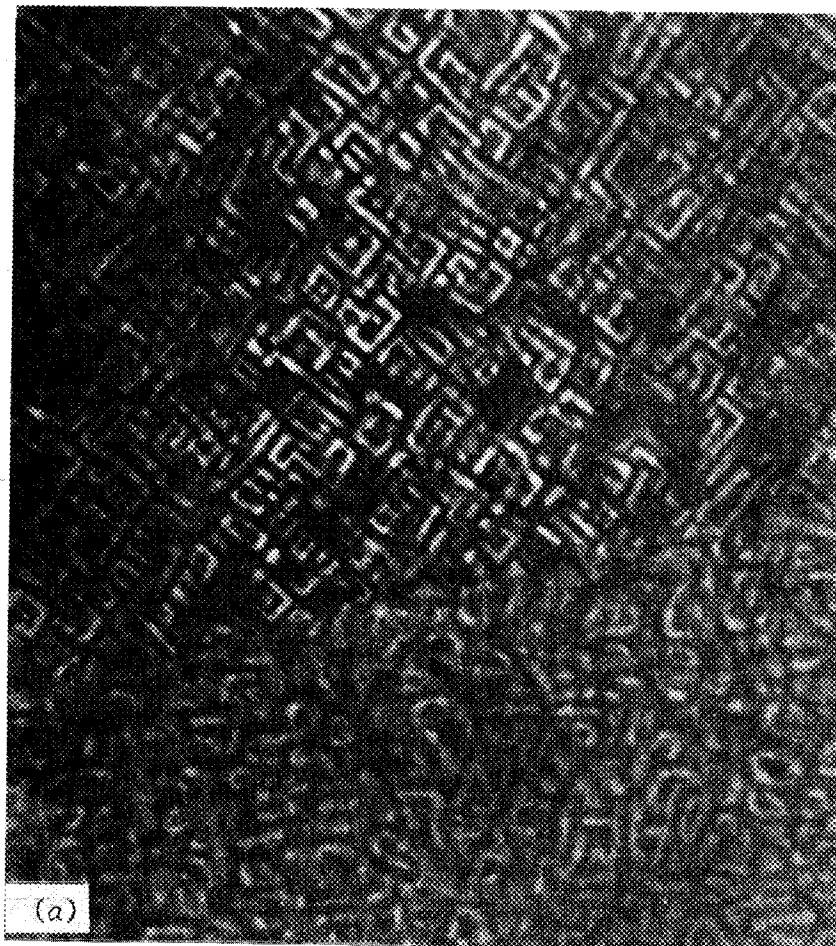


Fig. 8. Superlattice dark-field TEM micrographs of $(\text{Fe}_{30}\text{Ni}_{70})_3(\text{V}_{78}\text{Al}_{20}\text{Ti}_2)$ quenched from (a) 770°C and (b) 860°C , showing the morphology of the disordering phase transformation.

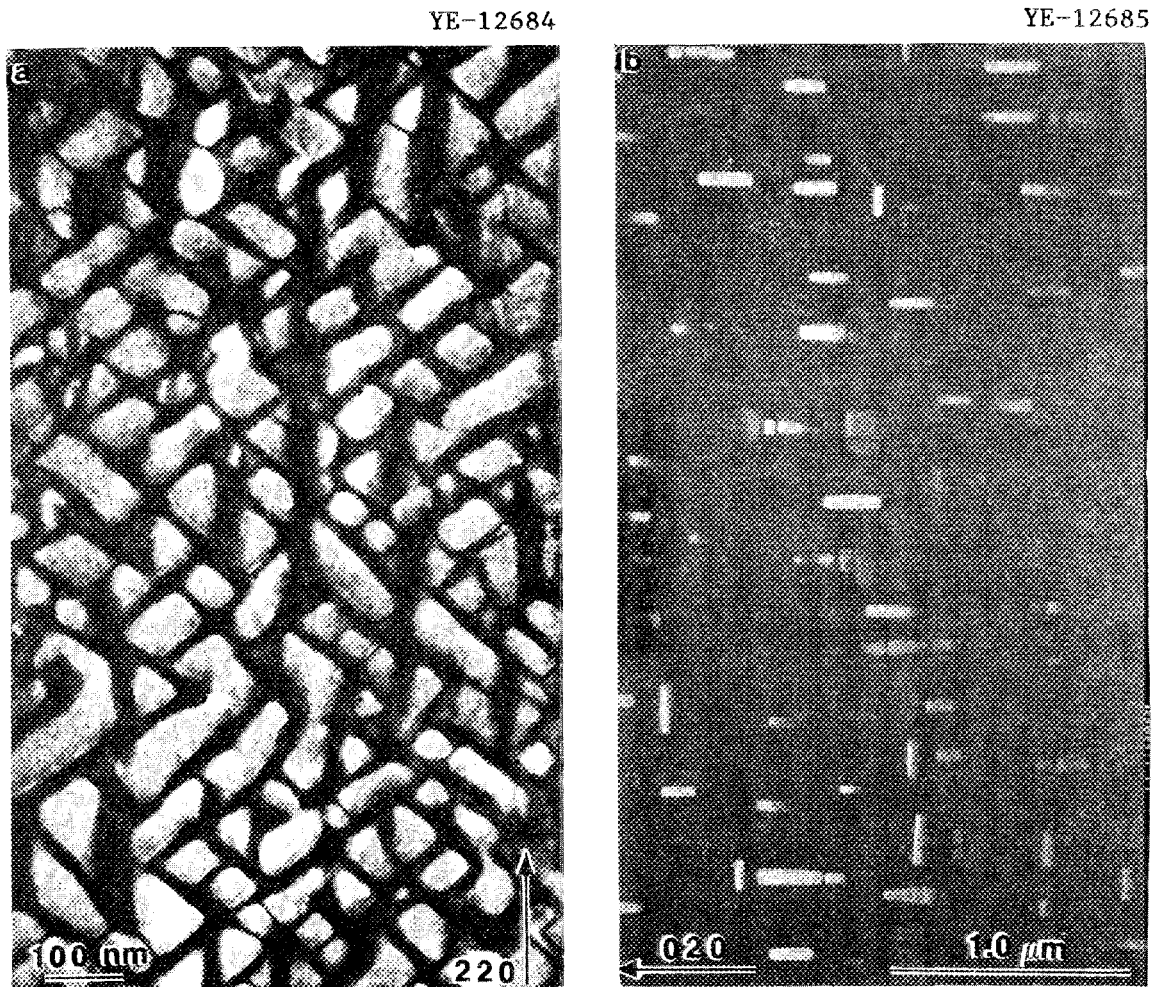


Fig. 9. Dark-field micrographs using superlattice reflections of LRO-55 quenched from (a) 860°C, electron beam direction near [112], and from (b) 965°C, electron beam direction near [001], showing the ordered regions as bright areas against a disordered (dark) background.

areas have a well developed crystallographic shape with [200] type faces. Energy dispersive spectroscopic (EDS) analysis in the TEM of these widely separated ordered precipitates revealed that they are enriched by 5 at. % in Al and 5% in Ni, and depleted by 5% in V and 5% in Fe as compared with the nearby matrix. Stereo micrographs showed that these precipitates were usually very thin. Because of the smallness of the precipitates, the EDS analyzed volume will include matrix. For this reason the above quoted numbers are an underestimate of the actual segregations. It appears that there is a tendency for the composition to migrate toward that of Ni_3Al .

LRO-55 ($x = 40$), after the normal stepwise ordering heat treatment, contains many large precipitates with the B_2 NiAl structure. These precipitates were found by EDS analysis in the TEM to have 10 at. % less Fe, 20% less V, 20% more Al, and the same amount of Ni. The composition of these precipitates is apparently migrating toward NiAl.

Work has clarified the steps in the transformation process for LRO-55 ($x = 40$), which differs from LRO-54 ($x = 20$) mainly in the presence of the second-phase B_2 particles. These steps have now been established to be

ordered cubic ($L1_2$) + B_2 → ordered cubic ($L1_2$) + disordered fcc → disordered fcc.

In summary, with the gradual replacement of vanadium by aluminum in the $(Ni_{70}Fe_{30})_3(V_{98-x}Al_xTi_2)$ alloys, there is a systematic change in the low-temperature ($<700^\circ C$) ordered structure, beginning with a tetragonal DO_{22} structure for $x = 0$ through 20, and cubic $L1_2$ for $x = 40$ and above. For $x > 40$, the microstructure becomes complicated through the presence of an additional ordered phase, NiAl with a B_2 structure at low temperatures.

Oxidation behavior of the LRO alloys was determined by exposure of specimens in air at $800^\circ C$. The alloy with $x = 35$ showed severe spalling, while the alloy with $x = 60$ (LRO-64) had no spalling. The LRO-64 specimen exhibited a high weight gain (due to formation of protective oxide scale) initially, followed by a much slower rate of weight gain with exposure time. The total increase in weight due to oxidation is 1.1×10^{-4} g/cm² between 200 and 1000 h exposure. Thus, LRO-64 has good oxidation resistance.

Partial replacement of vanadium atoms with aluminum atoms in the $(Fe,Ni)_3V$ alloy system is found to increase strength but lower creep resistance. In addition, the NiAl phase which forms in the $(Fe,Ni)_3(V,Al)$ alloys weakens the long-range order in the fcc matrix. In order to minimize the NiAl phase and to improve creep resistance, a new series of LRO alloys was prepared with basic compositions of $(Fe,Ni)_3(V,Al,Fe)$ and with a small amount of hafnium and manganese added for further enhancement in metallurgical and mechanical properties. Hafnium at levels of 0.5 and 1.0 at. % was added for creep resistance and manganese for improvement of fabricability. Sixteen new alloys were prepared by arc melting and drop

casting. Among them, eight alloys were fabricated into sheet stock by repeated cold rolling with intermediate anneals at 1050°C. The other eight alloys cracked during cold fabrication. In these LRO alloys, iron atoms may occupy both nickel and aluminum sublattice sites, thereby increasing the iron solubility in the alloys.

Mechanical properties of these new LRO alloys containing about 10 at. % aluminum were determined by tensile testing at temperatures to 1000°C. Figure 10 is a plot of the yield strength of LRO-77 $[(\text{Ni}_{86.4}\text{Fe}_{13.3}\text{Mn}_{0.3})_3(\text{Al}_{40}\text{V}_{35}\text{Fe}_{20}\text{Hf}_4\text{Mn}_1) + 0.01 \text{ wt } \% \text{ B} + 0.04 \text{ wt } \% \text{ Ce}]$ as a function of test temperature. Boron was added to this alloy as a grain boundary strengthener, and cerium was added as a grain boundary

ORNL-DWG 83-16174

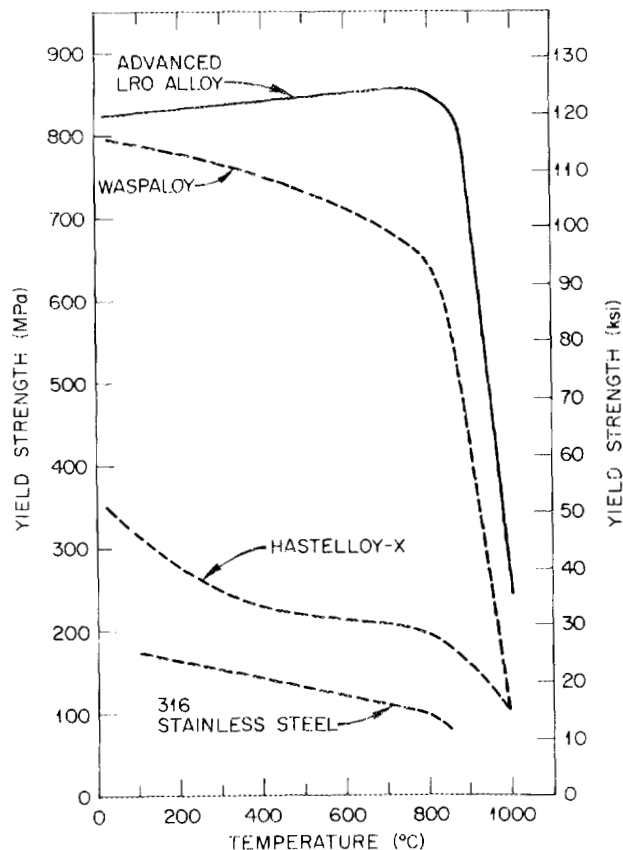


Fig. 10. Comparison of the yield strength of advanced LRO alloy with commercial solid-solution alloys type 316 stainless steel and Hastelloy X and particle-strengthened alloy Waspalloy.

scavenger of impurities. The yield strength of LRO-77 increases with temperature and reaches a maximum around 800°C. The LRO alloy is much stronger than commercial solid-solution alloys such as Hastelloy X and type 316 stainless steel and also is stronger than Waspaloy (a commercial gamma'-strengthened superalloy), particularly at higher temperatures. For instance at 1000°C, the strength of LRO-77 is 241 MPa (35,000 psi), which is more than double that of Hastelloy X and Waspaloy. The LRO-77 has a tensile ductility of 29% at room temperature. The ductility decreases with temperature and reaches a minimum of about 16% at about 900°C.

In the development of LRO alloys for advanced steam turbine applications, efforts have been concentrated on characterizations of fatigue and crack growth of (Fe,Ni)₃V alloys. High cycle fatigue (HCF) data were obtained for the niobium-modified LRO-37, designated as LRO-49 [(Fe₅₀Ni₅₀)₃(V₉₃Ti₄Nb₃)]. The testing under vacuum [6.7×10^{-2} mPa (5×10^{-6} torr)] at 600°C was carried out on samples of two grain sizes, 22 and 125 μm. Data in Fig. 11 clearly indicate the beneficial effects of fine grain on fatigue life. Comparison with earlier work on LRO-37 reveals that LRO-49 has superior HCF resistance at lower stress levels. Fatigue cracking is transgranular in all test samples of LRO-49.

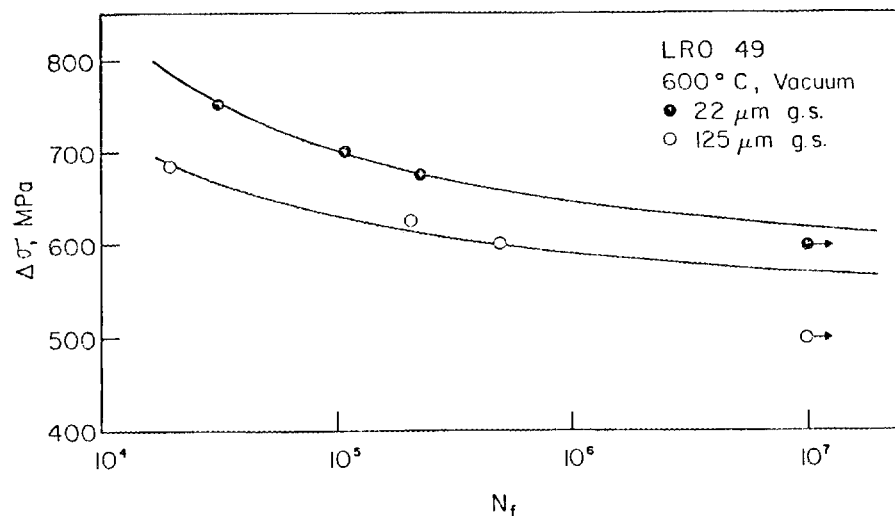


Fig. 11. High cycle fatigue data for LRO-49 at two grain sizes. Frequency = 20 Hz; σ_{\min} = 34.5 MPa. Source: N. S. Stoloff, Rensselaer Polytechnic Institute.

Low cycle fatigue testing was also carried out on LRO-49 in argon at a frequency of 0.33 Hz; results are shown in Fig. 12. Note that, based on total strain, LRO-49 falls within a scatter band of data for other alloys tested at Rensselaer under similar conditions. Based on plastic strain, it appears that LRO-49 at 600°C is superior to P/M (powder metallurgy) Rene 95 and Astroloy at 650°C, two high-strength gamma'-strengthened superalloys, except at low plastic strain levels. Retesting at low strain is planned to verify the data shown in Fig. 12.

Fractography performed on LRO-49 revealed intergranular surface cracks, but cracking shifted to a transgranular mode in the fatigue zone, with striations.

Crack growth behavior was also evaluated in LRO-60 and -42, both cerium-modified LRO-37 alloys. Figure 13 shows crack growth data for two

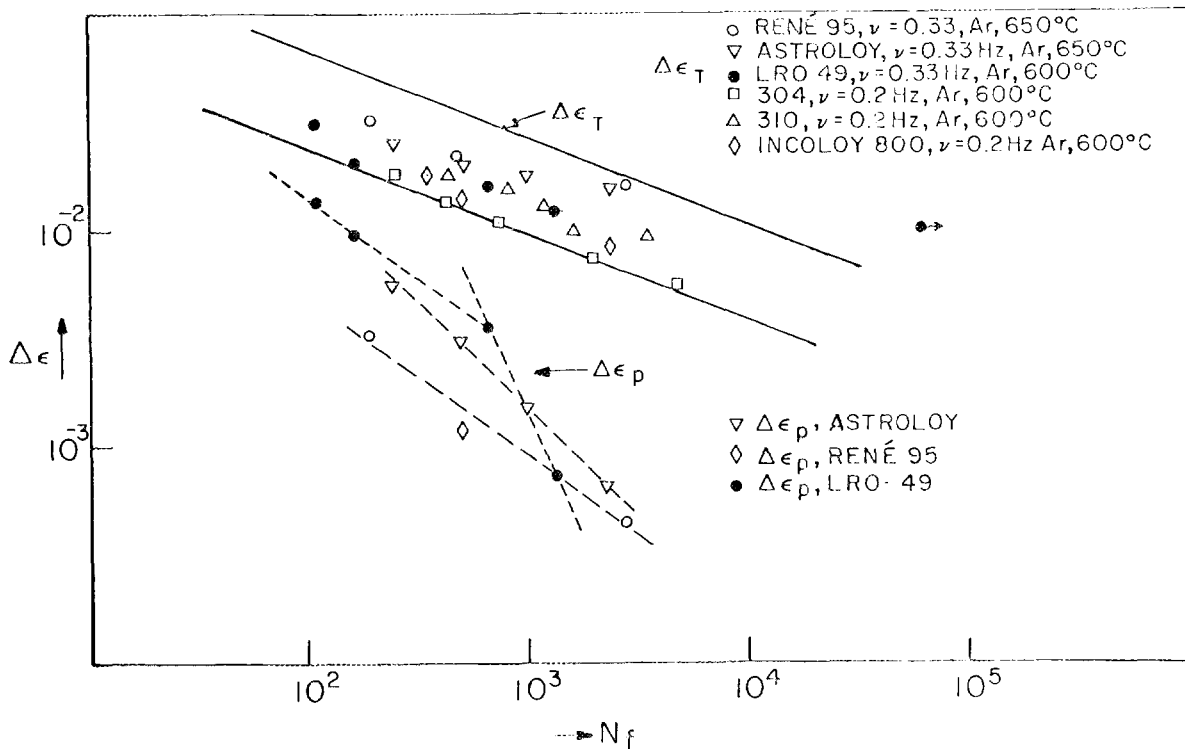


Fig. 12. Low cycle fatigue data for LRO-49 compared with data for other structural alloys, all tested at Rensselaer Polytechnic Institute. *Source:* N. S. Stoloff, Rensselaer Polytechnic Institute.

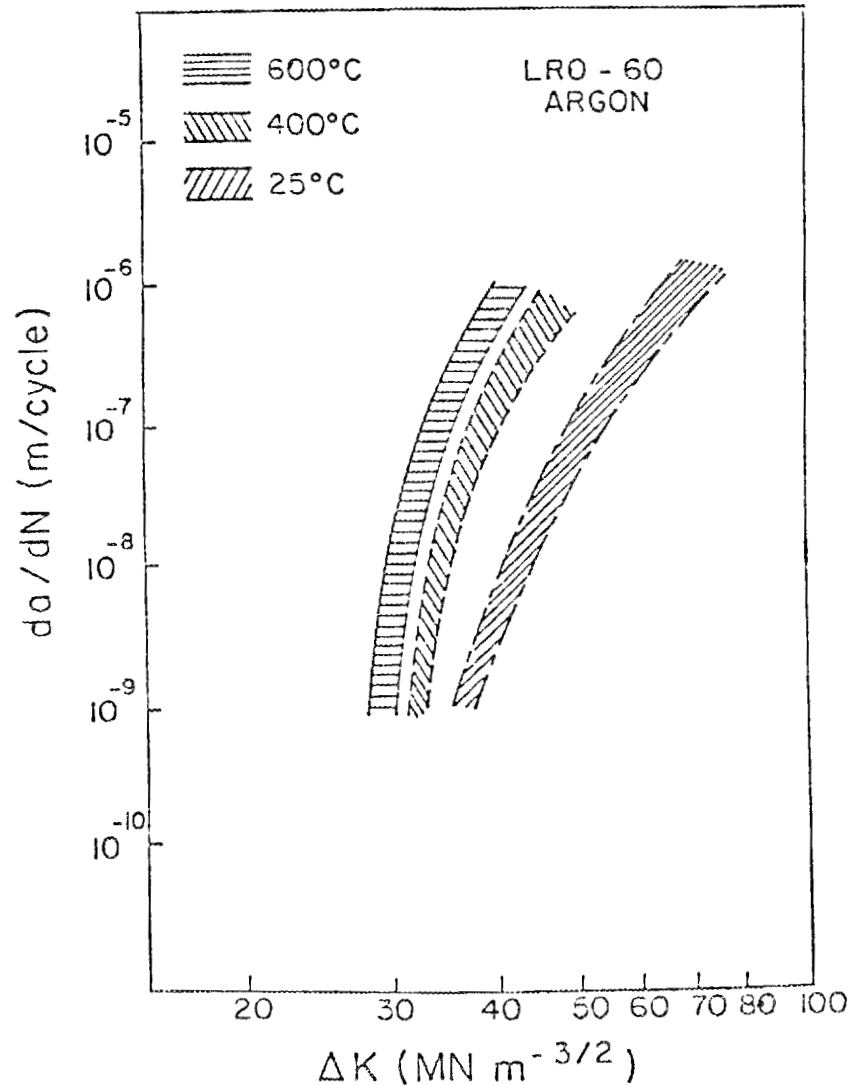


Fig. 13. Crack growth data for LRO-60. Each scatter band represents data for two samples, $\nu = 20$ Hz. Source: N. S. Stoloff, Rensselaer Polytechnic Institute.

specimens of LRO-60 at three temperatures - room temperature, 400°C, and 600°C - in an argon atmosphere. The data at 600°C compare very favorably at low stress intensity range, ΔK , with results from the literature and from Rensselaer on other high-temperature alloys (Fig. 14). It is important to note that the LRO alloys have distinctly higher threshold ΔK than commercial superalloys. Most of the alloys shown in Fig. 14 were tested in argon or vacuum, except for Udimet 718 and A-286, which were tested in air.

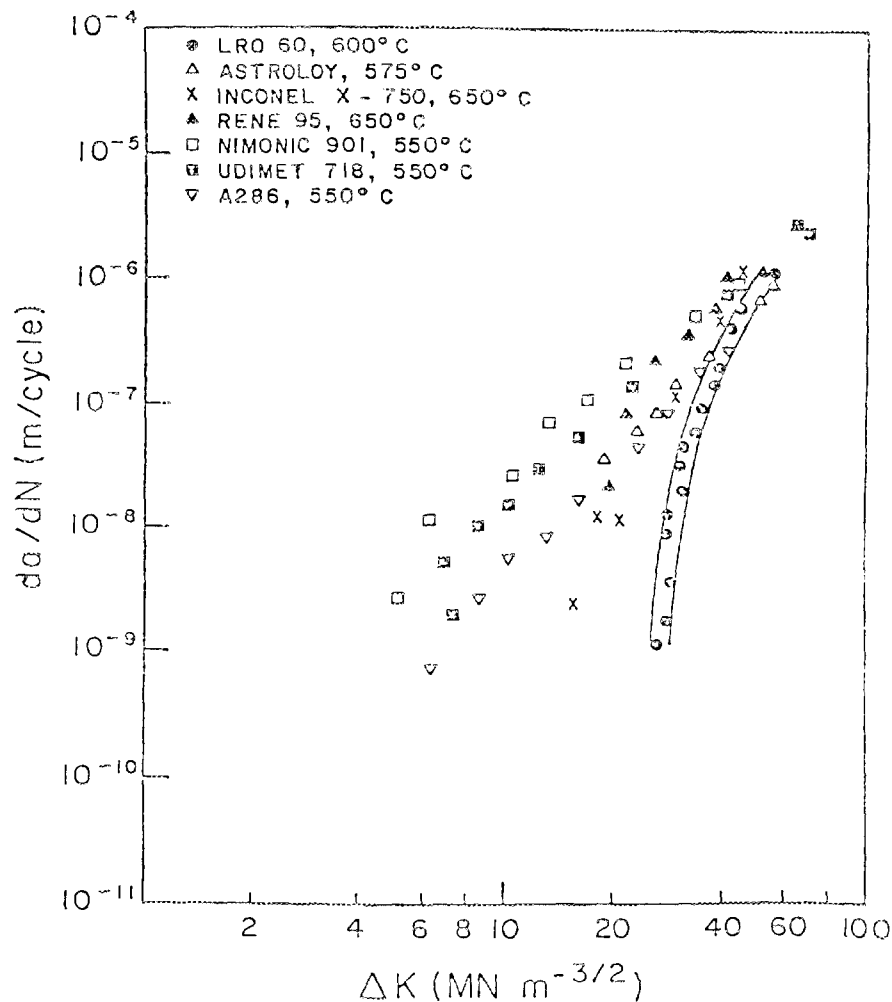


Fig. 14. Comparison of crack growth data for LRO-60 with that of other high-temperature alloys. Astroloy tested in argon, $R = 0.05$, $\nu = 10$ Hz; Inconel X-750 tested in vacuum, $R = 0.05$, $\nu = 10$ Hz. Rene 95 tested in argon, $R = 0.05$, $\nu = 20$ Hz. Nimonic 901, Udinet 718, and A-286 tested in air at $R = 0.1$, $\nu = 40$ Hz. Source: N. S. Stoloff, Rensselaer Polytechnic Institute.

Additional crack growth experiments using LRO-60 and LRO-42 were conducted with long-range order and test environment as experimental variables. Room-temperature tests on disordered LRO-60 in argon and in hydrogen gas at 0.101 MPa (1 atm) pressure showed no effect of hydrogen over the entire range of crack growth (Fig. 15). However, tests on ordered material revealed about a ten-fold increase in crack growth rate at all stress levels (Fig. 15), accompanied by a change from transgranular

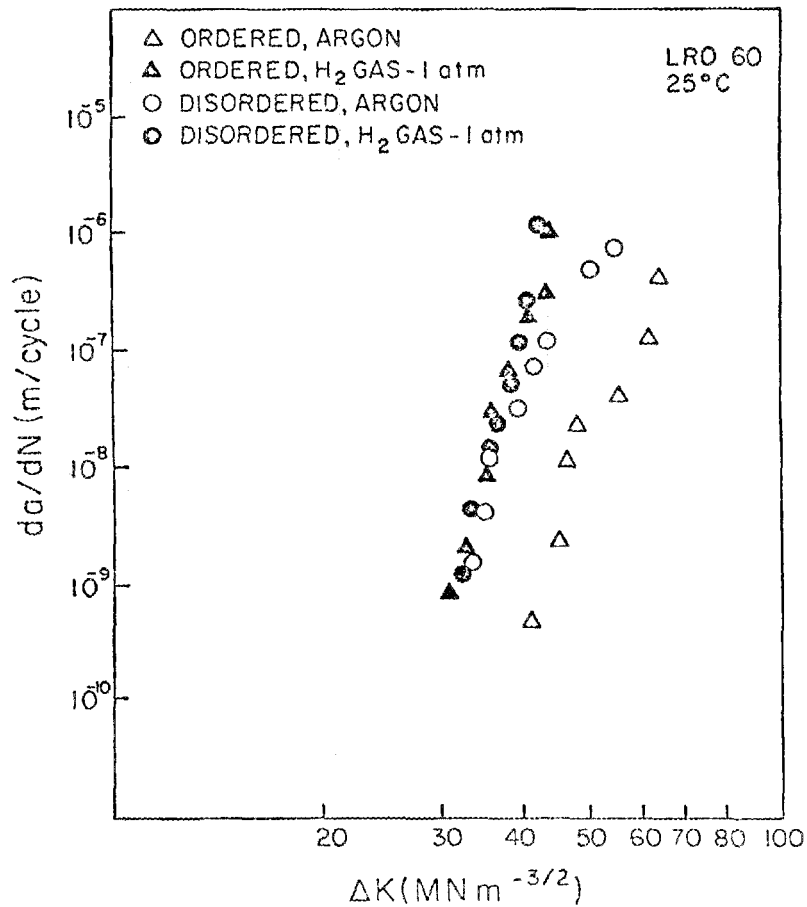


Fig. 15. Crack growth data for ordered and disordered LRO-60 in argon and hydrogen gas. *Source:* N. S. Stoloff, Rensselaer Polytechnic Institute.

to intergranular fracture (Fig. 16). Formation of long-range order slows crack growth in argon (Fig. 15). Figure 17 shows the effect of testing environments on crack growth in LRO-42. The result further indicates that testing in hydrogen gas is more detrimental than testing cathodically charged material.

Theoretical work on calculation of phase relationships has concentrated on the thermodynamics of ordered phases in multicomponent ordered systems based on Fe-Ni-Co-V. Values of the formation energies of compounds of vanadium, iron, cobalt, and nickel were received from the IBM Watson Research Laboratory, allowing progress to be made on the problem of translating such energies into compositional dependent compound models, solid solutions, and the liquid phases. Phase stability calculations were

ORNL PHOTO 1474-86

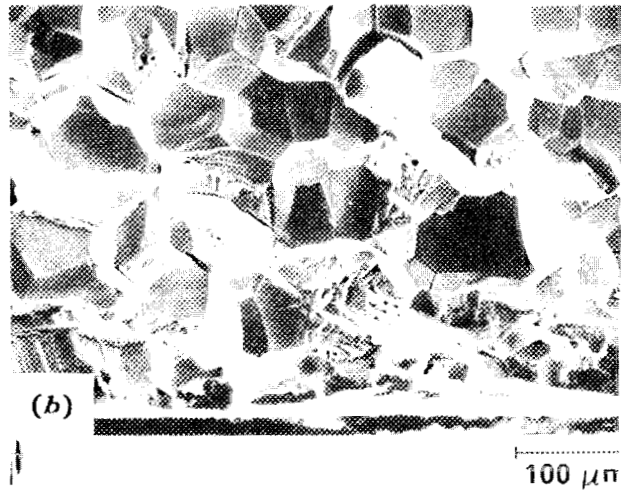


Fig. 16. Fractographs of LRO-60 fatigued in 1 atm hydrogen gas. (a) Disordered, transgranular. (b) Ordered, intergranular.

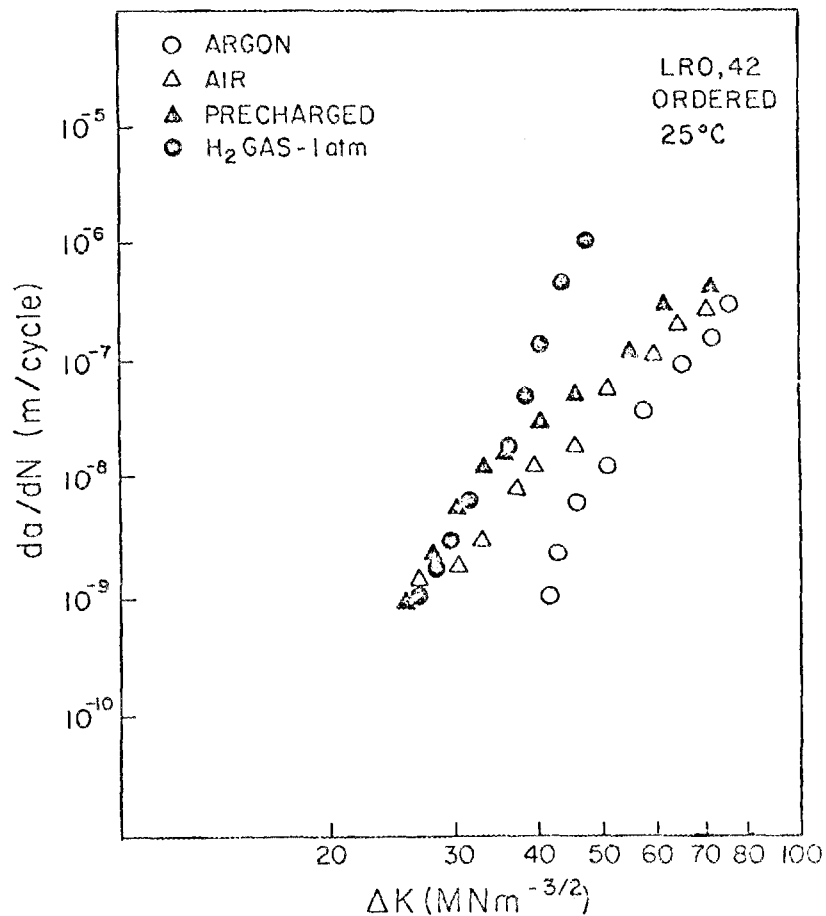


Fig. 17. Crack growth data for ordered LRO-42 in several environments. *Source:* N. S. Stoloff, Rensselaer Polytechnic Institute.

carried out at 1000°C on the Fe-Ni-Co-V system where the V content was restricted to 25 at. %. Figure 18 shows the equilibrium between the face centered and the body centered cubic structures. The tie lines shown fall approximately but not exactly in this cut. The calculations indicate that the size and shape of the two-phase field are only weakly temperature dependent at such elevated temperatures. The recent refinements of the solution model that includes the vibrational entropy contribution and the temperature dependence of the nonrandomness have not yet been incorporated into these calculations. Work is continuing in trying to develop models of ordered phases such that the calculations can be extended to include the equilibrium between the solid solutions and the ordered phases.

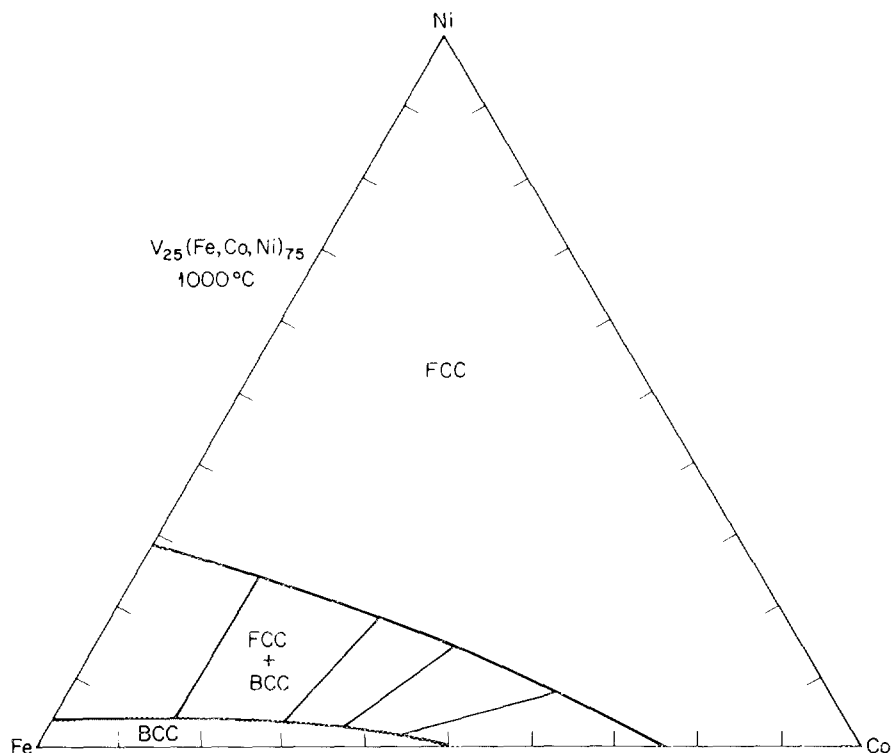


Fig. 18. Equilibrium between the face centered and body centered cubic structures formed in the $(\text{Fe,Co,Ni})_3\text{V}$ alloy system at 1000°C .

There has been considerable interest in the LRO alloys in industry. The Cabot Corporation has successfully prepared about 23 kg (50 lb) of LRO-37 and rolled it into 0.76-mm-thick (0.03-in.) sheets by using standard commercial processes commonly used for superalloys. The sheets have been tested at ORNL and appear to have as good tensile properties as material prepared in small quantities at ORNL. The work at Cabot has been sponsored by the DOE Fusion Program, while the ORNL characterization work has been sponsored by ECUT. The Bendix Corporation is testing specimens provided by ORNL of LRO-34 and -37 for potential use as high-speed brake material for military and commercial aircraft. This work is being supported by Bendix at about a one person-year level. Universal Cyclops is investigating the preparation of various LRO alloys via powder metallurgical techniques for a variety of undisclosed high-temperature applications. This work, too, is being supported by Universal Cyclops at about a two person-year effort.

WEAR TESTING OF DUCTILE LRO AND NICKEL ALUMINIDES - J. J. Wert
(Vanderbilt University)¹³⁻¹⁵

The purposes of this task are (1) to perform initial wear tests of the ductile long-range-ordered (LRO) alloys and nickel aluminides developed in the work described above and (2) to analyze the deformation-induced microstructures in order to elucidate the metallurgical parameters responsible for the observed wear behavior. Four types of tests are run: (1) an abrasive wear test in which the end of a 0.32-cm-diam (1/8-in.) pin of the selected alloy is worn by contact with a rotating disk covered with fine SiC grit, (2) an adhesive wear test in which the pin is run against a disk either of the same alloy or of a hardened steel, (3) a test in which wear marks are scratched into the surfaces of foils prepared for observations in the transmission electron microscope (TEM), and (4) an erosion test in which 0- to 50- μm particles of Al_2O_3 impinge upon the test specimen at about 65 m/s.

Abrasive wear tests have been completed for all materials under consideration. Each of the LRO and aluminide materials exhibited wear rates similar to those of 304L and 316 stainless steels. On the contrary, 52100 steel displayed a wear rate lower than that of all other materials by at least 30%. The superior wear resistance of 52100 under abrasive conditions has been attributed to the presence of chromium carbides.

Progress in the adhesive wear testing and TEM analysis has shown that the LRO and aluminide materials retain their structure throughout the wear process. Selected area diffraction patterns taken from wear tracks in these materials display typical spot type lattice reflections as opposed to a ring pattern which may be found after deformation in many other materials. The behavior of the LRO materials can be explained by the operation of only one slip system which is of the type $\{111\} \langle 110 \rangle$. Cross slip is strongly inhibited in the LRO and aluminide materials because of the low stacking fault energy and preferred ordered state. Therefore, it is suspected that a subcell structure which is the basis of the stacking fault correlation in wear theory does not form in these materials. Formulation of the wear mechanism operating in these materials is in progress.

DIFFUSION STUDIES OF DUCTILE LRO AND NICKEL ALUMINIDES - Y. T. Chou
(Lehigh University)^{16,17}

Research was initiated at Lehigh University to study diffusion in ductile $(\text{Ni,Fe})_3\text{V}$ and $(\text{Ni,Fe})_3(\text{V,Al})$ LRO alloys and in ductile Ni_3Al alloys. The major activities in this period were assembly of equipment and the preparation of diffusion samples. Studies will be made in both polycrystalline and bicrystal specimens. Analyses will be made via both electron microprobe analysis and radioactive tracer techniques.

MECHANICAL ALLOYING OF DUCTILE NICKEL ALUMINIDE ALLOYS - C. C. Koch
(North Carolina State University)

Work was initiated at North Carolina State University late in the period to determine the possibilities of further strengthening the ductile nickel aluminide alloys by mechanical alloying approaches. Small particles of a hard, second phase such as an oxide will be mechanically dispersed throughout the Ni_3Al microstructure by powder metallurgical means.

METALLIC BRAZING FILLER METALS FOR CERAMIC-CERAMIC AND CERAMIC-METAL JOINING - A. J. Moorhead (Oak Ridge National Laboratory)¹⁸⁻²⁴

The objective of this task is to develop brazing filler metals that will wet and bond directly to structural ceramics and metals for high-performance applications at elevated temperatures, at high stress levels, and in oxidizing environments. The task is necessary because joining is one of the key technologies that will enhance or restrict the use of ceramic materials in such applications. There are no commercially available brazing alloys that will meet these needs, and, in fact, most commercial brazing filler metals will not wet ceramics.

An arc melter was modified such that 1-g buttons of experimental filler metals could be flattened after the final melting cycle. This technique has greatly reduced the amount of effort needed to produce alloys in a form usable for the wetting studies.

Three series of experimental brazing filler metals were arc melted and subsequently evaluated for wetting and bonding behavior on alumina

substrates in the sessile drop apparatus. These alloys consisted of (1) a series based on Ni_3Al with varying additions of titanium, (2) Ni_3Al with hafnium replacing some of the aluminum, and (3) a similar group with zirconium substituted for some or all of the aluminum. The decision to study these compositions was based on the impressive success in developing a series of structural Ni_3Al alloys with good ductility and oxidation resistance (see the subsection titled "Ductile Ordered Intermetallic Alloys"). However, to date no composition has been found among these alloys that possesses both factors necessary in good brazing filler metal, namely, the capacities for both wetting and adherence or bonding. Good wetting by the sessile drops has been observed in half of the compositions (wetting angles of $40\text{--}60^\circ$) but little or no adherence. In some of these samples there was an interaction layer at the interface region on the alumina. These samples are being examined by X-ray diffraction and the SEM to try to understand why little or no bonding occurred.

Good adherence on alumina was achieved, however, with one alloy in the NiAl-Ti series, but the wetting angle in this case was 90 degrees, which is too high for a brazing filler metal. This composition is being modified to try to improve wetting behavior. Equipment is being set up to allow study of the wetting and bonding behavior of all these compositions in pure hydrogen.

Much effort was devoted to the making and testing of composite double-cantilever beam (DCB) specimens to measure the fracture toughnesses of some of the experimental brazing filler metals. It is believed that these fracture toughness measurements are the first of their kind anywhere. The results of this work are summarized in Table 3. The results on partially stabilized zirconia (PSZ) and alpha silicon carbide ($\alpha\text{-SiC}$), in which the fracture toughness of the braze joint exceeds that of the bulk ceramics, are encouraging. However, there is concern about a color change (from cream color to dark brown) that occurs in the PSZ in the vicinity of the braze alloy. It is hypothesized that the effect results from oxygen being pulled from the PSZ by the filler metal. Efforts have begun to determine what effect this substoichiometric condition has on the properties of the PSZ.

Table 3. Fracture toughness of ceramic-ceramic joints
joined with developmental filler brazing metals^a

Material(s)	K_{Ic} (MPa•m ^{1/2})	Failure
Bulk Al ₂ O ₃	6.7	
Al ₂ O ₃ TiCuBe/Al ₂ O ₃	4.2	Started and continued in braze material
Bulk Al ₂ O ₃ -Pt	7.0	
Al ₂ O ₃ -Pt/TiCuBe/Al ₂ O ₃ -Pt	4.7	Started and continued in braze material
Bulk PSZ	5.6	
PSZ/AgCuTi/PSZ	6.5	Started at braze/PSZ interface and went into PSZ
Bulk SiC	4.5	
SiC/NiCrTi/SiC	5.0	Started and continued in braze material

^aAll based on double-cantilever beam tests.

Other composite DCB specimens were brazed to measure the fracture toughness of brazements containing some of the experimental brazing filler metals. The samples of alumina brazed at 950°C with the alloy based on the Ag-Cu eutectic (with additions of Ni and Ti) in particular looked very good from a wetting standpoint (wetting angles near 0 degrees), but, unfortunately, they had relatively poor adherence. Selected samples from this series are being prepared for ceramographic analysis to try to ascertain the reason for the poor bond strength.

A number of samples were brazed in a partial pressure of hydrogen rather than in vacuum as in most previous work. This atmosphere was obtained in a vacuum furnace, which was evacuated to 1.33×10^{-2} mPa (10^{-6} mm Hg) and then brought to a low vacuum [1.33 Pa (100 μ m Hg)] by continuous addition of high-purity hydrogen. The samples consisted of hot-pressed alumina in contact with filler metals from a Ni-Al-Ti series and Carborundum's* sintered α -SiC brazed with compositions from a Ti-V-Cr series of alloys. The results in the alumina tests were not encouraging.

*The Carborundum Company, Niagara Falls, N.Y.

In no case did the drop adhere (even in a case where the wetting angle was significantly lower than in vacuum and in several of these compositions where adherence had been achieved in earlier tests in vacuum).

Polished cross sections of several brazed samples were examined with the electron microprobe. The samples consisted of Al_2O_3 , Nilsen* PSZ (MgO stabilized), and sintered α -SiC brazed with the experimental brazing filler metals. Preliminary evaluation of the results showed in each case that titanium tended to concentrate at the interfacial area, indicating that this element promoted wetting by lowering the interfacial energy between the ceramic and molten sessile drop. The titanium did not segregate to the surface of the braze filler, indicating that it does not influence wettability by lowering the surface tension of the alloy.

In order to try to determine the magnitude of the effect of active metal brazes on the fracture toughness of PSZ, DCB specimens were prepared (without a braze joint) in Nilsen PSZ material. The ungrooved surface of the specimens was coated with TiH_2 , which was then fired for 15 min at 1000°C simulating a brazing cycle. This technique apparently was at least partially successful in reducing the oxygen content of the PSZ because the material was darkened, although not as much as before when the composite DCB samples were prepared for measurement of the fracture toughness of the brazements. However, when the treated specimens were tested, K_{IC} values of 5.0 and 6.0 $\text{MPa}\cdot\text{m}^{1/2}$, which are the same as those measured earlier on the untreated PSZ, were found. These results are being analyzed to try to understand why the apparently significant loss in oxygen from the PSZ to the titanium coating (simulated braze alloy) did not affect the fracture toughness of this material.

Sessile-drop wettability studies were conducted on two new series of experimental brazing filler metals: (1) a series of Pd-base alloys with small additions of Ti, V, or Zr to promote wetting and bonding; and (2) a small group of $(\text{Ti-V-Cr})_3\text{Si}$ compositions with varying amounts of Ti, V, and Cr. Base materials in this study were hot pressed Al_2O_3 -2 wt % Cr and Carborundum's sintered α -SiC. The selection of Pd was made on the basis

*Nilsen (USA) Inc., Glendale Heights, Ill.

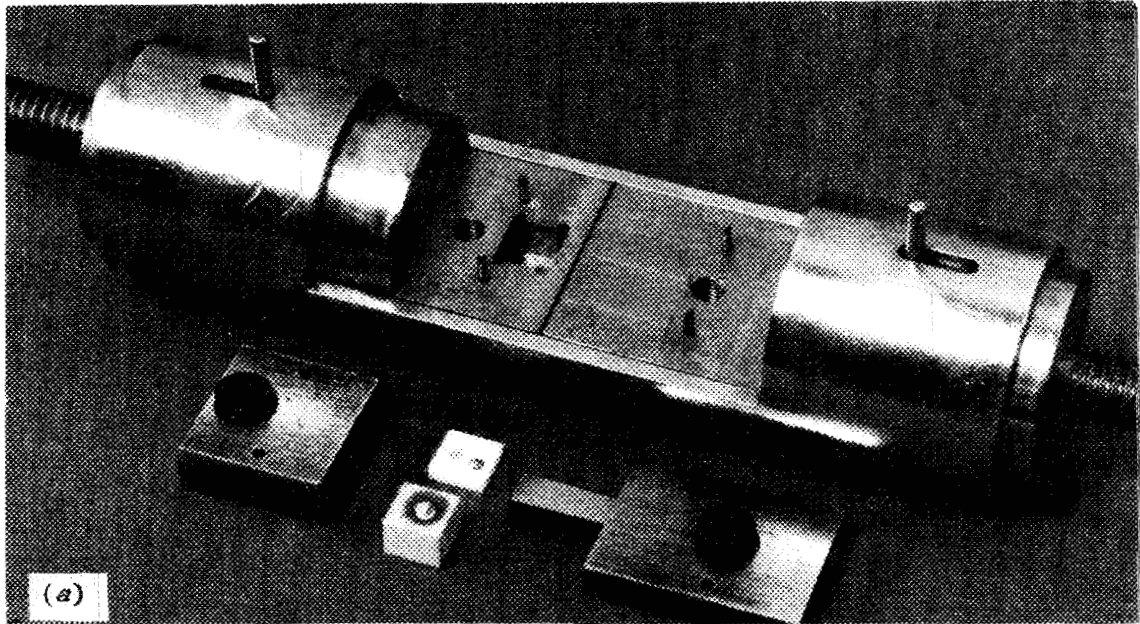
of oxidation resistance, ductility, and a somewhat lower coefficient of thermal expansion than some other major alloying components. The silicides were primarily considered for joining of the SiC where problems have arisen due to mismatch in coefficients of thermal expansion. Unfortunately, in these tests which were run in vacuum, none of the alloys wet satisfactorily, with wetting angles of about 90 degrees. These compositions will be evaluated further by heating in hydrogen to determine what effect that atmosphere has on the wetting behavior. In addition, Pd-base alloys will be made with active metal additions greater than the 1 wt % in this first series. Note that although the brazing temperature of these alloys ($\sim 1500^{\circ}\text{C}$) would be too high for direct brazing to metallic components in an advanced diesel engine, we are considering them because it may be feasible to braze a ceramic component to a metallic transition piece. This composite could in turn be brazed, for example, to ductile iron at a lower temperature.

Sessile-drop wettability studies were also conducted on alumina and α -SiC with three new series of alloys: Ti-Al, Pd-Cr, and Pt-Al. One or more alloys from each series wet and bonded to both substrates. In addition, the wetting angles were good, specifically, less than 90° in all cases and less than 60° in most samples. Some samples have been submitted for electron microprobe examination.

The apparent shear strengths of many of the sessile drops from these series were measured by the Sutton push-off test with the apparatus shown in Fig. 19. This has been a widely used test and, for the relatively low contact angles ($<90^{\circ}$) obtained in our experimental brazing filler metals, is considered to be a valid measure of shear strength. The results from these tests and some tests on PSZ are summarized in Table 4. A shortcoming of this test is that for low wetting angles, about 30° , the foot that pushes off the drop tends to ride up on the drop instead of pushing it off. In some cases, a portion of the drop is eventually sheared off, and the shear stress on the drop-substrate interface is then calculated. For some of our best-wetting filler metals, we will make samples for three- or four-point bend tests to measure bond strengths.

Table 4 also summarizes the results of the repeat of an earlier sessile-drop wettability test of MWF-50 (Ni_3Al) on an alumina substrate.

Y194143



Y194144

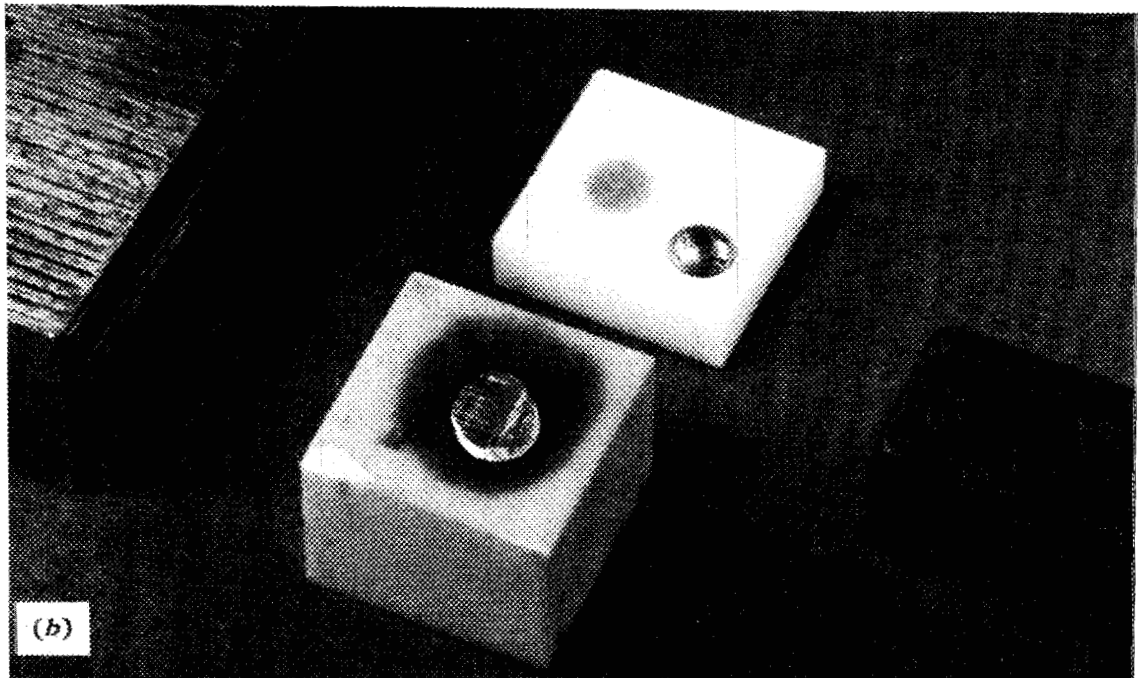


Fig. 19. Apparatus for Sutton push-off test of apparent shear strengths of bonds between sessile drops of developmental brazing metals and ceramic substrates. (a) Overview of apparatus. (b) Close-up of typical test specimens.

Table 4. Summary of contact angle and apparent shear strength of sessile drops on Coors^a AD-99 alumina and Nilsen PSZ (MgO stabilized)

Run	Filler metal		Contact angle, θ^b	Applied load (kg)	Shear strength ^c (MPa)	Brazing range (°C)
	Designation	Composition (at. %)				
Alumina substrate						
210	MWF-56	Cr-25Pd	50	6.4		1420-1700
251	MWF-57	Cr-39Pd	50	22.7	41	1320-1480
247	MWF-62	Pt-56Al		7.3	19	1470-1580
248	MWF-62	Pt-56Al	60	33.3	64	1470-1660
216	MWF-62	Pt-56Al	55	17.7	64	1470-1710
217	MWF-63	Pt-42Al	60	29.9	80	1470-1640
250	MWF-54	Ti-48Al-3V	40	21.3	31	1480-1500
256	MWF-50	Ni-25Al	90	5.9	24	1360-1580
252	MWF-65	Ni-25Al-0.05C	75	12.2	36	1360-1580
253	MWF-66	Ni-25Al-0.1C	70	19.5	44	1360-1580
257	MWF-66	Ni-25Al-0.1C	75	17.2	39	1360-1580
254	MWF-67	Ni-25Al-0.2C	75	23.1	111	1360-1580
222	MWF-7	Cu-20Au-18Ti	20	106.6	70 ^d	1020-1230
PSZ substrate						
237	MWF-2	Ag-34Cu-14Ti	15	50.0	52 ^d	880-1010
238	MWF-43	Ag-37Cu-0.8Ni-7.2Ti	25	12.3	33 ^d	840-1010

^aCoors Porcelain Company, Golden, Colo.

^bMeasured at room temperature.

^cSutton push-off test, room temperature.

^dPortion of drop sheared off, no failure at interface.

In the earlier test, in vacuum of approximately 6.7 mPa (5×10^{-6} mm Hg), there was no adherence, but, apparently as a result of better vacuum, a shear stress of 24 MPa was achieved in run 256. We also melted a series of 1- to 2-g buttons of MWF-50 with carbon additions aimed at improving wetting and bonding by reducing oxide films on the drops. Both the contact angles (θ) and the apparent shear strengths have been improved.

The sessile-drop apparatus was completely rebuilt to improve the system's vacuum capabilities and the balance between the inductances of the power supply and load. Significant improvements in both areas were successful, so that a vacuum of 0.67 mPa (5×10^{-5} mm Hg) is quickly achieved and the temperature capability of the system is now at least 1700°C. This one-decade improvement in vacuum seems to be significant because some sessile drops of compositions that had not adhered in earlier tests in vacuum of about 6.7 mPa (5×10^{-4} mm Hg) are now adhering.

As the result of a request by personnel of Cummins,* evaluation of the wetting behavior of some of the experimental brazing filler metals on PSZ made by NGK† has begun. This material is Y_2O_3 -stabilized as compared to the MgO-stabilized Nilsen material studied to date. Sessile-drop wetting tests show that this material is wet by both of the modified Ag-Cu-Ti filler metals (wetting angle $\theta = 20$ and 30° , respectively). In both cases there was some separation at the interface leaving a crater, with PSZ attached to the bottom of the drop, indicating that bonding had occurred.

A series of "sandwich" type coupons were brazed in which elemental metal foils (e.g., Cu and Ti or Cu and TiH) were used to form an in situ brazing filler metal. Brazing conditions were 5 min at 1000°C, but there is potential for lowering the temperature because there is a Ti-Cu eutectic at 880°C. A brazed sample of Nilsen MgO-stabilized PSZ looked promising and has been submitted for ceramographic examination.

WORKSHOP ON CERAMIC JOINING -- J. A. Carpenter, Jr. (Oak Ridge National Laboratory)

A workshop was held in late FY 1982 to establish research and development issues to be addressed by the ECUT Materials Project in the area of ceramic joining. A workshop report was drafted. Comments on the initial draft of the workshop report were received from the participants and a second draft prepared. The second draft was being reviewed in the ORNL approval chain.

*Cummins Engine Company, Columbus, Ind.

†NKG Spark Plug Company, Nagoya, Japan.

MODELING OF CERAMIC ATTACHMENTS - J. G. Hannoosh (Norton Company)

Initial approval of a sole-source contract to the Norton Company to develop finite-element models of certain typical ceramic joints was obtained during the final quarter of the year, and negotiations were in progress. In the initial phase of the work, solid joints between two beams of rectangular cross sections and two rods or disks of circular cross sections are to be modeled in order to be able to predict the stress states in and near the joints arising from differences in materials properties such as elastic moduli and coefficients of thermal expansion. Of particular interest are the effects at singularities such as corners and edges. The ultimate goal of the work is to provide guidance to designers as to what materials should and should not be joined in what geometries.

ASSESSMENT OF ELECTROMAGNETIC JOINING OF CERAMICS - R. S. Silberglitt (DHR, Inc.)

The objective of this effort is to assess the feasibility of joining ceramics to other ceramics or metals by using electromagnetic energy to heat the junction region. The research is concentrating on two key problems:

1. how to induce and control the electromagnetic heating of ceramic materials and
2. how to ensure that the joint formed will have the required properties, e.g., geometry, strength, corrosion resistance.

The first problem deals with electromagnetic heating equipment design and application and the second with ceramic materials science. These problems must be addressed in a coordinated fashion. Consequently, initial efforts concentrated on the materials aspects of ceramic joining in order to provide necessary input to the engineering design work.

Based upon a review of recent literature on ceramic joining, including the 1982 ECUT-sponsored workshop (see "Workshop on Ceramic Joining," above) and a 1982 National Materials Advisory Board (NMAB) joining study for the U.S. Department of Defense (DOD), attention was focused on the structural ceramics SiC, Si₃N₄, ZrO₂, and Al₂O₃ for applications such as high-performance heat exchangers, heat engines, and, perhaps eventually, fusion

reactors. The most important materials problems related to ceramic joining and how they might affect the design of the electromagnetic heating system, as derived from this literature review, are briefly described below.

1. Thermal expansion mismatch between the materials on different sides of the joint could induce cracking of the parts upon heating and/or cooling. This problem is very serious because an enormous temperature gradient will be created by the extreme localization of the electromagnetic energy in the joint region. Thus it will be essential to design an applicator system that can provide gradual and controlled heating and cooling.

2. Microstructural modifications due to phase changes or decomposition upon heating and/or cooling can significantly affect the dielectric loss tangent, $\tan \delta$, which determines electromagnetic absorption. This could destabilize the coupling of the electromagnetic energy applicator to the energy source or the ceramic load. The presence of phases with different loss tangents could also complicate the situation through the occurrence of runaway heating in the more lossy phases. For Si_3N_4 the decomposition reaction to silicon and nitrogen is a serious consideration because it could cause such severe property degradation that a perfectly joined part might turn out to be functionally useless. The sublimation of SiC is yet another potential problem. For these materials, it may prove necessary to incorporate a provision for joining in a controlled atmosphere. At present, cataloging is being done of all such microstructural changes which could affect the design or operation of an electromagnetic joining apparatus.

3. Bonding agents presently being used in ceramic joining could significantly influence the electromagnetic heating process. Metallic brazing compounds are unlikely to be useful in this application because metals are strong reflectors of electromagnetic radiation. Ceramic brazing compounds would be preferable (e.g., the oxynitrides used to join Si_3N_4), but as yet data on the high-temperature dielectric properties of such materials have not been obtained. These data will be required for prediction of electromagnetic absorption in the joint region.

In general, dielectric data for ceramics at temperatures approaching their melting points are scarce. This presents a problem because the

value of $\tan \delta$ for the materials under consideration is very small at room temperature (on the order of 10^{-4}). However, as the ceramic is heated, $\tan \delta$ and, hence, the electromagnetic absorption can increase by several orders of magnitude, as evidenced by the runaway heating phenomenon observed by others. At present, data for Al_2O_3 up to 1100°C are available, but room-temperature data only for the other materials. Searches are continuing for this data. Without it, extrapolation through a region of high nonlinearity in dielectric behavior will be necessary.

As a first step in determining the feasibility of this approach, power requirements have been estimated for ceramic joining, according to the calorimetric equation

$$P = \frac{60 m [C_p (\Delta T)]}{3413t},$$

where

- P = power required in kW,
- m = mass in g,
- C_p = heat capacity in cal/g $^\circ\text{C}$,
- t = heating time in min.

Table 5 displays the materials property data (derived from engineering handbooks and manufacturers' specifications) needed to estimate the power required to heat the desired materials to their melting point, assuming: 16.387 cm^3 (1 in.^3) of heating volume; initial temperature of 20°C (68°F); times of 1, 5, or 10 min required to reach melting points; and no losses and the availability of additional energy to accommodate phase changes, if any.

The results of this calculation are presented in Table 6. The power estimate figures shown in the table do not take into account any losses, i.e., they assume 100% microwave energy conversion efficiency. Losses in microwave conversion and in the cavity circuit would likely double or triple the power requirement so that for a 5-min heating time to the melting point, microwave power input of the order of 300 to 1000 W would be needed. Such power is well within the capability of conventional microwave generators.

Table 5. Materials properties data

Properties	Materials				
	PSZ	Al ₂ O ₃	SiC sintered	Si ₃ N ₄ hot pressed	Si ₃ N ₄ reaction bonded
Heat capacity, C_p (cal/g°C)	0.096	0.251	0.239	0.131	0.119
Density (g/cm ³)	5.75	3.80	3.10	3.30	2.50
Melting point (°C)	2600	2050	2500	1900	1900

Table 6. Power requirement estimate

Material	Power (W)		
	Time to achieve melting (min)		
	1	5	10
PSZ	1627	325	162
Al ₂ O ₃	2212	442	221
SiC sintered	1718	344	172
Si ₃ N ₄ hot pressed	929	186	93
Si ₃ N ₄ reaction bonded	639	127	64

Analysis of electromagnetic coupling options has begun by focusing on microwaves with frequencies in the gigahertz range, because they provide a combination of relatively good penetration and reasonable energy. However, it is intended ultimately to investigate the frequency dependence of this approach from perhaps 10^6 to 10^{11} Hz.

For microwaves, there are basically two types of application options, a lossless applicator (waveguide or cavity) and a lossy applicator, e.g., a leaky waveguide or a horn antenna. With the former approach it is much easier to concentrate the energy on the sample to be heated, whereas the

latter approach could be easier to use on complicated or large structures or in the field. To date, only lossless applicators have been analyzed.

In the waveguide approach, microwave energy is transmitted through a channel to the material to be joined. In order to ensure that sufficient energy is delivered to the joint, its impedance must be matched to that of the source. This can be accomplished by adding tuning stubs to the microwave channel and/or providing a movable back short. In this way, any load can be matched to the source. The difficulty of this approach is that, as noted above, $\tan \delta$ for ceramics varies strongly with temperature. Thus, as the material is heated, the channel will require constant retuning. In addition, this will make control of the temperature of the joint (e.g., through a feedback/servo mechanism, which is required to avoid thermal shock) very difficult to accomplish. For these reasons, the microwave cavity approach is believed to be a more promising alternative.

A microwave cavity is a resonant circuit that exchanges energy with the source. The advantage of using a cavity is that the energy returned to the source is dependent only upon the amount of energy absorbed by the cavity. Thus, no tuning is required, except for a back short, to excite a particular resonant mode (standing wave). The resonant modes of a microwave cavity are a function of the wavelength and the geometry of the cavity. The most desirable mode for our purpose for a rectangular cavity will probably be the H_{101} mode (transverse electric), which produces a peak field at the center of the cavity. This mode can be excited by adjusting the back short and measuring the field intensity within the cavity. A possible experimental setup using the cavity approach has been designed. In order to implement this concept we will require a highly sensitive detector to measure the temperature at the joint. Available options for this component are presently being reviewed.

In future work the cavity approach will be refined, its applicability to the materials and joining situations mentioned previously evaluated, and the lossy applicator approach investigated. The effectiveness of treating the joint region, either mechanically or with an external compound, will also be evaluated.

ASSESSMENTS OF SUPERALLOYS AND METAL FORMING -- R. S. Silberglitt
(DHR, Inc.)

Internal assessments to identify long-range energy conservation research and development needs and opportunities in the area of superalloys and metal forming were completed. The findings are summarized below. Copies of the full reports, not published, are available.

Superalloys

Because superalloys are relatively expensive materials and because, for many energy conservation applications, lesser materials (e.g., chromium- and molybdenum-alloyed stainless steels) can suffice, it was concluded that there are few superalloy energy conservation research opportunities. A further problem is that for higher-temperature applications (approaching 1000°C), ceramics appear to be more attractive than the superalloys. Within these limitations, however, some research opportunities worthy of ECUT consideration were identified. They include

1. high-temperature corrosion testing and data base development;
2. basic research on oxidation mechanisms (if the above testing indicates insufficient corrosion resistance);
3. investigation of high-temperature hydrogen permeation, adsorption, and embrittlement mechanisms; and
4. development of low-cost iron-base and aluminum-containing superalloys.

Metal Forming

In contrast to the superalloy case, it was concluded that there is ample room for energy conservation in metal forming. The most promising research areas consistent with the ECUT mission are

1. the tribology of metal forming,
2. computer modeling of metal-forming processes, and
3. near-net-shape isothermal forging and shape rolling.

LIGHTWEIGHT MATERIALS

RECOVERY AND REUSE OF PLASTIC SCRAP VIA BONDING AND SEPARATION -
COORDINATION - M. J. Curry, A. Spaak, and W. L. Hawkins (Plastics
Institute of America)²⁵⁻²⁷

The objective of these efforts is to provide the base technology needed to recycle or otherwise recover value from scrap plastics, particularly those in post-consumer wastes. Research continued on the recycling of automobile shredder residue through coordinated programs with the Universities of Lowell, Lehigh, and Texas at Austin, and the Polytechnic Institute of New York. Students have now been assigned to each of the four general research tasks discussed below. Table 7 shows the schools, faculty members, and students currently involved. Research results are discussed in subsequent sections.

Two students, David M. Busby and John S. Margosiak, are working with Professor Deanin at Lowell. These students are collaborating on the development of bonding agents and processing aids to improve the strength and flow properties of automobile shredder residue. Professor Pearce's student, P. K. Mukerji, has completed his thesis program on hydrogen-bonding additives. Dr. C. Do, a postdoctoral fellow, is preparing larger quantities of selected additives of this type; samples will be sent to Lowell for evaluation as bonding agents in automobile shredder residue. Concentration effects will be included in this study.

Professor Pearce at the Polytechnic Institute of New York has extended his research on synthetic bonding agents to include block copolymers as bonding agents in blends of styrene and ethylene oxide. Additional small amounts of the compatibilizing agents, which gave excellent results in improving the mechanical strength of shredder residue, are being synthesized in order to check the original results obtained at Professor Deanin's laboratory at the University of Lowell.

Professor Deanin at Lowell University has extended previous investigations of the melt flow characteristics of masticated fluff. He has also measured mechanical strength of samples of shredder residue modified with Professor Pearce's synthetic bonding agents.

William Crawford, under Professor Manson at Lehigh University, is continuing his studies of polymerization of selected monomers within shredder residue. Acrylic and furane-based monomers are under

Table 7. Current DOE/ECUT fellows

Task	School	Faculty member	Student	Degree candidate
Analytical and Separation Program	Stevens Institute of Technology	A. P. Plochocki	William Gripp	M.S.
Bonding Agents	University of Lowell	R. D. Deanin	D. M. Busby	M.S.
	Lehigh University	J. A. Manson	W. Crawford	M.S.
	Polytechnic Institute of New York	E. M. Pearce	K. Mukerji C. Do	Ph.D. Post-doctoral fellow
Processing Aids	University of Lowell	R. D. Deanin	J. S. Margosiak	M.S.

investigation. Compressive strength of the composites is being measured and fracture surfaces examined as a lead to improved compositions. Acrylic latexes are also being investigated as bonding agents for shredder residue.

Professors Paul and Barlow at the University of Texas at Austin have completed their investigation of adhesion and bulk properties for styrene-acrylonitrile (SAN) copolymers and polycarbonate (PC) blends.²⁸⁻³⁰ Using stress measurements, they have determined that the best adhesion of SAN to PC is obtained with the copolymer containing 25% of acrylonitrile. Polycaprolactam was studied as a compatibilizer for SAN-PC blends.

The Institute of Scrap Iron and Steel (ISIS) has provided initial support for developing a design concept for a pilot plant to clean, demetalize, grind, and modify (with bonding agents) several thousand kilograms of automobile shredder residue. A proposal on a "floating pilot plant" concept was submitted to the DOE Office of Industrial Programs and is undergoing review. Under the proposed work, about 4,536 kg (10,000 lb) of auto

shredder residue would be cleaned, demetallized, ground, modified (with bonding agents), and processed into usable items by using existing equipment at various machinery and converting plants across the country.

Dr. Peter Lantos, the Plastics Institute of America consultant on market outlets, has visited about a dozen processing companies exploring their interest in cost and possible specifications for clean shredder residue. Product lines produced by these companies and molding techniques used are being reviewed in searching for market outlets and existing, applicable fabricating processes. Flow molding may be a preferred technique for fabricating products from shredder residue. Dr. Lantos is concluding his phase of this market development effort.

PREPARATION AND TESTING OF LABORATORY SPECIMENS OF COMPATIBILIZER-BONDED AUTO SHREDDER RESIDUE -- R. D. Deanin (University of Lowell)³¹⁻³³

The "clean light fluff" fraction from scrap autos contains enough thermoplastic fraction so that it can be compression-molded into structural panels stronger than many current building materials. Melt flow is poor and color is mottled at best. Studies in the previous year¹ showed that masticating the fluff on a differential-speed two-roll mill could homogenize it to a good uniform black color and break down fibrous structures to permit improved melt flow, but flow was still inferior to that of commodity thermoplastics. Further, while 1980 clean light fluff milled and homogenized fairly well, "1990" material was much harder to handle, remaining coarse and inhomogeneous.

The "1990" clean light fluff was more finely ground to produce better homogeneity and processability. Milling was studied over a range of times from 2.5 to 20 min and temperatures from 140 to 222°C (285-432°F.) Most of this range produced fairly good flow and end-use properties, but overheating at 191 to 222°C (376-432°F) caused thermal degradation, poor flow, and poor appearance and end-use properties.

Standard process conditions were therefore chosen as follows:

"1990 clean light fluff," finely ground,
milling 7.5 min at 163°C (325°F),
molding 3.5 min at 160-170°C (320-338°F).

Because melt flow was lower than the norm for easy-processing commodity thermoplastics, a number of processing aids were added in concentrations of 5, 10, and 20% by weight. Results are summarized in Table 8. Five of the seven additives improved melt flow up into the range of general-purpose commodity thermoplastics. In the table, they are arranged in order from most to least effective in this respect.

Studies during the last quarter explored a wider range of additives to improve melt flow and end-use properties. The "1990" clean light fluff prepared by the Plastics Institute of America was used in most studies, although standard 1980 clean light fluff was used in a few cases. Results are reported in Table 9. The two most recent batches of residue are labeled F (received in February 1983) and M (received in May 1983). Additives were used in 5 to 20% concentrations, incorporated by milling 7.5 min at 163°C (325°F), and compression molded 3.5 min at 177°C (350°F). The molded sheets were cut into test bars and tested according to ASTM procedures. Melt flow was standard Condition E. The table begins with three clean light fluff controls and then lists a series of additives used individually. The latter part of the table describes the use of pairs of additives, beginning with Chemplex 5240 polyethylene and Rohm & Haas Acryloid K-175, which were particularly promising for improving melt flow in the previous year, and then adding second components to improve end-use properties as well.

Overall, Chemplex 5240 polyethylene and Rohm & Haas Acryloid K-175 remained most promising for improving melt flow, but Dow 61501.02 polyethylene was not far behind. Blendex 310 ABS raised flexural strength. Half of the additives raised tensile strength, and half of them raised impact strength. Best additives for impact strength were chlorinated polyethylene, ethylene/vinyl acetate, ethylene/propylene thermoplastic elastomers, ABS, and dicyclohexyl phthalate.

Even these tests are far from exhaustive, but they do illustrate the variety of additives which can be used in modest amounts to upgrade the processability and end-use properties of moldings made from clean light fluff.

Table 8. Properties of test plaques processed^a from "1990 clean light fluff"
auto shredder residue with various processing aids

Additive	Amount (Wt %)	Melt index condition (g/10 min)	Flexural modulus		Flexural strength		Tensile strength		Izod impact strength			
			(GPa)	(ksi)	(MPa)	(psi)	(MPa)	(psi)	Notched		Unnotched	
									(mJ•m)	(ft-lb in.)	(mJ•m)	(ft-lb in.)
None	0	0.19	0.77	112	5.94	861	2.82	409	24	0.7	31	0.9
Allied HDPE 540-A	5	1.2	0.80	116	6.14	890	2.63	381	24	0.7	24	0.7
	10	1.9	0.48	70	3.56	517	2.26	328	24	0.7	24	0.7
	20	15.6										
R&H Acryloid K-175	5	1.2	0.65	95	6.44	934	3.16	458	21	0.6	21	0.6
	10	2.2	0.57	83	6.53	947	2.79	403	21	0.6	21	0.6
	20	5.0	0.36	52	4.94	717	1.91	277	17	0.5	21	0.6
Chemplex HDPE MI 40	5	0.66	0.79	115	8.43	1223	3.16	458	21	0.6	24	0.7
	10	1.4	0.61	89	9.24	1340	3.59	520	21	0.6	21	0.6
	20	2.6	0.75	109	11.09	1609	3.40	493	21	0.6	28	0.8
Amoco PP MI 30	5	0.98	0.80	116	5.50	797	2.79	405	17	0.5	17	0.5
	10	1.6	1.01	147	7.63	1106	3.08	447	17	0.5	17	0.5
	20	2.0	0.54	78	7.94	1151	4.74	687	21	0.6	21	0.6
Amoco High-Flow PS	5	0.99	1.00	146	7.03	1020	3.13	454	21	0.6	21	0.6
	10	0.82	0.98	143	7.98	1158	2.92	424	17	0.5	21	0.6
	20	1.4	0.72	105	6.48	940	4.01	581	17	0.5	17	0.5
R&H Acryloid K-120-N	5	0.47	0.50	73	6.13	889	2.14	311	17	0.5	17	0.5
	10	0.34	0.96	139	5.70	826	2.32	336	17	0.5	17	0.5
	20		0.89	129	11.49	1667	4.10	595	17	0.5	21	0.6
R&H Exp. Prod. A	5	0.38	0.84	122	7.58	1099	3.36	527	21	0.6	24	0.7
	10		0.72	105	6.81	987	2.88	418	17	0.5	21	0.6
	20		0.66	96	7.05	1023	3.42	496	21	0.6	21	0.6

^aProcessing conditions: Fine ground, fluff milled with aid 75 min at 163°C (325°F), and molded 3.5 min at 160 to 170°C (320-338°F).

Table 9. Properties of test plaques processed^a from "1980 and 1990 clean light fluff"
auto shredder residue with various processing aids

Fluff	Additive	Amount (Wt %)	Melt index condition (g/10 min)	Flexural modulus		Flexural strength		Tensile strength		Izod impact strength			
				(GPa)	(ksi)	(MPa)	(psi)	(MPa)	(psi)	Notched		Unnotched	
										(mJ•m)	(ft-lb in.)	(mJ•m)	(ft-lb in.)
1980			0	0.45	66	3.17	460	0	0	24	0.7	24	0.7
1990(F) ^b			0.19	0.77	112	5.93	860	2.83	410	24	0.7	31	0.9
1990(M) ^b			0.32	1.36	197	10.20	1480	3.65	530	14	0.4	17	0.5
1990	Dow 2375.30 PE	5	0.18	0.95	138	10.14	1470	4.83	700	17	0.5	17	0.5
		10	0.26	0.83	121	10.62	1540	5.93	860	17	0.5	24	0.7
		20	0.31	0.47	69	7.31	1060	4.41	640	21	0.6	28	0.8
1990	Dow 5320.15 PE	5	0.46	1.21	176	10.48	1520	5.65	820	17	0.5	17	0.5
		10	0.44	1.06	154	8.76	1270	5.65	820	17	0.5	28	0.8
		20	1.31	0.98	143	10.76	1560	5.65	820	24	0.7	24	0.7
1990	Dow 61501.02 PE	5	0.52	0.87	127	9.17	1330	3.79	550	17	0.5	14	0.4
		20	0.50	1.13	164	10.89	1580	4.83	700	14	0.4	17	0.5
		30	1.82	1.00	145	10.27	1490	4.34	630	17	0.5	21	0.6
1990	Dow EAA-433	5	0.32	1.04	151	10.27	1490	4.90	710	21	0.6	21	0.6
		10	0.16	0.70	102	8.89	1290	5.17	750	17	0.5	21	0.6
		20	0.48	0.41	59	8.76	1270	5.65	820	28	0.8	28	0.8
1990	Dow CPE	10	0.07	0.21	31	6.90	1000			17	0.5		
		20	0.02	0.17	25	6.14	890			35	1.0		
1980	Dow CPE	10	0	0.33	48	4.62	670			31	0.9		
		20	0.03	0.13	19	3.52	510			45	1.3		
	Dow CPE + EVA	10	0.27	0.12	18	3.45	500			42	1.2		
1990	BW Blendex 310	5	0.11	1.10	160	8.27	1200	2.69	390	17	0.5	17	0.5
		10	0.06	1.35	196	10.41	1510	4.00	580	17	0.5	17	0.5
		20	0.02	1.33	194	13.51	1960	5.31	770	21	0.6	28	0.8

Table 9. (continued)

Fluff	Additive	Amount (Wt %)	Melt index condition (g/10 min)	Flexural modulus		Flexural strength		Tensile strength		Izod impact strength			
										Notched		Unnotched	
				(GPa)	(ksi)	(MPa)	(psi)	(MPa)	(psi)	(mJ•m)	(ft-lb in.)	(mJ•m)	(ft-lb in.)
1990	BW Blendex 336	5	0.07	1.05	153	8.96	1300	4.28	620	17	0.5	17	0.5
		10	0.04	1.00	145	10.62	1540	5.03	730	17	0.5	24	0.7
		20	0	0.72	104	8.69	1260	4.62	670	31	0.9	35	1.0
1990	UCC PCL-300	5	0.20	0.64	93	6.21	900	3.03	440	21	0.6	17	0.5
		10	0.20	0.68	99	7.03	1020	3.17	460	17	0.5	24	0.7
		20	2.04	0.59	86	6.14	890			21	0.6	24	0.7
1990	UCC PCL-700	5	0.45	0.63	92	7.10	1030	3.38	490	35	1.0	21	0.6
		10	0.36	0.74	107	7.79	1130	3.93	570	21	0.6	21	0.6
		20	0.59	0.70	102	8.89	1290	4.48	650	24	0.7	24	0.7
1990	Triphenyl Phosphate	5	0.12	0.65	94	7.65	1110	3.79	550	21	0.6	21	0.6
		10	0.19	0.25	36	5.17	750	2.55	370	24	0.7	28	0.8
		20	0	0.13	19	3.17	460	1.86	270	21	0.6	28	0.8
1990	Dicyclohexyl Phthalate	5	0.17	0.64	93	7.31	1060	3.31	480	21	0.6	21	0.6
		10	0.17	0.29	42	4.48	650	2.62	380	21	0.6	24	0.7
		20	0	0.11	16	3.17	460	1.93	280	38	1.1	38	1.1
1990	Chemplex 5240 PE	20	2.6	0.75	109	11.10	1610	3.38	490	21	0.6	28	0.8
	R&H Acryloid K-175	10	2.2	0.57	83	6.55	950	2.76	400	21	0.6	21	0.6
1990	Chemplex + 5 Uniroyal TPR-1600	20	1.76	0.65	94	7.10	1030	2.48	360	24	0.7	21	0.6
	Chemplex + 10 Uniroyal TPR-1600		2.28	0.61	89	7.31	1060	3.10	450	31	0.9	38	1.1

Table 9. (continued)

Fluff	Additive	Amount (Wt %)	Melt index condition (g/10 min)	Flexural modulus		Flexural strength		Tensile strength		Izod impact strength			
				(GPa)	(ksi)	(MPa)	(psi)	(MPa)	(psi)	Notched		Unnotched	
										(mJ•m)	(ft-lb in.)	(mJ•m)	(ft-lb in.)
1990	Chemplex + 5 Uniroyal TPR-1900	20	2.26	0.74	107	7.93	1150	2.90	420	21	0.6	24	0.7
	Chemplex + 10 Uniroyal TPR-1900	20	1.67	0.63	92	7.86	1140	3.59	520	24	0.7	31	0.9
	Chemplex + 20 Uniroyal TPR-1900	20	1.50	0.52	75	7.03	1020	3.79	550	42	1.2	55	1.6
1990	R&H + 10 Uniroyal TPR-1900	10	0.53	0.37	54	3.86	560	0.89	129	21	0.6	28	0.8
	R&H + 20 Uniroyal TPR-1900	10	1.50	0.29	42	4.34	630	2.00	290	28	0.8	38	1.1
1990	Chemplex + 5 BW Blendex 310	20	1.98	1.06	154	10.83	1570	3.72	540	17	0.5	21	0.6
	Chemplex + 10 BW Blendex 310		2.15	0.98	143	11.45	1660	3.93	570	17	0.5	24	0.7
	Chemplex + 20 BW Blendex 310		1.03	0.86	125	10.55	1530	4.27	620	14	0.4	17	0.5
1990	R&H + 5 BW Blendex 310	10	1.46	0.61	88	5.58	810	2.28	330	17	0.5	17	0.5
	R&H + 10 BW Blendex 310		1.11	0.60	87	5.24	760	1.72	250	14	0.4	17	0.5
	R&H + 20 BW Blendex 310		0.78	0.77	112	9.24	1340	4.13	600	14	0.4	21	0.6

Table 9. (continued)

Fluff	Additive	Amount (Wt %)	Melt index condition (g/10 min)	Flexural modulus		Flexural strength		Tensile strength		Izod impact strength			
				(GPa)	(ksi)	(MPa)	(psi)	(MPa)	(psi)	Notched		Unnotched	
										(mJ•m)	(ft-lb in.)	(mJ•m)	(ft-lb in.)
1990	Chemplex + 5 BW Blendex 336	20	1.39	0.74	107	9.45	1370	4.21	610	17	0.5	24	0.7
	Chemplex + 10 BW Blendex 336		1.54	0.74	107	10.62	1540	4.69	680	21	0.6	31	0.9
	Chemplex + 20 BW Blendex 336		0.50	0.50	73	9.65	1400	4.00	580	21	0.6	31	0.9
1990	R&H + 5 BW Blendex 336	10	1.04	0.64	93	6.48	940	2.00	290	17	0.5	17	0.5
	R&H + 10 BW Blendex 336		0.23	0.58	84	7.17	1040	2.28	330	17	0.5	21	0.6
	R&H + 20 BW Blendex 336		0	0.43	62	7.24	1050	2.83	410	17	0.5	24	0.7
1990	Chemplex + 5 Wood Flour	20	1.23	0.91	132	9.17	1330	2.90	420	17	0.5	21	0.6
	Chemplex + 10 Wood Flour		1.58	1.14	166	11.65	1690	5.17	750	17	0.5	21	0.6
	Chemplex + 20 Wood Flour		0.85	1.01	147	9.31	1350	4.62	670	17	0.5	21	0.6

^aMilled 7.5 min at 325°F, compression molded 3.5 min at 330°F, and cut into test bars.

^b_F = received in February 1983, M = received in May 1983.

DEVELOPMENT OF HYDROGEN-BONDING COMPATIBILIZERS FOR AUTO SHREDDER
RESIDUE - E. M. Pearce (Polytechnic Institute of New York)^{3,4}

The compatibility between polymers in a binary or ternary system is a function of several factors, especially intermolecular interaction, molecular weight, and molecular weight distribution. In previous work it was shown that polystyrene modified with trifluorocarbon-1-ol and hexafluoropropan-2-ol exhibited strong hydrogen bonding character and was compatible with polyethylene oxide whenever the binary system was rich in modified polystyrene content. In fact, the 10% hexafluoropropan-2-ol modified polystyrene was compatible with a large number of polymers (e.g., polyacrylates, polyesters, polycarbonates, etc.).

Attempts were made this year to use this knowledge to develop a suitable compatibilizer based on modified block copolymer of styrene and ethylene oxide to study the influence of molecular weight, mole ratio of each component, and degree of modification. Poly(ethylene oxide-styrene-ethylene oxides) with molecular weight approximately 60,000 and molecular-weight distribution 1.3 were synthesized by using α -methyl styrene/potassium initiator with mole ratio of styrene to ethylene oxide of 1:3, 1:1, and 3:1 and modified somewhat with trifluorocarbon-1-ol by Friedel Craft acylation using trifluoroacetic anhydride followed by reduction with sodium borohydride. These modified block copolymers exhibited different solubility patterns and developed frothing character even at less than 5% modification. Their blending characteristics were studied. Preliminary experiments gave promising results such as a sharp decrease in crystallinity, a lowering of melting point of polyethylene oxide, and a single glass transition temperature (T_g) in between the T_g 's of the individual components. However, this latter aspect will be pursued further to reconfirm that there is no overlapping of transition temperatures.

Block copolymers of the type poly(styrene-ethylene oxide) with molecular weight ranges of 100,000 and 150,000 and molecular weight distribution of 1.1 with mole ratios of styrene to ethylene oxide of 3:1 and 1:1, respectively, have also been prepared. Whenever α -methyl styrene/potassium was used as initiator, the molecular weight could be controlled within 20% of the desired value. However, it was difficult to control the molecular weight when using cumyl potassium initiator even when cumyl potassium was freshly prepared just before polymerization.

The concept was extended to block copolymers because the chemical bond between the two segmental blocks gives the necessary restriction of possible arrangements, thereby decreasing the entropy. This loss of entropy increased the critical molecular weight of the blocks for micro-phase separation. The polystyrene block modified with hydroxyl groups should further improve the compatibility between the blocks and also with other polymers in binary and ternary systems.

Therefore the block copolymers poly(styrene- β -ethylene oxide) (AB type) and poly(ethylene oxide-styrene-ethylene oxide) (BAB type) were synthesized by anionic polymerization of different molecular weight and mole ratio of styrene to ethylene oxide. These block copolymers were modified by trifluoromethyl carbinol (~8 and ~16%). Analytical techniques were also developed for the characterization of these modified block copolymers.

The binary blends of block copolymers with polystyrene showed marked improvement in the compositional range for compatibility. The suppression of total crystallinity was up to 90%, and the melting point depression was significant. Mostly AB-type block copolymers consistently gave a larger suppressed crystallinity than those of BAB-type. A single T_g was observed for the amorphous phase. The shift in T_g for polystyrene was approximately 25°C and was most significant for BAB-type block copolymers. Dynamic mechanical analysis studies are being done to confirm our observations regarding the single T_g.

The binary mixture with poly(ethylene oxide) gave mixed results. The compositional range was wider with respect to suppression of crystallinity and shift in melting point. However, the blends rich (~76%) in polyethylene oxide did give 20 to 30% suppression of crystallinity.

The film-forming property of the modified block polymer with polystyrene and polyethylene oxide was better and in general gave clearer films.

On comparing different block copolymers with regard to the ability to compatibilize, it was found that the AB-type polymer gave better results as compared with the BAB type. It was also observed that the mole ratio of 1:1 for BAB block copolymer showed improved compatibility.

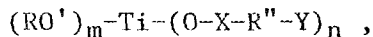
IN SITU POLYMERIZATION FOR BONDING AUTO SHREDDER RESIDUE - J. A. Manson
(Lehigh University)^{3,5}

Research is continuing with acrylic and furfuryl alcohol-based (Furathane-FA) resin composites; exploratory experiments were also made with several epoxy (thermoset) systems. The aim of the work with the acrylics was to investigate ways of increasing the interfacial bonding between the aggregate and matrix. Work is continuing with the FA resins to investigate the relationship between composition, reaction conditions, and mechanical properties. Also, several commercial epoxy systems were tried with cryogenically ground aggregate.

Acrylic Binders

In the recycling of automobile scrap, the scrap was initially viewed as a non-energy-intensive filler in a polymeric composite. In general, however, fillers usually supply little or no reinforcement unless there is good interfacial interaction between the resin and filler surfaces. In previous work,¹ acrylic matrix systems were developed which gave a corresponding decrease in mechanical properties with increasing filler content. This indicates rather poor interfacial adhesion. The use of the aggregate as a filler would be mechanically more favorable if coupling agents could be used to improve the interfacial bond between the filler and the polymer matrix. Besides increasing the level of mechanical properties, a coupling agent may reduce the melt viscosity of the composite system and thus aid considerably in the use of injection molding techniques.

Titanate coupling agents KR7, KRTTS, and K39DS were received from Kenrich Petrochemicals, Inc. These agents were recommended for use because methyl methacrylate has a poor affinity for polypropylene, which makes up more than 40% by weight of both the 1980 and 1990 aggregates. The titanate coupling agent may be represented as



where the (RO') group reacts with protons on the filler surface and the remainder of the molecule can then interact with the polymer to provide coupling.

The titanates were added to the monomer at 1/4% of the monomer weight, they were mixed well on a magnetic stirring plate, and polymerizations were effected as usual. The results are presented in Table 10.

Table 10. Properties of acrylic matrix of composites using auto shredder residue with various coupling agents

	Compressive strength (MPa)		Compressive strength/weight ratio		Modulus (MPa)		Density (g/cm ³)	
	MMA ^a	MMI ^b	MMA	MMI	MMA	MMI	MMA	MMI
Bulk aggregate	22.6	28.4	1.323	1.622	43.8	37.7	0.983	1.046
+ KR7	18.1	21.2	1.098	1.187	37.8	34.4	0.950	1.053
+ KRTTS	18.3	23.4	1.144	1.299	33.6	40.9	0.928	1.048
+ K39DS	19.1	22.1	1.198	1.235	26.3	34.9	0.940	1.054
+ Acrylic acid	<i>c</i>	9.5	<i>c</i>	0.611	<i>c</i>	17.3	<i>c</i>	0.892
Ground	17.9	12.9	0.943	0.718	35.3	13.3	1.081	1.070

^aMMA = poly(methyl methacrylate).

^bMMI = monomer mixtures containing 5% each of poly(methyl methacrylate) and trimethylolpropane trimethacrylate.

^cSamples did not polymerize.

The KRTTS gave a modulus for the MMI (see footnote *b* in Table 10) system at least equal to that of the control (bulk), using plain aggregate, and the smallest decrease in compressive strength. However, optimum conditions for improvement in strength have not yet been found.

Samples were then prepared by changing the reaction conditions while retaining the same percentage of titanate coupling agent as before. The syntheses were carried out in a 0.5-L reaction vessel purged with gaseous nitrogen and equipped with a mechanical stirrer. Methyl methacrylate (1/4% titanate coupling agent by weight monomer) was added to the aggregate (already in the vessel) and the temperature controlled to 55°C with constant stirring. This step in the synthesis should allow the titanate coupling agent time to act on the aggregate and increase the interfacial interaction. Once the temperature was constant, the initiator (2% benzoyl peroxide or 0.5% azobisisobutyronitrile, both based on monomer weight) was added to the system, and the reaction was allowed to continue for approximately 30 min in a 55 to 65°C temperature range. These mixtures were then poured into 25- by 95-mm cylindrical molds, and they were aired overnight in a 70°C water bath (to control the exotherm) and then at 80°C for another 24 h. Mechanical data on these systems are being obtained.

Along with treating the aggregate with coupling agents, cryogenic grinding and pH treatment have been attempted. Grinding the aggregate

might be expected to produce some active sites on the polyolefin surfaces (which probably constitute the major component) for adhesion of the polymer matrix. The aggregates were ground on a hand mill after using liquid nitrogen to embrittle the plastic scrap before grinding. This allows the scrap to be reduced to a much finer size with more efficiency. A broad size distribution was found for both 1980 and 1990 aggregates. Compressive tests were completed on the 1980 aggregate in the acrylic systems as shown in Table 10. Results show a drop in the compressive strength, strength-to-weight ratio, and modulus for both acrylic systems with an increase in the bulk density for both. The more dramatic effects due to the ground aggregate came from the acrylic system (MMI) consisting of methyl methacrylate with 5% poly(methyl methacrylate) (PMMA) and 5% trimethylolpropane trimethacrylate (TMPTMA).

Acid-base interaction between the polymer matrix and the aggregate should also enhance both the adhesion and the mechanical properties of the composite. Since the aggregate being used is very heterogeneous in composition, it would be very beneficial if the aggregate could be treated to give a more homogeneous type of surface.

The aggregate was soaked in acrylic acid, and then the acid was evaporated from the surface. It was intended that this treatment would result in good adhesion to the polymer and low agglomeration between particles for better distribution throughout the polymer matrix. As shown in Table 10, it resulted in brittle composites with significantly lower compressive strengths in moduli. Also, for unknown reasons, the polymerization of pure polymethyl methacrylate (MMA) was inhibited.

Furfuryl Alcohol-Based Resin Binder (FA)

Research on the synthesis of samples from furfuryl-alcohol-based resins is continuing in order to determine how the mechanical properties behave as a function of composition and reaction conditions.

Samples containing an aggregate/FA resin ratio of one, 20% $ZnCl_2$ (catalyst-based on FA resin weight) and 2% trichlorotoluene (TCT, initiator-based on FA resin weight), were compression-molded for 15 min in a temperature range from 80 to 150°C. Sheets suitable for machining samples for tensile, flexural, and Izod impact testing were completed.

After testing, parameters such as time of compression molding, pressure, and ZnCl_2 and TCT concentrations will be varied to find the optimum mechanical properties.

The ZnCl_2 catalyst must be added to the mixture to reduce the pH and allow polymerization to proceed. It is recommended not to dissolve it in water because higher water contents in FA resins have been reported to adversely affect the mechanical properties. If ZnCl_2 is added directly to the FA resin, agglomeration results without reaction. Addition of molten ZnCl_2 to the FA monomer results in violent reactions.

It was therefore decided to treat the aggregate with ZnCl_2 by first dissolving it in water. The water was then removed by drying to constant weight. The aggregate's appearance changed dramatically from that of a light fluffy material to a harder, more dense solid. This agglomeration of scrap was periodically broken down during the drying period.

Samples of this type aggregate have been cast by using aggregate treated with 60% ZnCl_2 (based on weight of FA resin) and 3% trichlorotoluene (TCT) initiator (based on weight of FA resin) with an aggregate/resin ratio of one. The samples show a low-gloss black finish with a density of approximately 1.5 g/cm^3 .

In addition, it was found possible to blend the ZnCl_2 with the aggregate before polymerization. To avoid a too fast reaction, the concentration of ZnCl_2 was reduced to 20% (based on the weight of FA resin); 2% TCT initiator was used with the same aggregate/FA resin ratio. This allowed a longer working time. Samples were then compression-molded for 6 min with 3629 kg (8000 lb) load at temperatures ranging from 93.5 to 121°C (200 to 250°F). These samples showed a glossy dark finish with a density of approximately 1.15 g/cm^3 and a shrinkage of approximately 4%.

Epoxy Resins (Thermosets)

Two epoxy systems (which work well with cryogenically ground aggregate) have been obtained from Atlas Minerals & Chemicals, Inc. Samples of both resin systems were prepared by warming the resin to approximately 30°C (while stirring mechanically), adding the hardener, and mixing in the aggregate (40% by weight mixture). Final cure was obtained in a 35°C oven for approximately 48 h to ensure complete polymerization. The viscosities of each system were surprisingly low, making it easy to prepare

good-looking samples in both cylindrical and bar shapes. Although mechanical data have not yet been obtained, it is obvious by inspection that each epoxy system produces specimens that are mechanically different; Epoxy A produces rather stiff (brittle) composites while the other, Epoxy B, produces rubbery (ductile) composites. Epoxy B would not be used for a building material, but other applications such as laminates would be possible. The addition of the cryogenically ground scrap and the scrap in the bulk state will be investigated further.

General

Future plans are

1. to continue to explore ways of increasing the interfacial bond between the aggregate and the acrylic matrix through coupling agents and acid-base interactions,
2. to cast samples with consolidated aggregate received from Lowell University,
3. to explore the use of ground thermoset resins as aggregates to model the trend toward the increased use of such materials in automobiles,
4. to explore the high chemical reactivity of the furan resin as an opportunity for high production rates at low temperatures, and
5. to continue to define the mechanical properties as a function of composition and reaction conditions.

SEPARATION AND ANALYSIS OF AUTO SHREDDER RESIDUE - A. P. Plochocki
(Stevens Institute of Technology)³⁶⁻⁴⁰

In close cooperation with the Plastics Institute of America, five "model" (representative) samples of plastic shredder residue were prepared, four being remnants of plastics contained in 1980 cars as collected at different shredding facilities and one being a sample blended to simulate residue from a 1990 car. A program of separations via density gradient techniques, identifications of components by semiquantitative gas chromatography, and evaluations of melt flow via capillary plastometry was charted out. For the latter, a melt flow tester (ASTMD 1238) was selected and its design (die) modified so as to generate meaningful data when the residues are blended with inexpensive thermoplastics and, possibly, compatibilizers.

Information on some European processes and products based on plastics scrap utilization was collected and evaluated from the standpoint of potential product targeting.

In parallel, research aimed at testing the melt rheology "blending rule," required for suggestions on shredder residue/thermoplastic binary polyolefin systems composition, was started. The isotactic-polypropylene/low density polyethylene (i-PP/LDPE) and/or isotactic-polypropylene/linear-low density polyethylene (i-PP/LLDPE) were selected for initial screening of compoundability. It is assured that melt fluidity synergism encountered in those systems may substantially ($\leq 2 \times$) increase the amount of the shredder residue possible to incorporate over the maximum loading attainable with homopolymers. A major part of the compoundability study consisted of installing and mastering the operation of a Haake Buehler melt (distributive) mixer. The mixer will be used in discrete composition sampling studies aimed at determining the high melt fluidity composition (HMFC) in the above listed polyblends and for subsequent compounding of the shredder residue with HMFC polyblends. Morphology of the residue is studied with sieve analysis and optical microscopy.

PLASTICS REUSE VIA DECOMPOSITION - J. F. Kinstle* (Oak Ridge National Laboratory and University of Tennessee)

This portion of the ECUT program concerns certain options for recycle/reuse of scrapped organic polymeric materials via methods involving the decomposition or rearrangement of the polymer macromolecule or even the monomer. Like other sections of the program, the polymeric scrap of concern is that from the auto shredder. In line with last year's meeting in Hershey (see Ref. 1, pp. 16-17) and reinforced by further considerations since then, the auto shredder scrap is appropriate because it is available in great amounts at particular sites, it is not unrealistically "pure" like sorted-out bottles etc., and it is not unrealistically "impure" like municipal waste.

Professor James F. Kinstle of the University of Tennessee accepted a part-time position at ORNL to coordinate ECUT's efforts on plastics reuse

*Now at Polaroid Corporation, Cambridge, Mass.

via decomposition. Initial efforts were centered on organizing an international symposium on Recycle/Reuse and delineating combinations of materials, processes, and investigators who should be involved in the reuse effort.

Partial chemical breakdown of the scrapped polymers to yield usable chemical intermediates conserves the greatest value, but a more complete breakdown to petrochemical feedstock or fuel is also an option. The least discriminatory option for obtaining benefit from scrapped polymeric materials is incineration with capture of thermal energy, which is still far preferable to just discarding the materials.

Literature reviews aimed at identifying the knowledge gaps in the area of plastics reuse via various molecular decomposition approaches were completed. The most appropriate polymeric material to focus on appeared to be that from the auto shredder (in agreement with conclusions of the Hershey meeting). The studies included individual "control" materials that represent major/typical components of the mixed feedstock such as polypropylene and nylon. Processes included those already studied (pyrolysis etc.) and new ones (extractions under unusual conditions etc.). Investigators were identified by documented expertise in appropriate conventional and unconventional areas. Ensuring knowledge of, but nonduplicity with, other related research efforts was viewed as crucially important.

The international "Symposium on Recycle/Reuse of Polymers" was held on August 31 and September 1, 1983, during the fall national meeting of the American Chemical Society in Washington, D.C. The major impression obtained from the symposium was that there are more developments in the recycle or reuse of polymer scrap around the world than previously thought. For example, incineration technology - including gaseous and particulate emissions and solid clinker considerations - seems to be quite well developed. Pyrolysis techniques (including inert gas and molten salt pyrolyses) have been studied more than some recognize, though further work in pyrolysis (especially with selected additives and/or concomitant application of other energy such as ultraviolet) probably is warranted. Selective partial breakdown can be very valuable, and further work is needed to assess its potential contribution.

At the University of Tennessee, literature reviews and limited experimental studies have been carried out on decomposition routes with

hydrolysis and nonaqueous solvolysis. These studies illustrate that hydrolysis of polymers - without added acid, base, or other catalyst - offers a viable method for reclamation of materials from scrapped polymers. The utility of the approach is not limited to polymers with obviously hydrolyzable structures like the polyesters or polyurethanes, but also includes more "resistant" materials like the styrene-crosslinked unsaturated polyester systems. For the simple segregated systems, the science is relatively complete, and the process engineering appears to be available. For the more resistant and, therefore, complex systems, the science is not complete nor are key variables defined sufficiently to allow processes to be formalized. Further work is necessary on the latter systems and is continuing on the styrene-crosslinked unsaturated polyester system and on the mixed polymer material obtained from the auto shredder.

Treatment of polymers with nonaqueous solvents can lead to dissolution and/or reaction. Therefore, such treatment has potential utility in extraction/separation or in chemical modification/degradation or - in the ideal case - perhaps in both. Multipolymer/single solvent extractions and single polymer/single solvent reactions have been investigated in prior work and in the present studies. Scouting work on multipolymer/multi-solvent schemes has been carried out. Certain problems have become apparent such as non-ideal solubility behavior, i.e., dissolution of one species even to a relatively minor extent often affects the ability of that solvent to dissolve or react with another species. It should be possible to use this "problem" to advantage. While combination systems will have to be treated individually and additional physical and analytical chemistry may have to be adapted to the study of such systems, it appears that this area has tremendous potential.

ASSESSMENT OF ECONOMIC POTENTIAL OF PLASTICS REUSE - T. R. Curlee (Oak Ridge National Laboratory)⁴¹⁻⁴⁴

The initial effort was a literature review and an assessment of the long-range economic potential of plastics reuse. All plastic waste streams were considered, not just those in automobile shreds. Technical and economic data were collected on expected waste streams, costs of various recycle technologies, and projected costs of competitive products. Results

indicated an abundance of preconceived notions (mostly negative) about the economic potential of plastics reuse, but a dearth of hard supporting data. The results of this assessment should be of great value to the area of plastics reuse in general and to the ECUT Project in particular in guiding its efforts in this area.

Further work was aimed at two major objectives. First, projections of the quantities and qualities of plastic wastes in the 1985 to 1990 time frame were made. These projections were made in terms of specific plastic resins and the forms in which the wastes are expected to enter the waste stream. Form implies either manufacturing nuisance plastics or one of eight postconsumer categories of goods. The projections indicated that the largest plastic waste category will be packaging. Considering all future waste projections, it was concluded that about 25%, or about 3.39 billion kilograms (7.48 billion pounds) per year, of the total quantity of plastic wastes can be easily diverted; about 79% is expected to be thermoplastics.

The second major objective was to review the available cost and revenue data concerning the various plastics recycle and disposal technologies. Three major conclusions were drawn from this part of the work. First, the available cost and revenue estimates are not sufficient in terms of quality or quantity to make any definitive statements about the economic viability of any of the technologies. Second, given the available data, preliminary conclusions indicate that several recycle processes are competitive with currently used disposal processes. Third, the available data indicate that recycle processes that utilize municipal wastes are not clearly inferior to recycle processes that require relatively uncontaminated wastes. Additional work is required to make more definitive conclusions.

AGING OF RIGID URETHANE FOAM INSULATION - L. Glicksman (Massachusetts Institute of Technology)⁶⁵⁻⁵³

The overall objective of this task is the development of experimentally verified models to predict thermal characteristics from measurable material properties in order to predict the reduction with time of the insulating qualities (R-value) of rigid urethane foam insulation and, if possible, to suggest ways of mitigating it. The R-value of this type

of insulation is thought to decrease over time by as much as 40% as the blowing gas (Freon 11) trapped in the cells of the foam diffuses out and is replaced by air. The work in this task involves the modeling of heat transfer and gaseous diffusion; accordingly, progress is reported below under those topics.

Heat Transfer

The study of heat transfer in foam insulations entailed the development of simplified procedures for material properties measurement including the thermal conductivity of both the solid polymer and entrapped gases, the modified extinction coefficient, and the fractional distribution of polymer in the struts vs the fraction in the cell walls. Very simple procedures were developed for the determination of both the modified extinction coefficient and the thermal conductivity of the solid polymer. It was found that the modified extinction coefficient may be determined directly by using a spectrometer fitted with an integrated hemispherical collector. A finite difference program simulating the absorbing and scattering processes that occur in the spectrometer was used to verify the validity of the test. For the polyurethane foam and fiberglass it was determined that the error increased with the amount of backscatter and increasing albedo. This error is usually within 10% for normal phase functions and a modest albedo, and always less than 15% even in the extreme case of high albedo and highly back-oriented phase function. The extinction coefficient is not constant for all thicknesses, and minimum error is achieved in the range of optical thicknesses of 0.75 to 1.5 (approximately 40-20% transmission). For polyurethane foam, the error was found to be 3%. Considering the fact that radiation accounts for approximately 25% of the total heat flux, this simplified procedure should cause a total heat flux error of less than 1%. The procedure was also verified for fiberglass using measured phase functions.

A search of the literature on the thermal conductivity of solid polyurethane has shown that reported values vary by more than a factor of 2, from 0.166 W/m^{-°C} (1.16 Btu-in./ft²-h-°F) to 0.347 W/m^{-°C} (2.42 Btu-in./ft²-hr-°F). It was postulated that the variation in conductivity might be due to two factors: variations in polymer chemistry and the thermal history of the foaming process. The thermal history of a foam affects

the amount of crosslinking in the polymer as well as the amount and type of gas that may be dissolved in the solid polymer. A simple test to measure the thermal conductivity of a solid polymer in the as-foamed state was developed during the past year.

This test is a transient, hot-wire, thermal conductivity test. The measurement procedure involves embedding a small-diameter heater wire between foamed polyurethane samples, which are then crushed to nearly the solid density under a pressure of about 345 MPa (50,000 psi). The crushing cylinder arrangement is shown in Fig. 20. To measure the effect of entrapped gases on the conductivity, two tests were performed: one on foam that is only crushed, therefore containing freon as well as atmospheric gases; and one on foam that is granulated before crushing, therefore containing only atmospheric gases.

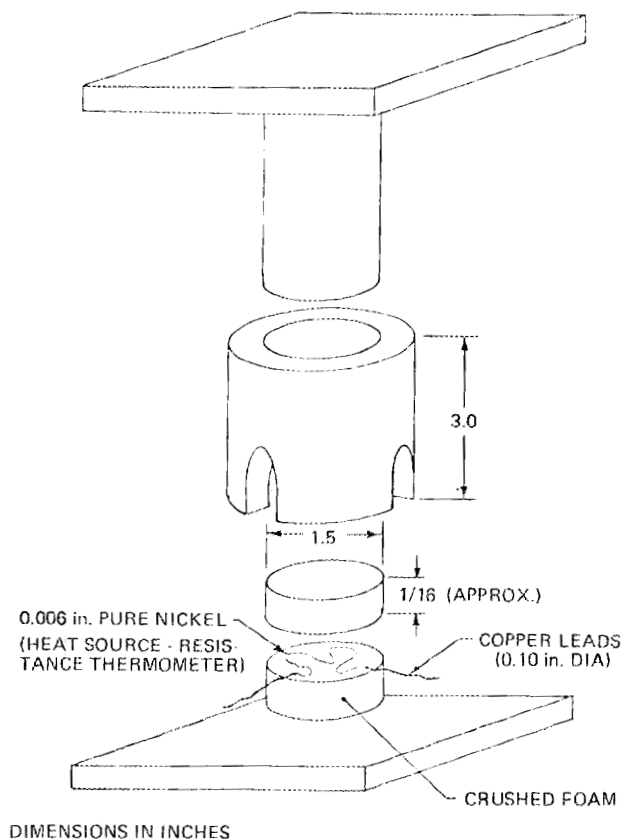


Fig. 20. Schematic of apparatus for crushing plastic foam samples and measuring the thermal conductivity of the crushed foam plastic. Source: L. Glicksman, Massachusetts Institute of Technology.

A current is produced in the wire, causing the temperature of the wire to increase. The thermal conductivity of the material surrounding the wire may be inferred from the rate of temperature increase of the wire.

The heat transfer from the wire has been modelled as a constant line heat source in an infinite medium. A well known solution for this problem exists, from which the thermal conductivity of the surrounding medium is easily extracted. Because the method of measuring the temperature of the wire is by monitoring its change in resistance, the strength of the power generation must change as well. This difficulty was overcome by numerically generating correction factors using the general time varying power solutions. It was found that the corrections are 5 to 10% of the measured thermal conductivity for the amount of power variations observed.

Samples of three urethane foams (Owens Corning B87, Dow 33-4B, and Dow 34-5A) were crushed at total pressures below about 345 MPa (50,000 psi), after which the thermal conductivities of the crushed compacts were measured. The results are shown in Fig. 21. They clearly show that pressures above 240 MPa (35,000 psi) are needed to achieve the true conductivities of the foamed plastic.

Also shown in Fig. 21 are representative solid urethane thermal conductivities previously reported in the literature. Note the wide variation. Note, too, that all three foam plastics tested tend to yield essentially the same ultimate value.

An analysis of the uncertainties involved in the testing resulted in an overall test experimental uncertainty of approximately 8%. This includes the uncertainty due to the power deviation of the hot wire, the nonuniformity of the temperature of the wire due to conduction along its length, electrical noise and offsets, and the uncertainties in the measured temperature coefficient of resistivity and the measured length of the hot wire. Considering that conduction through the solid accounts for approximately 25% of the total heat flux through the foam, an 8% uncertainty in polymer conductivity reduces to only a 2% uncertainty in the effective R-value of the foam. This is quite acceptable.

The calibrations of the experiment were checked by testing a sample of gum rubber whose thermal conductivity was previously measured by

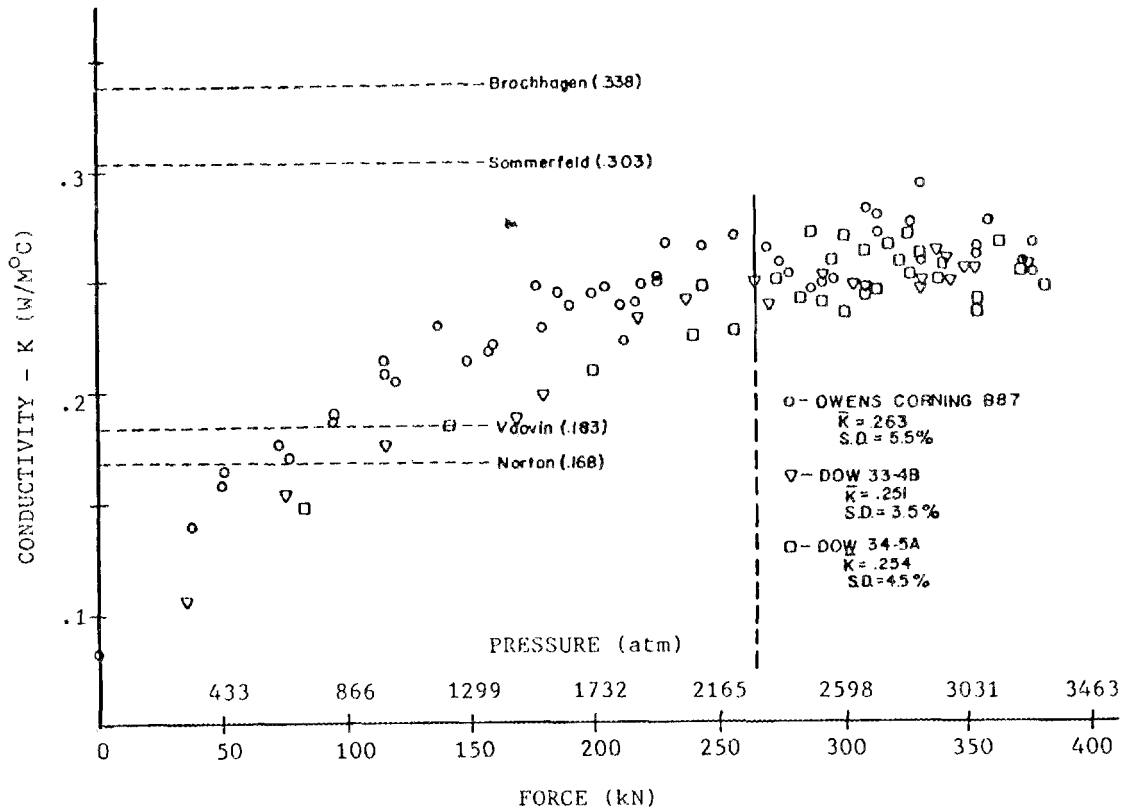


Fig. 21. Plot of measured thermal conductivity of samples of commercial polyurethane foam thermal insulations vs crushing pressure. Also shown (dashed lines) are thermal conductivity values for solid urethane as reported in the literature by other workers. Source: L. Glicksman, Massachusetts Institute of Technology.

Dynatech Corporation.* Ten samples, tested by the method described above, resulted in an average K of 0.173 W/m-°C (1.34 Btu-in./ft²-hr-°F) with a standard deviation of 4.8%, which compares favorably with Dynatech's measured value of 0.165 W/m-°C (1.28 Btu-in./ft²-hr-°F).

A major problem in this test was confirming that it is actually the polymer conductivity that is measured, because some of the gases trapped in the closed cells remain in the sample after crushing. The trapped gases cause a contact resistance between layers of the foam, and they may cause the measured conductivity to be lower than the solid polymer conductivity. The effect of entrapped gases was evaluated by testing two types

*Cambridge, Mass.

of foam samples. Fresh foam, primarily containing Freon, was crushed and tested. Secondly, foam was granulated in a kitchen blender, and the foam fluff was tested. In the first case, Freon is the trapped gas, whereas in the second case, the majority of the Freon is released on blending, and air is the trapped gas. Freon has a substantially lower conductivity than air, so comparison of the test results should indicate the magnitude of the contact resistance problem. The results showed essentially the same conductivity for both whole and granulated foam, indicating that the entrapped gases, and hence contact resistance, have little effect when testing the foam at 290 MPa (65,000 psi).

The test repeatability was also checked by performing tests on the same foam sample a week apart. The results were identical.

Thermal conductivity tests of 24 samples of polyurethane yielded a mean polymer conductivity of $0.261 \text{ W/m}^{\circ}\text{C}$ ($1.82 \text{ Btu-in./ft}^2\text{-hr}^{\circ}\text{F}$) with a standard deviation of 5.2%. A total of 260 tests were conducted. The maximum deviations from the mean are 10%. Considering that the experimental uncertainty is approximately 10%, no measurable variation in polymer conductivity was observed. The value of $0.261 \text{ W/m}^{\circ}\text{C}$ is recommended for use in the heat transfer model. Testing of each foam is not required.

During the next year attempts will be made to fully characterize several foam samples. This will serve as a check on both the material property measurements and the heat transfer model.

Diffusion

Initial results from experimental sectioning of four polyurethane foams were obtained. Measurements of foam cell wall thickness, strut cross sectional area, and surface-to-volume ratio were obtained from optical and scanning electron photomicrographs. These geometrical factors are needed in both the diffusion and heat transfer parts of the overall aging model.

The sectioning of the polyurethane foams with densities of 0.0283, 0.0304, 0.0432, and 0.0447 g/cm^3 (1.77, 1.90, 2.70, and 2.79 lb/ft^3) was completed. It was found that the cell size and the strut cross sectional area decrease as the foam density increases. Mass distribution measurements indicated that only 13 to 30% of the polymer material is in the

walls, while the rest is in the struts. This important observation was used to modify the original model, which assumed that 100% of the polymer is in the walls and thus was predicting much lower permeability than the data were indicating. Permeability predicted by the modified model (i.e., by using the correct wall thickness and mass distribution) was found to be within 10 to 20% of the actual measurements.

The effect of the low-viscosity resin, which was used for scanning electron microscope photographs of the foam, was tested. No significant change at the strut cross section was noticed, but it was found that wall thickness does increase from 30 to 50% when the resin is used. It was concluded that the resin affects only the surface of the polymer and therefore changes the thickness of the thin walls, while the much thicker struts are unaffected.

Permeability measurements by using foam samples of 0.635, 0.95, and 1.27 cm (1/4, 3/8, and 1/2 in.) were performed. The samples were exposed to a pressure difference of 14 to 96.6 kPa (2 to 14 psi) of O₂, CO₂, or N₂. The temperature influence on the permeability was also studied. Data were taken for carbon dioxide and oxygen in a polyurethane foam sample. It was found that the permeation rate at 60°C increased 6 times for the oxygen and 3 times for the carbon dioxide; therefore, it was concluded that the 2- or 3-month accelerated aging test might not adequately simulate the actual aging.

Reverse flow was observed during the polyurethane foam permeability test: whenever the low pressure (downstream) side of the permeability test apparatus was flushed, the slug in the capillary tube moved toward the cell indicating that the gas volume at the low pressure side is decreasing. In order to get reliable data, the sample was exposed to a relatively high pressure drop for several weeks and flushed. Following this, data were taken and a constant permeability was obtained in the pressure range from 10.3 to 82.75 kPa (1.5 to 12 psi) (provided the cell had not been flushed at least 1 h before the data were taken). The results obtained for different temperatures are as follows:

0.0304 g/cm³ (1.9 lb/ft³) μ foam;
 at 25°C, permeability (Pe) = 4.17×10^{-7} cm³_{stp}-cm/cm²-S-cm;
 Hg with range $\pm 8.3\%$;
 at 35°C, Pe = 6.03×10^{-7} with range $\pm 3.8\%$;
 at 56°C, Pe = 11.6×10^{-7} with range $\pm 9.7\%$.
 (In the Pe units, S is the effective solubility of
 the gas in the solid polymer expressed as cm³/cm³-atm.)

Attempts were made to measure the permeability of the solid material. Bubbles formed on the free-rised foam surface were used as test samples. Because it was observed under the microscope that small diameter bubbles have less cracks or holes, only small bubbles were cut out and glued to a rubber ring. Then CO₂ and Freon at atmospheric pressure were applied to the opposite side of the samples. All samples were examined under the microscope, and all were found to have some cracks.

Following these tests, two changes were made: the apparatus was improved to bring down the initial CO₂ and Freon pressure shock on the sample, and rigid Plexiglass was used instead of the rubber ring to make sure that the glued bubbles did not experience mechanical stress. With these changes the first nonleaking sample was obtained, but, whenever the CO₂ side of the apparatus was flushed, reverse flow was still observed similar to the reverse flow observed during the foam tests.

Because the tiny film does not have any capacity to absorb or emit gases, it was concluded for some time that some other part of the apparatus was absorbing and emitting gases. It is now felt that, after flushing, the Plexiglass and rubber are acting as sinks for pure CO₂ and as sources for the other gases. Every Epoxy adhesive could be expected to outgas and add volume to the permeated gas. This could explain the previously obtained nonlinear relation between the permeation rate and pressure drop. Further modifications on the apparatus are being made.

At the same time, more data were taken to quantify the permeation rate at the foam/foil interface. Samples, outer diameter 22.86 cm (9 in.) and inner diameter 5.08 cm (2 in.), were cut and exposed to overpressure at the outer diameter. The permeation rate was measured at the inner diameter. The same very high permeation rate data were taken with a

sample with a plastic facing. The only sample that exhibited no flow rate at all was one with a heavy steel facing.

PLASTIC-COATED LOW-TEMPERATURE HEAT EXCHANGERS - P. D. Roach
(Argonne National Laboratory)⁵⁴

The objective of this task is to test plastic coatings for applications in waste heat recovery systems which must extract heat from gaseous waste streams containing potentially corrosive gases such as SO_2 at temperatures below 200°C . The work attempts to identify plastics which are thin enough not to impede the heat flow excessively yet thick enough to protect the underlying heat exchanger material. In addition, costs must be held within commercial feasibility. Primary emphasis is on developing materials that will withstand the hot sulfur-bearing flue gases generated in industrial furnaces and boilers.

Four new sample pieces consisting of very thin [0.00254-cm (0.001-in.)] plastic coatings on carbon steel tubes were tested primarily to explore the feasibility of very thin coatings. The plastics used were Xylac polyethersulfone (PES), Dykor polyvinylidene fluoride (PVDF), Ryton polyphenylene sulfide (PPS), and Lectrofluor 604P (proprietary).

Testing was relatively brief because all samples showed quite rapid deterioration in the hot sulfuric acid vapor. The samples showed severe corrosion of the underlying metal tube in about 100 h of testing. Such very thin coatings are not adequate protection because the acid vapors can reach the metal through small defects or porosity of the coating.

Extended testing of a quite thick plastic coating has led to an unexpected failure. The coating was a 0.076-cm-thick (0.030-in.) spray coating of polyphenylene sulfide (PPS). After more than 3600 h of testing, metallic corrosion developed at one spot under the coating. This led to local swelling and cracking of the coating and perforation of the underlying stainless steel tube. Thinner coatings of PPS performed well after comparable test times.

The failure of the thick coating can probably be attributed to excessive stresses caused by differential thermal expansion between the plastic and the metal. Thinner coatings can more easily stretch to accommodate this expansion. This result also confirms the value of

extended testing. It cannot be assumed that a sample that survives 1000 or 2000 h of testing will then survive indefinitely. The emphasis in the current program is long-term testing of the samples that have performed well for thousands of hours.

Two other samples, identified by the vendor as XYLAC 4600 and XYLAC 4400, were also corrosion tested. Although coating thicknesses of approximately 0.005 cm (0.002 in.) were promised by the vendor, the actual thickness was much less (by a factor of 3 to 10). These new samples were installed in the corrosion test apparatus for exposure to hot sulfuric acid vapor. After relatively short exposure (40 and 90 h, respectively), the samples showed severe metallic corrosion. These are similar results to those observed with other very thin plastic coatings. Either of these plastics may be entirely satisfactory in adequately thick (0.013- to 0.025-cm) coatings.

Several plastic-coated heat exchanger tubes have now accumulated over 5000 h in the corrosion test apparatus. The perfluoroalkoxy (PFA) sample is now badly blistered, indicating corrosion of the underlying metal tube. However, both samples of Ryton PPS (polyphenylene sulfide) have withstood the sulfuric acid vapor environment very well. These coatings, of thickness 0.0127 and 0.254 cm (0.005 and 0.010 in.), are essentially unchanged after 5070 and 3760 h, respectively, in the test apparatus. Ryton is the only plastic that has survived this long.

MATERIALS BY DESIGN

The overall objective of this newly initiated work element is to establish the technical feasibility of modeling properties of materials, especially interfacial and surface properties, by using calculations of the electronic structures of many atoms in order to design, optimize, and control various phenomena important to energy conservation. The scope of the effort was expanded beyond surface catalysis phenomena to include surface phenomena important in tribology and grain boundary and adhesion phenomena important in the materials sciences.

It was determined that assessments should be conducted in three areas to determine the states of the arts and the potential for future

applications to practical modeling of the above phenomena. These three areas to be addressed are electronic and molecular theory, computer technology, and experimental techniques.

The power of the experimental techniques would determine how well the predictions of the models could be verified. A potential subcontractor to carry out the assessments for molecular theory and computer technology was identified. However, the attempt at a sole-source procurement for the assessment was rejected by UCC-ND Purchasing (now Martin Marietta Energy Systems, Inc.); therefore, procedures for competitive bidding were implemented. An announcement of the Request for Proposal (RFP) for the assessment appeared in page 31 of the September 2, 1983, issue of *Commerce Business Daily*. Copies of the RFPs were mailed to about 90 prospective bidders on September 26, 1983. Proposals were due on November 21, 1983. A review panel of ORNL researchers was named.

NEW ASSESSMENTS AND INITIATIVES

The objective of this work element is to explore, to a limited extent, conceptual ideas as they arise during a fiscal year in order to assess their potential for further funding in the future.

CUBIC BORON NITRIDE AND DIAMOND-LIKE CARBON COATINGS BY CVD -
D. P. Stinton (Oak Ridge National Laboratory)

A small effort was initiated to explore the feasibility of producing cubic boron nitride (BN) and diamond-like carbon coatings via the chemical vapor deposition route. Diamond and cubic BN are, respectively, the hardest and second hardest substances known. They are produced in bulk form through high-temperature and high-pressure processes but not as coatings. It is believed that if such coatings could be produced, they would find myriad uses as bearing and wear-resistant surfaces. The approach being taken for this task is to use activation of the process gases via either a plasma or a hot filament prior to deposition on the substrate.

Several attempts were made to produce diamond-like carbon coatings from methane and hydrogen by the hot-filament activation technique. All attempts resulted in oxidation of the tungsten filament and deposition of

metallic tungsten on the reactor walls and substrate. Oxidation of the filament continued to be a problem even after several modifications to the coating system. Potential sources of oxygen contamination are from air leaking into the system or contamination of the coating gases with oxygen. The solution to these problems is the use of an ultra-high-vacuum system and the use of devices to remove oxygen from the gas streams. Because limited funding precludes such efforts at the present time, the hot filament activation work was terminated.

Development of a system that employs plasma activation for the deposition of cubic BN coatings is continuing. For this system, the coating gases are activated in a plasma before coming into contact with the substrate. The chief advantage of this technique is the ability to deposit films at unusually low substrate temperatures. As a result, metastable materials and films which are mismatched in thermal expansion with the substrate can be deposited without severely stressing the film as the coated substrate cools to room temperature.

The system consists of an RF (radio frequency) generator inductively coupled to a quartz reaction chamber, coating gas metering equipment, vacuum pumping equipment, and an off-gas handling system. A 20-kW variable range Lepel generator is used to produce an argon plasma. This generator was received and installed.

The reactions which are being used to explore the production of cubic BN are as follows:

1. $\text{BCl}_3 + \text{NH}_3 \longrightarrow \text{BN} + 3\text{HCl}$, and
2. $\text{B}_2\text{H}_6 + 2\text{NH}_3 \longrightarrow 2\text{BN} + 6\text{H}_2$.

An argon plasma was established in this system at the reduced pressure of 0.67 kPa (50 torr). A very stable plasma could be established with proper control of the gas flow, generator power, and fine tuning of the generator to the load. However, small flows of hydrogen or other coating gases were found to extinguish the argon plasma. The plasma was extinguished because very little of the RF power was coupled with the plasma. Numerous modifications to the induction coil and coating chamber failed to transfer significant amounts of energy to the plasma. A commercial vendor (TAFA) has been located that produces plasma torches to operate with RF

generators. Their design has been optimized to obtain the maximum amount of power from the generator. A 2.54-cm-diam torch is being purchased that should capture 90 to 95% of the power when attached to our coating chamber.

Radio frequency plasmas have been emphasized in this work instead of dc arc plasmas because the absence of electrodes should reduce contamination. Thermal plasmas of this type should operate at 8000 to 9000 K and have relatively gradual thermal gradients. The velocity of gases through a thermal plasma is considerably lower than for a dc arc plasma, resulting in an increased residence time of from 5 to 20 msec. One disadvantage of an RF plasma is that it is difficult to get coating gases to thoroughly mix with the denser plasma. Distributor designs become very important to ensure that coating gases pass through the plasma. The TAFA plasma torch which is being purchased has a distributor design that has proven to thoroughly mix the coating gases with the plasma. An additional method to get good gas mixing uses a water cooled copper probe which can be introduced directly into the plasma. Coating gases can then be introduced into the plasma through the cooled probe. A second advantage of such a probe is that gases can be introduced into the tailflame of the plasma by inserting the probe through the plasma to the tailflame. This will very likely be necessary in this work because the introduction of NH_3 into an argon plasma will very likely extinguish the plasma. The energy necessary to ionize appreciable quantities of hydrogen gas is greater than the energy available from the RF generator presently used. Introduction of gases into the tailflame should dissociate the NH_3 but not affect the argon plasma.

CERAMIC COMPOSITES - G. C. Wei* (Oak Ridge National Laboratory)⁵⁵

A small effort was initiated to explore the possibility of using SiC whiskers to improve mechanical performance of ceramics. This is a joint effort with ARCO, Inc., which is supplying the whiskers. In order to fabricate net-shape, large specimens ($\sim 76 \times 12 \times 6$ mm) for evaluations, graphite dies with cheek pieces and square punches were prepared for uniaxial hot pressing. In principle, hot isostatic pressing can also be applicable if proper materials can be identified.

*Now at GTE Sylvania Laboratories, Waltham, Mass.

Specimens of ARCO SiC whiskers in Al₂O₃ matrix, mullite matrix, B₄C matrix, ZrO₂ matrix, or Si₃N₄ matrix were fabricated to high densities by uniaxial hot pressing. The SiC whiskers appear compatible with Al₂O₃, mullite, or B₄C matrix materials at hot-pressing temperatures, as specimens of over 99% theoretical density have been successfully fabricated. On the other hand, ZrO₂ or Si₃N₄ appear to react with the SiC whiskers resulting in bulk densities less than 95% of theoretical. Optical microscopy of the SiC-whisker, Al₂O₃-matrix, mullite-matrix, and B₄C-matrix materials revealed that the whiskers were preferably aligned perpendicular to the hot-pressing direction.

Many samples were sent for determinations of modulus of rupture and critical fracture toughness, K_{IC} . It was found that the SiC-whisker Al₂O₃-matrix material had remarkable and significant improvements in K_{IC} over conventional hot-pressed or sintered Al₂O₃ ceramics for cracking in the direction perpendicular to the orientation of the whiskers at temperatures up to 1200°C in air. More specimens of different compositions and whisker lengths will be prepared via various processing techniques for mechanical testing in order to understand the toughening and strengthening mechanisms.

A different type of alumina powder with a finer particle size than that of the alumina powder previously used was employed. In addition, an ultrasonic homogenizer was used for mixing the whiskers with the powders. These two process modifications greatly improved the uniformity of the microstructure of the hot-pressed samples. Metallographic examination showed the preferred orientation of SiC whiskers, but with a much more uniform distribution, qualitatively, in planes orthogonal or parallel to the hot-pressing axis. As a result, statistically, the modulus of rupture of these samples was increased by about 2% over that of the previous samples.

Analyses of the transient densification curves (linear shrinkage vs time) of the whisker-powder mixtures during hot pressing revealed several interesting features. First, most (~90%) of the densification was completed at temperatures as low as 1600°C. Second, the final densification rate (from ~90% density to 100% density) was temperature dependent with an activation energy of only 2 eV. Third, the densification rate in the

final stage was proportional to the hot-pressing stress to the 1.6 power. The 2-eV activation energy and the 1.6 stress power dependence of the final stage of the hot pressing suggest a boundary mechanism controlled with plastic flow. Therefore, attention must be directed at ways of enhancing boundary transport and deformation for further development of pressureless-sintered whisker-reinforced alumina.

In summary, under this task, a new material has been successfully developed, namely, SiC-whisker-reinforced alumina possessing improved toughness and strength. Further development of this material, including optimization of the whisker content, pressureless sintering, etc., is expected to be continued under the sponsorship of the DOE Ceramics Technology for Advanced Heat Engines Project.

MAGNETRON-SPUTTERED AMORPHOUS METAL WEAR-RESISTANT COATINGS --
S. K. Khanna (Jet Propulsion Laboratory)^{56,57}

A small effort was initiated at the Jet Propulsion Laboratory (JPL) to assess the wear resistance of amorphous metallic coatings produced by magnetron sputtering. It is known that amorphous metallic alloys with their homogeneous microstructure and lack of long range order tend to be much more resistant to chemical corrosion than the same alloys in their crystalline forms, and there is some evidence that the same applies to wear resistance. However, such alloys are usually produced in either powder or narrow ribbon form by liquid quenching. Clearly, it is impossible to use them in this form for protective purposes as most attachment processes involve heat treatments which would cause the amorphous phase to crystallize. In this present work it was shown that hard adherent amorphous metallic coatings can be deposited onto a steel surface by magnetron sputtering, thereby improving the wear resistance of the steel dramatically.

A sputtering target of $(W_{0.6}Re_{0.4})_{76}B_{24}$ was fabricated by hot pressing at 1200°C and 20.7 MPa (3000 psi) thoroughly mixed powders of W, Re, and B into the desired composition. The target was finally machined to the exact size required. W-Re-B films were deposited on microscope glass slides using a dc sputter "S-gun" (Sputtered Films, Inc.) for characterization studies. Typical sputtering parameters were: base vacuum about 10^{-7} torr;

carrier gas, argon at 5 μm pressure; power fed to the run at about 1000 W; substrate to target distance about 12.7 cm (~5 in.); substrates maintained at room temperature.

Films were checked for crystal structure by using X-ray diffraction (Fig. 22). The presence of only a broad diffuse halo pattern instead of sharp diffraction peaks confirmed the amorphous structure of the as-deposited films.

To obtain an accurate value for the crystallization temperature, a film deposited on quartz was heated in argon atmosphere, and its resistance was monitored as a function of temperature (Fig. 23). The sudden drop in the resistance at about 1275 K (~1000°C) indicated film crystallization at that temperature. It should be noted that this high crystallization temperature opens the possibility of using these coatings for high-temperature applications not previously thought possible.

The depth profile of the chemical composition of a film was studied with a Cameca secondary ion mass spectrometer (SIMS). Figure 24 shows the remarkable uniformity of the composition over the film thickness.

Films were deposited on 52100 steel discs and pins for the hardness and wear resistance measurements. To obtain good adhesion and hardness of the films on the steel substrates, sputtering parameters were systematically varied. The best results were obtained when the sputtering pressure was about 10 μm of argon. The steel substrate temperature was maintained at 350°C, and the substrate was subjected to a light sputter etch just prior to the film deposition. Microhardness of the hard adherent films (measured by indentation technique) vs the load is shown in Fig. 25. The hardness value of 2400 kg/mm² is about that for silicon carbide.

Wear resistance was measured by the pin-on-disc method. Figure 26 shows the wear/sliding distance vs load. It is clear from the figure that there is about three orders of magnitude improvement in the wear behavior of 52100 steel coated with amorphous metallic $(W_{0.6}Re_{0.4})_{76}B_{24}$ over the uncoated 52100 steel.

INSTRUMENTS FOR HARSH ENVIRONMENT - K. G. Kreider (National Bureau of Standards, Gaithersburg)^{5,8}

The objective of this task is to supply critical generic background on high-temperature thin-film devices for use in noncontinuous combustion

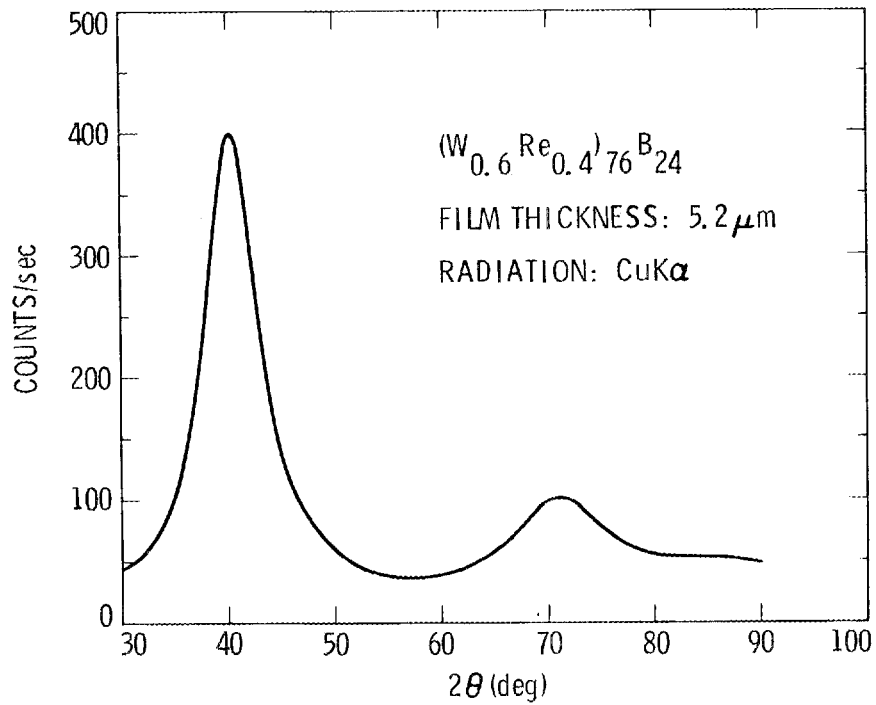


Fig. 22. X-ray diffraction scan of magnetron-sputtered W-Re-B film.
 Source: S. K. Khanna, Jet Propulsion Laboratory.

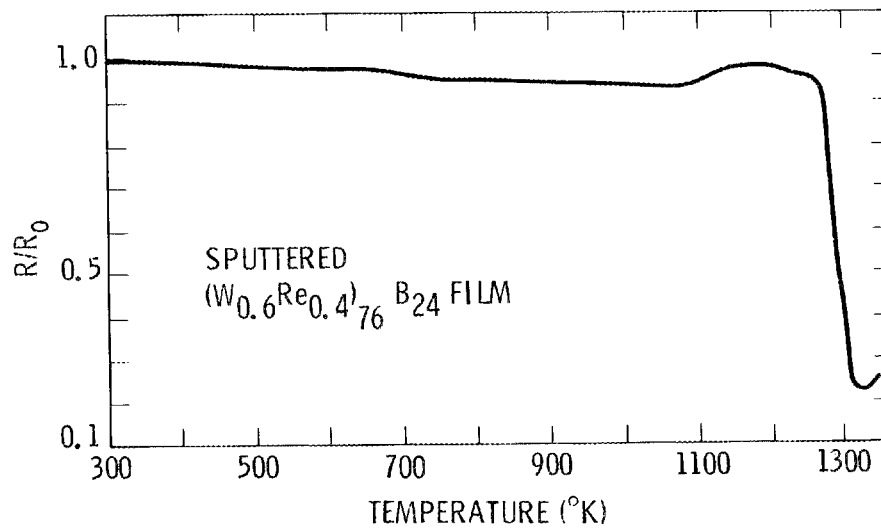


Fig. 23. Relative resistance of magnetron-sputtered W-Re-B as a function of temperature. R_0 is the resistance at room temperature.
 Source: S. K. Khanna, Jet Propulsion Laboratory.

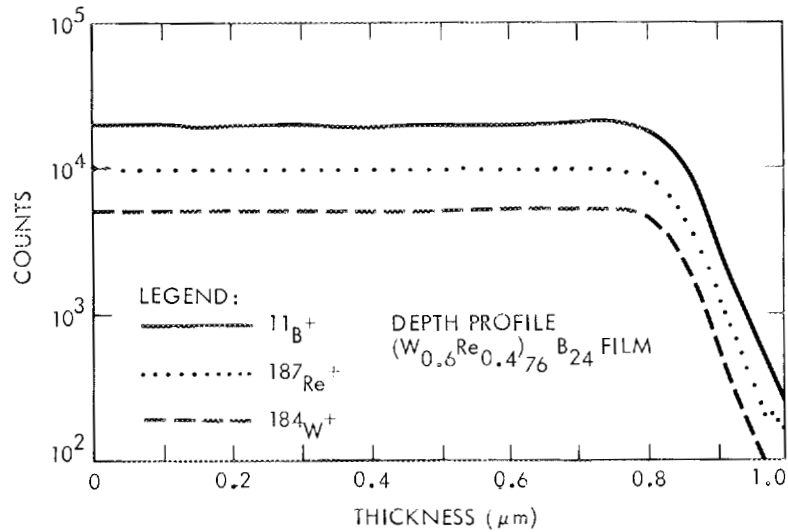


Fig. 24. Depth profile by secondary ion mass spectroscopy (SIMS) of magnetron-sputtered W-Re-B film. Source: S. K. Khanna, Jet Propulsion Laboratory.

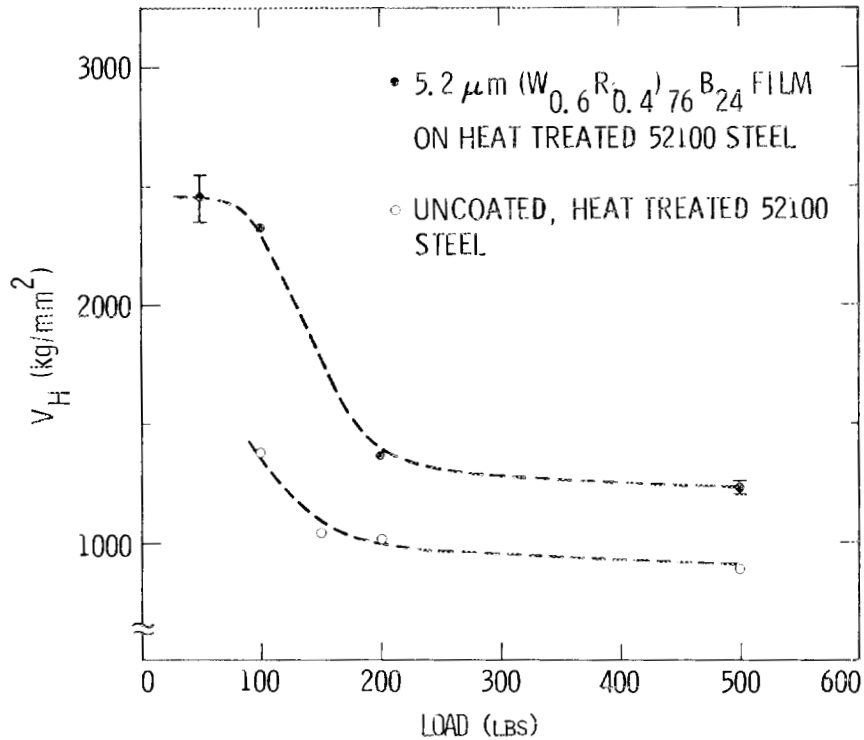


Fig. 25. Hardness (Vickers) measurements as function of indenter load for W-Re-B film magnetron-sputtered onto a 52100 bearing steel substrate. Source: S. K. Khanna, Jet Propulsion Laboratory.

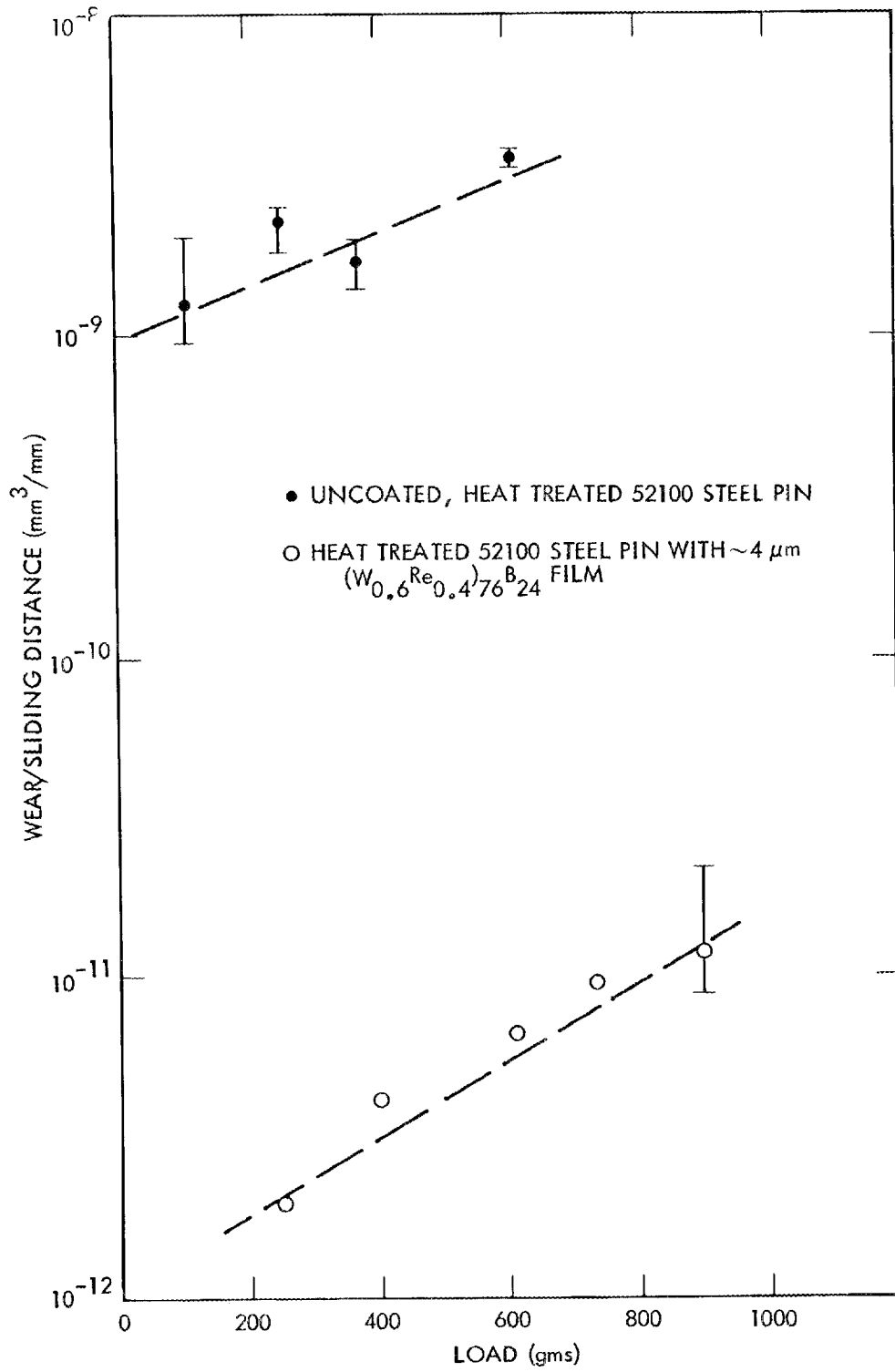


Fig. 26. Effect of load on the wear rate of a W-Re-B coated and an uncoated 52100 steel surface. *Source:* S. K. Khanna, Jet Propulsion Laboratory.

environments. The thin-film devices are for application in internal combustion engines on moving parts, such as valves and pistons, where knowledge of surface temperatures and strains will help in the design of efficient engines. The program will supply information on methods of signal generation and construction in practical thin-film devices. Solid state and surface physics studies of the films have been undertaken to understand the preferred methods of constructing durable thin-film devices.

The existing method of high-temperature thin-film construction uses a thermally grown metal oxide to electrically insulate the sensing element from the substrate. The development of practical surface sensors for use in harsh environments is primarily dependent on the development of a coating which is compatible with the substrate material and capable of growing useful insulating surface oxide layers. For automobile engine alloys, the iron-base alloy Fe-25 Cr-5 Al-0.1 Y has been selected from the group of M-Cr-Al-Y high-temperature alloys which form adherent aluminum oxides during oxidation. An extensive investigation of the electrical properties of the aluminum oxides grown on these alloys led to the initial selection of Fe-Cr-Al-Y. The dielectric strengths of oxides grown on this alloy (5×10^4 V/cm at 1093°C) are high, and the electrical resistivities are relatively high ($\sim 10^8$ ohm-cm at 1093°C). In addition, the alloy has desirable mechanical properties throughout the operating range of the sensors, and devices using this alloy are unusually durable.

Each element of the sensor is chosen for its specific electric, chemical, or mechanical properties, and, as a result, it is necessary to combine materials with widely varying types of chemical bonding. The metal oxide is an insulator with strong ionic bonds, the coating is a high-temperature metal alloy, and the sensing element is usually a noble-metal alloy. Therefore, when the temperature of the assembly is changed, thermal mechanical strains develop within the assembly.

In an automobile engine, the most probable areas of application are the measurement of temperatures and strains on valves, the engine cylinder walls, and areas of the pistons and rings. Accordingly, this task will develop a substrate/coating/oxide/electrode system that will withstand the thermomechanical strains and the environment of the component surfaces.

Because of the difficulties that industrial developers have had with the adherence, dielectric breakdown, and reliability of thin-film sensors on turbine engine hardware, it is felt that an important contribution that can be made relates to the understanding of the fundamentals of the aluminum oxide-sensor interface. In the first year of this project, a basic study of the rhodium, aluminum, and oxygen reactions at the interface was undertaken. The system selection has been made partially because rhodium-containing platinum alloys have been found more adherent than pure platinum. Studies of the platinum/oxygen system have indicated the difficulty in bonding oxides to platinum and suggest the use of extremely thin transition layers to enhance bonding of metals such as rhodium.

Surface analytical techniques have been used to study the initial stages of aluminum oxide growth on rhodium. By characterizing the fundamental processes occurring at aluminum oxide-rhodium interfaces, these investigations help to define the best procedures for fabricating temperature sensors and demonstrate the stability of the interface region. Low-energy electron diffraction (LEED) and Auger electron spectroscopy (AES) were used to characterize, as a function of temperature and coverage, individual overlayers of aluminum and oxygen on a Rh(111) crystal and interaction between these species during coadsorption experiments. Aluminum oxide formation rates were observed to depend both on the overlayer coverages and on the surface temperature.

Activities have included preparing the 4340 and cast-iron test coupons, coating these coupons with Fe-Cr-Al-Y, metallographic studies, thermal oxidation, vacuum reactive sputtering of Al_2O_3 , platinum thin-film sputtering, and evaluating thin-film coating quality. An 18:8 stainless steel (347) has been added to the substrate alloys of 4340 and 1177 cast iron. The 4340 alloy is used in engine valves for its high strength-to-weight ratio in combination with its toughness.

These two alloys are being studied with and without a coating of Fe-Cr-Al-Y (Fe + 18 Cr, 11 Al, 0.7 Y) approximately 100 μm thick. The coating provides oxidation resistance and a proven base for the oxide dielectric insulating layer of Al_2O_3 . The native oxide of the Fe-Cr-Al-Y is Al_2O_3 ; not only is this oxide a superior base for the sputtered Al_2O_3

layer, but experience in using this combination for turbine blade temperature sensors indicates that good adherence of the Al_2O_3 layer to the platinum and the platinum-10% rhodium layer is possible.

The native oxide on the Fe-Cr-Al-Y can be used in the as-received condition, which is very thin, or it can be matured by oxidation in air at elevated temperatures as in the fabrication of turbine alloy sensors. Initial experiments on thermally oxidizing the Fe-Cr-Al-Y were quite successful in developing the oxide on the coating, but disastrous oxidation of the substrates precludes the use at the high temperatures ($>1075^\circ\text{C}$) used in the turbine sensor technology. The second oxidizing heat treatment has been performed at 760°C , which is below the austenitizing temperature of 843°C (1550°F).

An alternative to growing the Al_2O_3 layer is to directly sputter it onto the substrates. Both 4340 and 1177 alloys have been reactively sputtered with Al_2O_3 to form the dielectric insulator. Good adherence was observed directly on the Fe-Cr-Al-Y. These Fe-Cr-Al-Y coatings were made by vacuum sputtering at an outside facility according to standard procedures used for nickel and cobalt alloys. The coatings are formed at high temperatures (approximately 800°C) and have large grains ($10\text{-}20\ \mu\text{m}$) on the surface. Finishes used include as-received and with a 600-mesh polish. Cleaning is accomplished in an ultrasonic bath of acetone followed by methyl alcohol.

This technology is similar to that used to fabricate thermocouple sensors on aircraft turbine blade and vane alloys. After sputtering of the Al_2O_3 layer, which should be approximately $2\ \mu\text{m}$ thick to ensure good insulating and good dielectric breakdown properties, an anneal is used to convert the amorphous Al_2O_3 to the alpha phase. Then the sample is ready to receive the two thermocouple legs of platinum and platinum-10% rhodium. Two samples have been fabricated, one of each alloy with platinum film thermocouple legs; the adherence appears adequate.

To test the adherence and insulating properties, two tests have been designed for the simulated thermocouple film sensor. Both tests are performed on the test coupon, which is approximately $1.5 \times 1.5 \times 0.5\ \text{cm}$, of 4340 or 1177 alloys. The coupon has the sputtered aluminum oxide insulator on top of the Fe-Cr-Al-Y with its oxide. The thermocouple films of

platinum and platinum-10% rhodium are sputtered 0.4 cm wide with 0.4 cm overlap and are ready to be tested for adherence, insulating properties, and dielectric strength. The adherence tests include a thermal cycling test in which the coupon is cycled between <100 and $>1000^{\circ}\text{C}$ ten times with a 3-min cycle time. This is accomplished by directly heating the films with a brazing torch. The electrical properties are tested by following the resistance to ground (substrate) and resistance through the thermocouple element while heating to 900°C in an air furnace. These tests have been used previously for the turbine hardware coupons and are a strong indication of the durability and stability of the film sensor.

Considerable effort has been expended in optimizing the Al_2O_3 sputtering procedure to ensure good adherence and good stoichiometry of the coating. The best procedure appears to include RF sputtering of aluminum in an oxidizing (7-10% oxygen in argon) atmosphere at a partial pressure of 2 mm. The sputtering gun is a commercial planar magnetron which permits a deposition rate of 0.1 to 0.2 mm/s at a 10-cm standoff distance using 300 W.

After the fabrication conditions for these test coupons are optimized, a thermocouple test in a furnace is planned. This test coupon must be long enough to maintain a large thermal gradient between ends of the film thermocouple. The test coupons will be basically similar, but they will be 15 cm long, and evaluation will be compared to standard Type S thermocouples to elevate accuracy and stability.

Scanning electron microscopy (SEM), energy dispersive X-ray analysis (EDX), and electron spectroscopy for chemical analysis (ESCA or XPS) will be used to optimize and analyze the morphology, composition, and contamination of the oxide films and interfaces in the film sensors.

SUPERCRITICAL FLUID EQUATIONS OF STATE - J. F. Ely (National Bureau of Standards, Boulder)

An interagency agreement was completed for this work. It is part of a joint effort with other government funders to develop separation techniques utilizing supercritical fluids.

COATINGS FOR HIGH TEMPERATURE ENERGY CONVERSION SYSTEMS - A. V. Levy
(Lawrence Berkeley Laboratory)

The objectives of this effort are (1) to assess the state of the art of plasma-sprayed and chemically vapor-deposited ceramic coatings and (2) to test the friction and wear characteristics and analyze certain thermal barrier and wear resistant coatings being considered for use on the piston rings and cylinder walls of the adiabatic diesel engine. Plasma-sprayed coatings to be tested include $Y_2O_3-ZrO_2$, WC-Co, Cr_3C_2 , $Al_2O_3-TiO_2$, TiB_2 , and TiC_2 . The coatings are tested to determine the friction and wear rates in a Falex 6 washer-on-disk wear tester modified to achieve $760^\circ C$ ($1400^\circ F$) in air. Coatings are analyzed before and after testing to determine compositions, microstructure, surface texture, wear mechanisms, and wear rates.

Work is currently focused on modifying the Falex 6 to extend the testing temperature range from room temperature to $760^\circ C$ ($1400^\circ F$). Wear test specimens have also been sent to Cummins Engine Co. for application of ceramic coatings. The modifications of the Falex 6 tester will basically replace the existing upper testing shaft with a split shaft incorporating a thermal resistance barrier. This barrier will be composed of alternating ceramic and stainless steel washers to interrupt and dissipate heat conducted up the shaft from the testing zone. The lower specimen table design will also be altered to reduce heat flow and provide a base to support the furnace structure surrounding the testing zone. The basic furnace design uses a heater core powered by cartridge heaters to provide the necessary heat input. This core will be surrounded by alumina insulation within a stainless steel furnace cover. The temperature of various elements in the testing system will be monitored by temperature sensing elements located at strategic places. The heater output will be controlled accordingly.

The furnace, when constructed, will be subjected to test runs prior to mounting on the Falex machine. After this, the furnace will be mounted on the machine itself, and several tests will be conducted to determine the temperature behavior of the system and the corrosion behavior of the test specimens.

LASER SURFACE MODIFICATIONS OF CERAMICS - J. Narayan and R. F. Davis
(North Carolina State University)^{59,60}

A small subcontract has been let to the North Carolina State University to investigate the nature and implications of surface modifications induced by driving or diffusing certain metal ions into ceramic surfaces by laser irradiation. This work will be performed at North Carolina State University under the guidance of Narayan and Davis. Thin layers of Cr, Fe, or Ni will be deposited onto flat surfaces of α - or β -SiC, Si₃N₄, or Al₂O₃ and then irradiated by lasers. Fracture strength and toughness, friction and wear behavior, fatigue resistance, microstructure, and compositional variations will be determined and compared with similar properties of uncoated samples. The aforementioned properties will also be related to the wavelength of the laser radiation, the pulse duration, and the energy density. The major output expected from this research is an initial determination of the effects of such treatment.

ION IMPLANTATION OF ZIRCONIA - J. K. Cochran, Jr. (Georgia Institute of Technology)⁶¹⁻⁶⁵

Subcontract action has been initiated for work at the Georgia Institute of Technology, the objective of which is to determine if it is feasible to toughen the surface of partially stabilized zirconia by implanting excess Zr⁺ ions. The surface of cubic-ZrO₂ (stabilized with 9.8 mole % Y₂O₃) will be implanted with 200 KeV Zr⁺ ions at doses of 1.5, 3, and 6 X 10¹⁶ ions/cm². The implanted specimens are heat treated in air for 4 h at 1200, 1300, and 1400°C in order to oxidize the implanted zirconium. RHEED, microhardness, fracture toughness, and wear measurements are made before and after heat treatment to determine if tetragonal or monoclinic ZrO₂ precipitates have formed from the implanted zirconium and to determine any resulting changes in the properties measured.

FY 1983 PUBLICATIONS

1. D. N. Braski and S. A. David, "Weld Microstructure of (Ni,Fe)₃(V,Ti) Long-Range Ordered Alloy," *Metall. Trans. A* **14A**, 1785 (1983).
2. S. Ashok, K. Kain, J. M. Tartaglia, and N. S. Stoloff, "High Cycle Fatigue of (Fe,Ni,Co)₃V Type Alloys," *Metall. Trans A* **14A**, 1997 (1983).

3. C. T. Liu, H. Inouye, and A. S. Schaffhauser, "Long-Range Ordered Alloys Modified by Group IV-B Metals," U.S. Patent 4,410,371, 1983.
4. G. C. Wei, "Beta-Silicon Carbide Powders Produced by Carbothermic Reduction of Silicon in a High-Temperature Rotary Furnace," *J. Am. Ceramic Soc.* **66**(7), C111-C113 (July 1983).
5. J. W. Barlow and D. R. Paul, "Mechanical Compatibilization of Immiscible Blends," paper presented at International Symposium on Phase Relationships and Properties of Multicomponent Polymer Systems, Anacardi, Italy, May 30-June 3, 1983, available through authors at Department of Chemical Engineering, Center for Polymer Research, The University of Texas at Austin, Austin, TX 78712.
6. T. D. Taugott, "Mechanical Properties and Morphologies of HDPE-PET Blends," master's thesis, The University of Texas, December 1982.
7. M. A. Schuetz, "Heat Transfer in Foam Insulation," master's thesis, Massachusetts Institute of Technology, December 1982.
8. P. D. Roach and R. E. Holtz, *Plastic Heat Exchangers for Waste Heat Recovery - Final Report*, ANL-83-81, Argonne National Laboratory, Argonne, Ill., September 1983.

ACKNOWLEDGMENTS

The authors thank the following for their contributions: Gloria Donaldson and Debbie McCoy for typing the draft, O. A. Nelson for editing it, and Mary Upton, D. L. Northern, and H. G. Sharpe for preparing the final report.

REFERENCES

1. L. E. Morris and J. A. Carpenter, Jr., *Materials Project of the Energy Conversion and Utilization Technologies (ECUT) Program Progress Report for Year Ending September 30, 1982*, ORNL/TM-8940, August 1984.
2. C. T. Liu and E. M. Schulson, "The Fracture of Ordered $(\text{Fe,Co})_3\text{V}$," *Metall. Trans. A* **15A**, 701 (April 1984).
3. C. T. Liu, "Physical Metallurgy and Mechanical Properties of Ductile Ordered Alloys $(\text{Fe,Co,Ni})_3\text{V}$," *International Metals Rev.* **29**(3), 168-93 (1984).

4. C. T. Liu and N. S. Stoloff, *Development and Characterization of Ductile Long-Range Ordered (LRO) Alloys (Fe,Co,Ni)₃V for High Temperature Structural Use*, ORNL-6032, August 1984.
5. D. N. Braski and S. A. David, "Weld Microstructure of (Ni,Fe)₃(V,Ti) Long-Range Ordered Alloy," *Metall. Trans. A* **14A**, 1785-91 (September 1983).
6. S. Ashok et al., "High Cycle Fatigue of (Fe,Co,Ni)₃ Type Alloys," *Metall. Trans. A* **14A** (1983).
7. N. S. Stoloff, "Ordered Alloys - Physical Metallurgy and Structural Applications," in *Metals Rev.* **29**(3), 123-35 (1984).
8. C. T. Liu et al., *Initial Development of Nickel and Nickel-Iron Aluminides for Structural Uses*, ORNL-6067, August 1984.
9. C. T. Liu and J. O. Stiegler, "Ordered Intermetallic Alloys - High Temperature Structural Materials of the Future," *Mater. Eng.* **100**(5), 29-33 (November 1984).
10. C. T. Liu and J. O. Stiegler, "Ductile Ordered Intermetallic Alloys," *Science* **226**, 636-42 (1984).
11. S. A. David et al., "Welding and Weldability of Nickel-Iron Aluminides," *Welding Journal* **64**(1), 22-25 (January 1985).
12. J. A. Horton, A. DasGupta, and C. T. Liu, "The Disordering Process in an L1₂ Ordered Alloy," p. 486 in *Proceedings 42nd Annual Meeting of the Electron Microscopy Society of America, Detroit, Michigan, August 13-17, 1984*, San Francisco Press, Inc., San Francisco, 1984.
13. B. J. Marquardt, "Wear Induced Deformation of Ni₃Al, (Fe,Co)₃, and (Fe,Ni)₃V," master's thesis, Vanderbilt University, Nashville, Tenn., December 1984.
14. B. J. Marquardt and J. J. Wert, "Wear Induced Deformation of Ni₃Al, (Fe,Co)₃V, and (Fe,Ni)₃V," in *Proceedings of the 1984 Annual Meeting of the Materials Research Society*, Boston, November 26-28, 1984.
15. B. J. Marquardt, P. M. Baker, and J. J. Wert, "Erosive Wear of Ductile Ordered Alloys," in *Proceedings of the International Conference on Wear of Materials*, meeting in Vancouver, Canada, April 1985.
16. T. C. Chou and Y. T. Chou, "Volume and Grain Boundary Diffusion in L1₂ Alloys with Special Reference to Ni₃Al Compounds," pp 461-74 in *Proceedings of the Symposium on High Temperature Ordered Intermetallic Alloys*, C. C. Koch, C. T. Liu, and N. S. Stoloff, eds., Materials Research Society, Pittsburgh, 1985.

17. T. C. Chou and Y. T. Chou, "Equilibrium Shapes of Ni₃Al Crystallites Formed During Diffusion Anneal," *J. Mat. Sci. Lett.*, **4**, 1340-1346 (1985).
18. A. J. Moorhead and J. J. Woodhouse, *Initial Development for Filler Metals for Direct Brazing of Structural Ceramics*, ORNL-6104, in final publication process.
19. A. J. Moorhead et al., "Fabrication, Testing, and Brazing of Dispersed-Metal Toughened Alumina," pp. 291-99 in *Proceedings of 20th Automotive Tech. Dev. Contractors' Coordination Mtg.*, Dearborn, Mich., Oct. 25-28, 1982, SAE P-120, April 1983.
20. A. J. Moorhead, T. N. Tiegs, and R. J. Lauf, "Dispersed Metal-Toughened Ceramics and Ceramic Brazing," pp. 223-29 in *Proceedings of 21st Automotive Tech. Dev. Contractors' Coordination Mtg.*, Dearborn, Mich., Nov. 14-17, 1983, SAE P-138, March 1984.
21. A. J. Moorhead, "Direct Brazing of Structural Ceramics for Uncooled Diesels," pp. 531-39 in *Proceedings of 2nd Automotive Tech. Dev. Contractors' Coordination Mtg.*, Dearborn, Mich., Oct. 29-Nov. 2, 1984, SAE P-155, March 1985.
22. A. J. Moorhead and P. F. Becher, "Development of a Test for Determining Fracture Toughness of Brazed Joints in Ceramic Materials," in review for submission to *Welding Journal*.
23. A. J. Moorhead, "Filler Metals for Direct Brazing of Ceramics," U.S. Patent pending.
24. A. J. Moorhead, "Oxidation Resistant Filler Metals for Direct Brazing of Structural Ceramics," U.S. Patent pending.
25. I. Peterson, "Recycling Mixtures of Plastics Is Becoming Technology Feasible, but What Do You Do with the Product," *Science News* **126** (Sept. 1, 1984).
26. "DOE-ECUT-PIA Program on Recycling Auto Scrap," report in *Inside R&D*, **13**(2), (Jan. 11, 1983).
27. A. Spaak, "Recycling a Mixture of Plastics -- A Challenge in Today's Environment," pp. 1158-63 in *SPE-ANTEC '85*.

28. J. W. Barlow and D. R. Paul, "Mechanical Compatibilization of Immiscible Blends," paper presented at *International Symposium on Phase Relationships and Properties of Multicomponent Polymer Systems*, Anacardi, Italy, May 30-June 3, 1983, available through authors at Department of Chemical Engineering, Center for Polymer Research, The University of Texas at Austin, Austin, TX 78712.
29. T. D. Traugott, "Mechanical Properties and Morphologies of HDPE-PET Blends," master's thesis, The University of Texas, December 1982.
30. J. D. Keitz, "Partial Miscibility of Polycarbonate with Poly(styrene-co-acrylonitrile) Copolymers," master's thesis, The University of Texas at Austin, December 1983.
31. R. D. Deanin and C. S. Nadkarni, "Recycling of the Mixed Plastics Fraction from Junked Autos. I. Low-Pressure Molding," *Am. Chem. Soc. Poly. Mat. Sci. Eng.* **50**, 408 (4/8-13/84); and in *Adv. Polym. Tech.* **4**(2), 172 (1984).
32. R. D. Deanin and A. R. Yniguez, "Recycling of the Mixed Plastics Fraction from Junked Autos. II. High-Pressure Molding," *Am. Chem. Soc. Polym. Mat. Sci. Eng.* **50**, 413 (4/8-13/84); and in *Adv. Polym. Tech.*, 1986 in press.
33. G. J. DeAngelis, B. Porter, and R. D. Deanin, "The Effect of Hydrogen Bonding Additives on the Clean Light Fluff Plastics Fraction from Automobile Shredders," *Soc. Plastics Eng., Ann. Tech. Conf.*, 1986 (in press.)
34. E. M. Pearce, "Polymer Compatibilization Through Hydrogen Bonding," *J. Macromol. Sci.-Chem.* **A21**(8&9), 1181-1216 (1984).
35. W. J. Crawford, "Use of Automobile Scrap as a Filler in Polymeric Composites," master's thesis, Lehigh University, June 1984.
36. A. P. Plochocki, "High Processibility, Filled Plastics Based on Melt Rheo-Synergism: Tentative Results for Inert Filler," *43rd ANTEC-SPEC*, TP 31, 1985.
37. S. S. Dagli, "Rheosynergistic Polyblends as the Matrix for Plastics Composites with Automotive Re grind," M. Sci. thesis, Che. E., Stevens Institute of Technology, 1985.
38. A. P. Plochocki, S. S. Dagli, and H. Emmanuilidis, *ACS Polymer Preprints* **26**(1), 288 (1984).
39. A. P. Plochocki et al., "Simulation of Melt VE Function for Binary Polyblends," submitted for *44th ANTEC*, TP32 (1986).

40. A. P. Plochocki and S. S. Dagli, *43rd ANTEC - SPE*, TP31, 972-75 (1985).
41. T. R. Curlee, "Recycling Plastics Wastes: Quantity Projections and Preliminary Competitive Assessment," *Materials and Society* **8**(3), 529-49 (1984).
42. T. R. Curlee, *The Economic Feasibility of Recycling Plastic Wastes: Preliminary Assessment*, ORNL/TM 9098, April 1984.
43. T. R. Curlee, "The Recycle of Plastics from Auto Shredder Residue: Incentives and Barriers," *Materials and Society* **9**(1), 29-43 (1985).
44. T. R. Curlee, "Plastic Wastes and the Market Penetration of Auto Shredders," *Technological Forecasting and Social Change* **28**(1), 29-42 (August 1985).
45. M. A. Schuetz, "Heat Transfer in Foam Insulation," master's thesis, Massachusetts Institute of Technology, December 1982.
46. M. Sinofsky, "Property Measurements and Thermal Performance Prediction of Foam Insulations," master's thesis, Massachusetts Institute of Technology, January 1984.
47. M. A. Schuetz and L. R. Glicksman, "A Basic Study of Heat Transfer Through Foam Insulation," pp. 341-47 in *Polyurethane - New Paths to Progress - Marketing Technology, Proceedings of the SPI 6th International Technical Marketing Conference*, 1983.
48. D. W. Reitz, M. A. Schuetz, and L. R. Glicksman, "A Basic Study of Aging of Foam Insulation," pp. 332-40 in *Polyurethane - New Paths to Progress - Marketing Technology, Proceedings of the SPI 6th International Technical Marketing Conference*, 1983.
49. M. A. Schuetz, L. R. Glicksman, and M. Sinofsky, "Radiation Heat Transfer in Foam Insulation," submitted to *ASME J. of Heat Transfer*, 1984.
50. L. R. Glicksman, A. G. Ostrogorsky, and D. W. Reitz, "Aging of Polyurethane Foam," submitted to *ASME J. of Heat Transfer*, 1984.
51. M. A. Schuetz and L. R. Glicksman, "A Basic Study of Aging of Foam Insulations," *J. Cellular Plastics* **20**(2), 114-21 (March-April 1984).
52. D. W. Reitz, M. A. Schuetz, and L. R. Glicksman, "A Basic Study of Aging of Foam Insulations," *J. Cellular Plastics* **20**(2), 104-13 (March-April 1984).

53. L. R. Glicksman, A. G. Ostrogorsky, and S. Chiappetta, *Effective Conductivity of Aging Polyurethane Foam*, ORNL/Sub/84-9009/1, March 1986.
54. P. D. Roach and R. E. Holtz, *Plastic Heat Exchangers for Waste Heat Recovery - Final Report*, ANL-83-81, Argonne National Laboratory, Argonne, Ill., September 1983.
55. P. F. Becher and G. C. Wei, "Toughening Behavior in SiC-Whisker-Reinforced Alumina," *Comm. of the Am. Cer. Soc.*, C-261 to C-269 (December 1984).
56. A. P. Thakoor et al., *J. Vac. Sci. Technol.* **A3**, 600 (1985).
57. A. P. Thakoor et al., *J. Appl. Phys.*, in press.
58. K. G. Kreider and S. Semancik, "Internal Combustion Engine Thin Film Thermocouples," *NBS IR 85*, 3110 (February 1985).
59. J. Narayan et al., "Ion-Beam and Laser Mixing of Nickel Overlayers on Silicon Carbide," *J. Appl. Phys.* **56**(6), (Sept. 15, 1984).
60. J. Narayan, D. Fathy, and O. W. Holland, "Excimer Laser Mixing of Nickel Overlayers on Silicon Carbide," *Mater. Lett.* **3**(7,8), 261-64 (May 1985).
61. X. L. Mann, "The Effect of Heat Treatment on Al⁺ Ion-Implanted Yttria Stabilized Zirconia," master's thesis, Georgia Institute of Technology, August 1984.
62. K. O. Legg et al., "Modification of Surface Properties of Yttria Stabilized Zirconia by Ion Implantation," *Nuc. Instr. and Methods in Phy. Res.* **B7/8**, 535-40 (1985).
63. J. K. Cochran et al., "Ion Implanted Precipitate Microstructure and Mechanical Properties of Ceramic Surfaces," in *Proceedings of ASM Conference on Applications of Ion Plating and Implantation in Materials*, Atlanta, Ga., June 3-5, 1985 (in press). Also *J. of Mat. for Energy Systems*, **8** (No. 2), 121-127, 1986.
64. J. K. Cochran et al., "Microstructural Control of Ion Implanted Ceramic Surfaces," pp. 602-08 in *Proceedings of ASEE Annual Conference*, ed. L. P. Grayson and J. M. Bidenbach, V2, 602-08, 1985.
65. J. K. Cochran et al., *Toughening of Oxide Surfaces Through Ion Implantation*, First Annual Report, ORNL Subcontract 19BD78D2C X-17, March 1985.

ORNL/TM-9695
 Distribution
 Category UC-95a

INTERNAL DISTRIBUTION

- | | | | |
|--------|-------------------------------|--------|-----------------------------|
| 1-2. | Central Research Library | 35. | C. T. Liu |
| 3. | Document Reference Section | 36. | L. K. Mansur |
| 4-5. | Laboratory Records Department | 37. | M. M. Martin |
| 6. | Laboratory Records, ORNL RC | 38. | H. E. McCoy |
| 7. | ORNL Patent Section | 39. | D. L. McElroy |
| 8. | P. Angelini | 40. | M. K. Miller |
| 9. | J. Bentley | 41. | A. J. Moorhead |
| 10. | W. D. Bond | 42-46. | L. E. Morris |
| 11. | R. A. Bradley | 47. | A. C. Schaffhauser |
| 12. | A. J. Caputo | 48. | G. M. Slaughter |
| 13. | R. S. Carlsmith | 49. | J. O. Stiegler |
| 14. | P. T. Carlson | 50. | D. P. Stinton |
| 15-19. | J. A. Carpenter, Jr. | 51. | R. W. Swindeman |
| 20. | R. S. Crouse | 52. | V. J. Tennery |
| 21. | T. R. Curlee | 53-55. | P. T. Thornton |
| 22. | A. DasGupta | 56. | F. W. Wiffen |
| 23. | J. R. DiStefano | 57. | R. O. Williams |
| 24. | W. P. Eatherly | 58. | R. J. Charles (Consultant) |
| 25. | D. M. Eissenberg | 59. | G. Y. Chin (Consultant) |
| 26. | W. Fulkerson | 60. | H. E. Cook (Consultant) |
| 27. | J. A. Horton | 61. | Alan Lawley (Consultant) |
| 28-32. | A. Jordan | 62. | W. D. Nix (Consultant) |
| 33. | M. P. Kertesz | 63. | J. C. Williams (Consultant) |
| 34. | E. H. Lee | | |

EXTERNAL DISTRIBUTION

64. ADVANCED MECHANICAL TECHNOLOGY, INC., 141 California Street, Newton, MA 02158
 F. J. Carignan
- 65-67. ARGONNE NATIONAL LABORATORY, Components and Technology Division, 9700 South Cass Avenue, Argonne, IL 60439
 A. I. Michaels
 F. A. Nichols
 P. D. Roach
68. Bell Associates, 17300 Mercury Blvd., Houston, TX 77058
 P. S. Gupton
69. DHR, INC., 6849 Old Dominion Drive, McLean, VA 22101
 R. S. Silberglitt

70. GENERAL ELECTRIC COMPANY, Lighting Research Operation, Nela Park,
Cleveland, OH 44112
Gary Weber
71. GEORGIA INSTITUTE OF TECHNOLOGY, School of Ceramic Engineering,
Atlanta, GA 30332
J. K. Cochran, Jr.
72. GTE Laboratories, 40 Sylvan Road, Waltham, MA 02154
G. C. Wei
73. James C. Holzwarth, 2629 Saturn Drive Lake, Orion, MI 48035
74. INSTITUTE FOR DEFENSE ANALYSES, 1801 N. Beauregard Street,
Alexandria, VA 22311
T. F. Kearns
75. JET PROPULSION LABORATORY, 4800 Oak Grove Drive, Pasadena, CA
91103
Satish Khanna
76. LAWRENCE BERKELEY LABORATORY, University of California, Berkeley,
CA 94720
A. V. Levy
- 77-78. LEHIGH UNIVERSITY, Materials Research Center, Bethlehem, PA 18015
Y. T. Chou
J A. Manson
79. LOCKHEED PALO ALTO LABORATORIES, Materials Science, Organization
5230, Bldg. 201, 3251 Hanover Street, Palo Alto, CA 94304
E. C. Burke
- 80-81. MASSACHUSETTS INSTITUTE OF TECHNOLOGY, 77 Massachusetts Avenue,
Cambridge, MA 02139
M. B. Bever
L. Glicksman
- 82-83. NATIONAL BUREAU OF STANDARDS, National Measurements Laboratory,
Center for Materials Science, Chemical Stability and Corrosion
Division, Washington, DC 20234
S. M. Hsu
K. G. Kreider
84. NATIONAL BUREAU OF STANDARDS, Thermophysical Properties Division,
Center for Chemical Engineering, National Engineering Laboratory,
Boulder, CO 80303
J. F. Ely

- 85-87. NORTH CAROLINA STATE UNIVERSITY, Raleigh, NC 28750
R. F. Davis
C. C. Koch
J. Narayan
- 88-89. NORTON COMPANY, Goddard Road, Northboro, MA 01532-1545
P. O. Charreyron
J. G. Hannoosh
- 90-91. PLASTICS INSTITUTE OF AMERICA, INC., Stevens Institute of
Technology, Castle Point Station, Hoboken, NJ 07030
M. J. Curry
A. Spaak
92. POLAROID CORPORATION, Polymer Department, 750 Main Street,
Cambridge, MA 02139
J. F. Kinstle
- 93-94. POLYTECHNIC OF NEW YORK, Brooklyn, NY 11201
E. M. Pearce
G. C. Tesoro
95. RENSSELAER POLYTECHNIC INSTITUTE, Materials Engineering
Department, Troy, NY 12181
N. S. Stoloff
96. Maxine Savitz, 5019 Lowell St., Washington, DC 10016
97. STEVENS INSTITUTE OF TECHNOLOGY, Castle Point Station,
Hoboken, NJ 07030
A. P. Plochocki
98. TECHNOLOGY STRATEGIES, INC., 10722 Shingle Oak Ct., Burke, VA
22015
E. C. Van Reuth
99. UNIVERSITY OF LOWELL, Plastics Engineering Department,
One University Avenue, Lowell, MA 01854
R. D. Deanin
100. UNIVERSITY OF MASSACHUSETTS, Room 701, GRC, Amherst, MA 01003
R. S. Porter
- 101-102. UNIVERSITY OF TEXAS AT AUSTIN, Department of Chemical Engineering,
Austin, TX 78712
J. W. Barlow
D. R. Paul

103. VANDERBILT UNIVERSITY, Station B, P. O. Box 1621,
Nashville, TN 37235
J. J. Wert
104. VIRGINIA POLYTECHNIC INSTITUTE, College of Engineering,
329 Norris Hall, Blacksburg, VA 24061
W. Hibbard
- 105-111. DOE, ENERGY UTILIZATION RESEARCH, Office of Conservation and
Renewable Energy, Forrestal Building, 1000 Independence Avenue,
Washington, DC 20585
J. J. Brogan
J. J. Eberhardt (5 copies)
T. M. Levinson
112. DOE, RESEARCH AND DEVELOPMENT, Office of Conservation and
Renewable Energy, Forrestal Building, Independence Avenue,
Washington, DC 20585
Allen Streb
113. DOE, OAK RIDGE OPERATIONS OFFICE, P.O. Box E, Oak Ridge, TN 37831
Office of Assistant Manager for Energy Research and Development
- 114-271. DOE, TECHNICAL INFORMATION CENTER, Office of Information Services,
P.O. Box 62, Oak Ridge, TN 37831

For distribution as shown in DOE/TIC-4500, Distribution
Category UC-95a (Energy Conservation-Utilization and
Information Dissemination)